UNIVERSITAT DE BARCELONA

Aplicació de tècniques voltamperomètriques i cronopotenciomètriques de redissolució a l'especiació d'ions metàl·lics

Núria Serrano i Plana

Departament de Química Analítica
Barcelona, 2007

III. RESULTATS I DISCUSSIÓ

CAPÍTOL 8

Estudis cronopotenciomètrics de redissolució

CAPÍTOL 8. Estudis cronopotenciomètrics de redissolució per a l'especiació de metalls pesants emprant l'elèctrode de gotes de mercuri i l'elèctrode de pel·lícula de mercuri

Aquest capítol engloba tres treballs que tenen per finalitat, avaluar els avantatges i els desavantatges de la cronopotenciometria de redissolució respecte a la voltamperometria per redissolució anòdica en l'estudi de sistemes complexants amb lligands inerts i làbils senzills i macromoleculars i en sistemes multi-metall.

Els treballs segueixen un mateix esquema: es realitzen valoracions voltamperomètriques i cronopotenciomètriques per a cada sistema objecte d'estudi, emprant l'elèctrode de gota penjant de mercuri (HMDE) i l'elèctrode de disc rotatori sobre el qual es diposita una fina pel·lícula de mercuri (MF-RDE). A partir dels potencials de pic (E_p) i de les àrees de pic (I_p per ASV o τ per SCP) en absència i presència de lligand, s'apliquen els diferents models de complexació amb la finalitat de determinar les constants

d'estabilitat dels complexos formats i, poder-les comparar entre si i amb els valors de la bibliografia.

8.1 Comparison of constant-current stripping chronopotentiometry and anodic stripping voltammetry in metal speciation studies using mercury drop and film electrodes

N. Serrano, J.M. Díaz-Cruz, C. Ariño, M. Esteban

Journal of Electroanalytical Chemistry 560 **(2003)** 105-116

Available online at www.sciencedirect.com
SCIENCE DIRECT®
Journal of Electroanalytical Chemistry 560 (2003) 105–116
Journal of Electroanalytical Chemistry
www.elsevier.com/locate/jelechem

Comparison of constant-current stripping chronopotentiometry and anodic stripping voltammetry in metal speciation studies using mercury drop and film electrodes

Núria Serrano, José Manuel Díaz-Cruz *, Cristina Ariño, Miquel Esteban

Departament de Química Analítica, Facultat de Química, Universitat de Barcelona, Av. Diagonal 647, E-08028 Barcelona, Spain

Received 13 March 2003; received in revised form 16 June 2003; accepted 1 July 2003

Abstract

Capabilities for heavy metal speciation of anodic stripping voltammetry (ASV) and constant-current stripping chronopotentiometry (SCP) in both mercury drop (HMDE) and mercury film rotating disk (MFE-RDE) electrodes are compared. For this purpose, the Cd(II)–glycine and Cd(II)–polymethacrylate (PMA) systems are used as models of simple labile and macromolecular labile complexes adsorbing onto the electrode, respectively. The results suggest that SCP could be a valuable alternative to the more widespread ASV in this kind of study. Concerning the electrode, the MFE-RDE is less user-friendly than the HMDE, but presents a better definition of both the hydrodynamic conditions during the deposition step and the stripping regime during the oxidation. An important interference in SCP is the dissolved oxygen, which can be minimised by combining relatively large oxidation currents and low stirring rates. Moreover, for Cd–PMA, double peaks have been observed in both ASV and SCP, which seems to be due to the lack of enough ligand excess to complex the metal ions released by the amalgam oxidation. Anyway, this problem can be minimised by optimising the rotation rate of the electrode and ensuring enough ligand excess.

Keywords: Stripping cronopotentiometry; Anodic stripping voltammetry; Mercury film electrode; Rotating disk electrode; Hanging mercury drop electrode; Heavy metal speciation

1. Introduction

Stripping techniques have been extensively applied to the analysis of heavy metal ions in environmental and biological samples [1–3]. This is especially due to their excellent detection limits, which allow one to assess the low metal concentrations frequently encountered in such samples. Moreover, their sensitivity to the presence of different metal species can be helpful in heavy metal speciation.

Stripping techniques basically consist of a deposition step where the metal is accumulated onto the electrode (by applying a constant potential and stirring of the solution) and a further stripping step where the accumulated metal is totally or partially dissolved from the electrode to the solution.

For heavy metal ions, the most widely used stripping technique is anodic stripping voltammetry (ASV), in which the accumulation is done by reduction of the metal ion in a mercury electrode and the stripping is performed by means of an oxidative potential scan (usually in the differential pulse mode). Then, the evolution of current as a function of potential is measured. In the case of mercury drop electrodes, a rest period between deposition and stripping steps is required to ensure a homogeneous distribution of the metal inside the drop. When thin mercury films are used, this intermediate step is not necessary [4]. Despite the widespread character of ASV, many problems have been reported in its application to samples containing organic matter, mainly due to adsorption of different species onto the electrode [5].

Stripping chronopotentiometry (SCP), also termed potentiometric stripping analysis (PSA), was introduced

* Corresponding author. Tel.: +34-93-403-4873; fax: +34-93-402-12-33.
E-mail address: jmdiaz@apolo.qui.ub.es (J.M. Díaz-Cruz).

0022-0728/$ - see front matter © 2003 Elsevier B.V. All rights reserved.
doi:10.1016/j.jelechem.2003.07.022

by Jagner and Graneli [6,7]. It is usually performed on mercury electrodes and includes a deposition step identical to that of ASV and a stripping step where the accumulated metal is reoxidised by the action of a chemical oxidant or by imposing a constant oxidising current. Both SCP modalities measure the evolution of the potential as a function of time and use the transition time (that between two consecutive potential jumps) as the main analytical parameter. SCP constitutes a valuable alternative to ASV, since it has been empirically proved to be less sensitive to the presence of important quantities of organic matter (mainly by comparison of SCP results with GFAAS and ICP-OES data) [5,7,8]. This is why SCP has been extensively applied to the determination of total amounts of heavy metals in foods, beverages and biological samples. However, up to now, few attempts have been made to exploit the interesting features of SCP in the field of heavy metal speciation.

Recently, Town and van Leeuwen [9,10] have published interesting theoretical considerations and experimental evidence on the use of constant-current SCP in a hanging mercury drop electrode (HMDE) for heavy metal speciation. In this work, they stress the importance of the stripping regime which, depending on the oxidising current, can be closer to the semi-infinite linear diffusion case or to the total depletion limit. They also have pointed out the dramatic increase of the interference of dissolved oxygen as the applied current decreases. Moreover, they recommend the measurement of the area under the baseline-corrected derivative of time as a function of potential to obtain a transition time free from capacitive background current and from problems caused by electrodic adsorption and ligand saturation during the stripping step.

The present piece of work tries to complement such promising SCP studies, carried out in HMDE, with additional experiments by both SCP and ASV using a rotating disk mercury film electrode (RDE-MFE). As compared to HMDE, RDE-MFE is less user-friendly and lacks a comparable high reproducibility but, in contrast, ensures a total depletion regime under a wider range of experimental conditions, and presents better defined hydrodynamic conditions during the deposition step.

2. Theory

Let us consider a heavy metal ion M which can be complexed in solution by a ligand L and reversibly reduced in a mercury electrode, according to the scheme:

$$\begin{array}{ccc} \mathrm{M} + m\,\mathrm{L} & \underset{\beta_m}{\rightleftharpoons} & \mathrm{ML}\ldots\mathrm{ML}_m \\ n\bar{e}\ \uparrow\downarrow & & \\ \mathrm{M(Hg)} & & \end{array} \qquad (1)$$

where the electrical charges have been omitted for the sake of simplicity. β_m denotes the overall complexation constant for the species ML_m

$$\beta_m = c^*_{\mathrm{ML}_m}/c^*_{\mathrm{M}}(c^*_{\mathrm{L}})^m \qquad (2)$$

with c^*_i denoting bulk concentration of the species i.

In a RDE-MFE, both ASV and SCP include, first, a deposition step with application of a constant potential E_d (negative enough to render the process mass transport-controlled) for a time t_d and, second, a stripping step where the metal reduced in the mercury film is reoxidised. Electrode rotation is usually applied in both steps.

Concerning the deposition step (identical in both ASV and SCP), the concentration of reduced M in the amalgam at the end of this period is given by

$$c_{\mathrm{M(Hg)}} = (I_d t_d)/(nFAl), \qquad (3)$$

where A is the area of the electrode, l is the thickness of the mercury film, t_d is the deposition time and I_d is the average limiting current registered during this time. The RDE character of the electrode ensures the fulfilment of the Levich equation [4] during the deposition, so that I_d can be expressed in the form

$$I_d = 0.62nFA\bar{D}^{2/3}\omega^{1/2}\nu^{-1/6}c^*_{\mathrm{TM}}, \qquad (4)$$

ω being the angular frequency of rotation (s^{-1}), ν the kinematic viscosity ($cm^2\ s^{-1}$), c^*_{TM} the total bulk concentration of the metal (mol cm^{-3}) and $\bar{D}$ the average diffusion coefficient of the labile species of the metal ion in solution ($cm^2\ s^{-1}$). According to the model by de Jong et al. [11–13], when association–dissociation equilibria for all complexes are fast (labile situation) $\bar{D}$ can be computed as a weighted average of the diffusion coefficients of the different metal species

$$\bar{D} = (c^*_{\mathrm{M}}/c^*_{\mathrm{TM}})D_{\mathrm{M}} + \Sigma_m(c^*_{\mathrm{ML}m}/c^*_{\mathrm{TM}})D_{\mathrm{ML}_m} \qquad (5)$$

with c^*_i, D_i denoting the bulk concentration and the diffusion coefficient of the species i, respectively. In the case of low-size ligands, the diffusion coefficients of the complexes can be considered equal to that of the free solvated metal ion, D_M, whereas in the case of macromolecular ligands they can be assumed to be equal to that of the free ligand, D_L (much lower than D_M).

By combining Eqs. (3)–(5) for the same total metal concentration and under identical voltammetric and hydrodynamic conditions, the concentration of metal in the amalgam can be written as

$$c_{\mathrm{M(Hg)}} = k\bar{D}^{2/3}c^*_{\mathrm{TM}}, \qquad (6)$$

where k is a constant.

The stripping step is quite different for ASV and SCP. In the case of ASV, a potential scan is applied in the positive direction to reoxidise the metal, and the area (or the height) of the stripping peak is taken as the analytical signal. A numerical solution has been found for ASV measurements in MFE which, for the usual range

of experimental conditions, approaches the following expression for the peak current I_{ASV} [4]:

$$I_{ASV} = (n^2F^2vlAc_{M(Hg)})/(2.7RT), \quad (7)$$

v being the scan rate.

In contrast with ASV, the stripping step of SCP is carried out by chemical oxidation promoted by a species in solution (usually Hg^{2+}) or by application of a constant anodic current. In any case, the potential (E) is recorded as a function of time (t). At the beginning of the reoxidation, E decreases greatly from the deposition potential to that given by the equilibrium between the reduced and oxidised forms of the metal on the electrode surface, according to the Nernst equation. As the metal is being stripped to the solution, there is a smooth change in the equilibrium potential but, when the concentration of reduced metal on the electrode surface virtually decreases to zero, there is a dramatic change in the electrode potential, which starts to be determined by a different electrochemical process, or simply approaches the potential of equilibrium between electrode and solution. The time between both sudden potential changes is termed the transition time τ, and it is the analytical parameter in SCP. When the constant current modality is used, two limiting situations are possible. For thick mercury films and large oxidation currents, the metal depletion from the mercury affects only the most external layer of the electrode and the semi-infinite linear diffusion regime applies. Then, for an approximately planar electrode, the Sand equation can be invoked to obtain [4,9]

$$\tau^{1/2} = nFAD_{M(Hg)}^{1/2}\pi^{1/2}c_{M(Hg)}/(2I_{ox}) \quad (8)$$

with $D_{M(Hg)}$ denoting the diffusion coefficient of the reduced metal inside the mercury and I_{ox} the constant oxidation current. It must be noted that in relatively small mercury drops the sphericity of the electrode can produce deviations in the behaviour predicted by this equation. In contrast, the use of thin mercury films and small values of I_{ox} leads to the total depletion regime, which implies reoxidation of all the metal previously reduced in the mercury. Then, independently of the geometry of the electrode, equations for total electrolysis can be applied to obtain [4,9]

$$\tau = nFAlc_{M(Hg)}/I_{ox}. \quad (9)$$

The comparison between Eqs. (8) and (9) suggests that a good indication of the regime can be obtained from the logarithmic plot of τ vs. I_{ox}

$$\log\tau = a + b\log I_{ox}. \quad (10)$$

Thus, a value of -2 for the slope b indicates a semi-infinite linear-diffusion and a value of -1, a total depletion regime.

In the voltammetric study of metal complexes the usual strategy is based on the comparison of the currents measured for the same total concentration of the metal in the presence and in the absence of the ligand [11–13]. Thus, in the case of ASV, a normalised current ϕ_{ASV} can be defined, according to Eqs. (6) and (7), as

$$\begin{aligned}\phi_{ASV} &= I_{ASV}\ (\text{with L})/I_{ASV}\ (\text{without L})\\ &= c_{M(Hg)}\ (\text{with L})/c_{M(Hg)}\ (\text{without L})\\ &= (\bar{D}/D_M)^{2/3}, \end{aligned} \quad (11)$$

where D_M refers to the diffusion coefficient of the free metal ion. When constant-current SCP is used, an analogous normalised parameter ϕ_{SCP} can be defined as a ratio between transition times

$$\phi_{SCP} = \tau\ (\text{with L})/\tau\ (\text{without L}). \quad (12)$$

In SCP, however, the relationship between ϕ and the diffusion coefficient ratio depends strongly on the stripping regime. For semi-infinite linear diffusion, combination of Eqs. (6) and (8) produces

$$\begin{aligned}\phi_{SCP,\text{linear diffusion}} &= [c_{M(Hg)}\ (\text{with L})/c_{M(Hg)}\ (\text{without L})]^2\\ &= (\bar{D}/D_M)^{4/3}, \end{aligned} \quad (13)$$

whereas in the case of total depletion, Eqs. (6) and (9) yield

$$\begin{aligned}\phi_{SCP,\text{total depletion}} &= c_{M(Hg)}\ (\text{with L})/c_{M(Hg)}\ (\text{without L})\\ &= (\bar{D}/D_M)^{2/3}. \end{aligned} \quad (14)$$

At this point it must be emphasised that, when HMDE is used instead of RDE, the hydrodynamic conditions during the deposition step are not well-defined. To solve this problem, the validity has been postulated of an expression similar to Eq. (6) but including a semiempirical parameter p ranging from 1/2 (semi-infinite linear diffusion) to 2/3 (convective diffusion, according to the Levich equation) which depends on the stirring conditions during the preelectrolysis step [14]

$$c_{M(Hg)} = k'\bar{D}^p c_{TM}^*, \quad (15)$$

where k' is again a constant. Despite some experimental studies suggesting that p could be closer to 2/3 than to 1/2 [15], in practice it is very difficult to determine its exact value for a given experimental device. This implies that Eqs. (11), (13) and (14) can be used for the HMDE but one must accept an important uncertainty in the value of the exponent of the diffusion coefficient ratio.

To summarize the facts described so far, it can be said that, independently of the technique or the electrode used (ASV or PSA, RDE or HMDE), an experimental ϕ parameter is expected to equal the term $(\bar{D}/D_M)^p$, which is related to metal speciation through Eq. (5)

$$\begin{aligned}\phi &= (\bar{D}/D_M)^p\\ &= \left[\left(c_M^*/c_{TM}^*\right) + \Sigma_m\left(c_{ML_m}^*/c_{TM}^*\right)\left(D_{ML_m}/D_M\right)\right]^p. \end{aligned} \quad (16)$$

In the case of simple labile complexes, their diffusion coefficients are practically identical to D_M, so that $\phi = 1$ and no complexation data can be deduced from this parameter. If a macromolecular labile complex is formed, every complexation site can be considered to be a ligand and, for the case of excess ligand, an average 1:1 metal-to-site complexation constant can be computed

$$K = c_{ML}/(c_M c_L). \quad (17)$$

Moreover, the diffusion coefficients of the macromolecular complexes are very similar to that of the ligand and a parameter ε (less than 1) can be defined as the ratio between the (average) diffusion coefficient of the complex and that of the free metal ion [11–14]

$$\varepsilon = D_{ML}/D_M. \quad (18)$$

This allows one to write Eq. (16) in the form [14]

$$\phi = [(1 + \varepsilon K c_L^*)/(1 + K c_L^*)]^p, \quad (19)$$

which makes possible the determination of ε and K by fitting of Eq. (19) to the experimental ϕ vs. c_L^* curves, provided the value of p is known.

Finally, for the potentials, the validity of the DeFord-Hume method has been postulated [16,17] for ASV data according to the expression [14]:

$$F_0 = \exp(-nF/RT\Delta E_{ASV} - \ln \phi_{ASV}) = 1 + \Sigma_i \beta_i (c_L^*)^i, \quad (20)$$

where F_0 is the Leden function of zero order and ΔE_{ASV} is the potential shift (usually negative) caused by the addition of the ligand to the free metal ion. Further experimental work confirmed empirically the validity of such an approach in the absence of electrodic adsorption [18].

Taking into account the case of ASV and comparing Eqs. (11), (13), (14) and (16), for SCP we postulate the applicability of Eq. (20) to the peak potential shifts (ΔE_{SCP}) found in dt/dE vs. E plots, substituting ϕ_{ASV} by $\phi_{SCP}^{1/2}$, in the case of semi-infinite linear diffusion, or by ϕ_{SCP}, in the case of total depletion:

$$F_0 = \exp(-nF/RT\Delta E_{SCP,\text{linear diffusion}} - 1/2 \ln \phi_{SCP,\text{linear diffusion}}) = 1 + \Sigma_i \beta_i (c_L^*)^i, \quad (21)$$

$$F_0 = \exp(-nF/RT\Delta E_{SCP,\text{total depletion}} - \ln \phi_{SCP,\text{total depletion}}) = 1 + \Sigma_i \beta_i (c_L^*)^i. \quad (22)$$

In all cases, Leden functions of higher order can be computed by applying

$$F_1 = (F_0 - 1)/c_L, \ldots, F_n = (F_{n-1} - \beta_{n-1})/c_L^*. \quad (23)$$

3. Experimental

3.1. Reagents

Polymethacrylic acid (PMA) was obtained from BDH, with an average molar mass of 26,000 g mol^{-1} (according to BDH). Using this value, Cleven [19] estimated a diffusion coefficient close to 1.5×10^{-7} cm^2 s^{-1}.

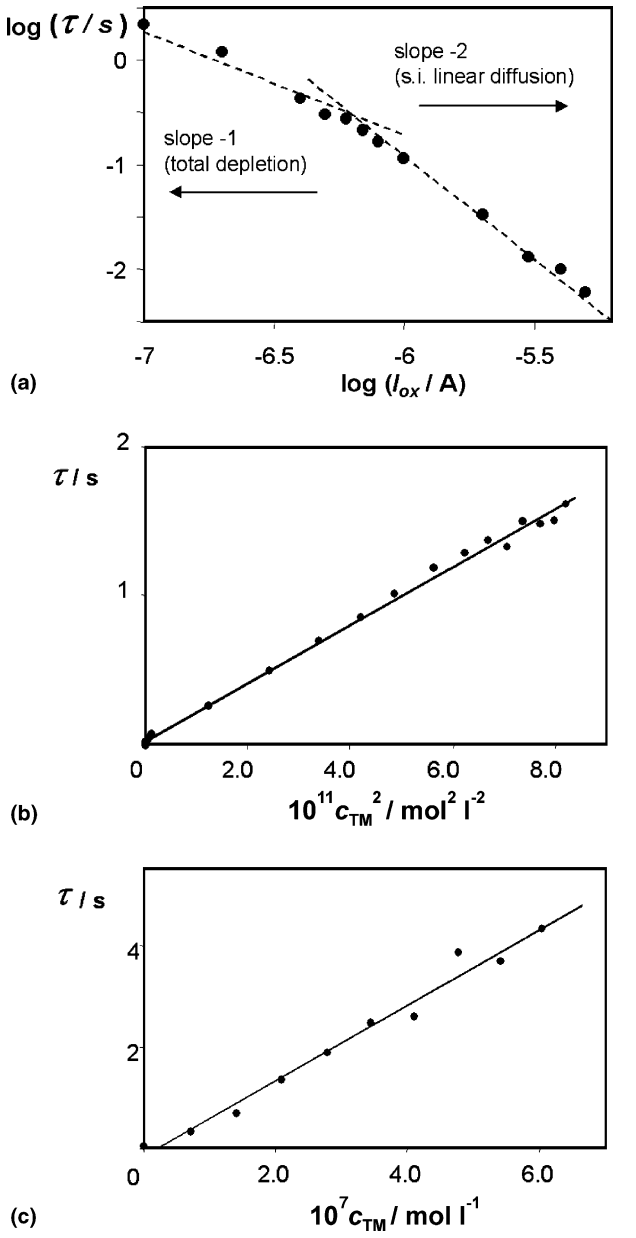

Fig. 1. Study of the SCP stripping regime in HMDE from the transition times (τ) measured for a solution containing Cd(II) and 0.01 mol l^{-1} of KNO_3 using a deposition time of 120 s: (a) $\log \tau$ vs. $\log I_{ox}$ plot for a Cd(II) concentration of 10^{-6} mol l^{-1} compared with the theoretical lines with slope −1 (total depletion) and −2 (semi-infinite linear diffusion); (b) τ vs. c_{TM}^2 plot (where c_{TM} is the total metal concentration) using an oxidation current $I_{ox} = 10^{-6}$ A; (c) τ vs. c_{TM} plot using an oxidation current $I_{ox} = 10^{-9}$ A.

It must be pointed out, however, that the diffusion coefficient can change considerably depending on the degree of dissociation of PMA as a consequence of conformational changes caused by electrostatic interactions between carboxylate groups. Stock solutions of ca. 0.1 mol l^{-1} (in monomeric units, containing one carboxylic group each) were prepared by dilution, and the total number of carboxylic groups was determined by conductimetric acid–base titration. Partially neutralised PMA solutions were prepared daily from these stock solutions by adding the amount of KOH necessary to deprotonate 70% of the carboxylic groups (degree of dissociation 0.7). All PMA solutions were stored in the dark at 4 °C to prevent decomposition.

Glycine was obtained from Sigma (purity higher than 99%). Stock solutions of 2.2 mol l^{-1} were prepared by dissolving an accurate weight of the solid in water.

All other reagents used were Merck analytical grade. Cd^{2+} stock solutions were prepared by dissolving $Cd(NO_3)_2 \cdot 4\ H_2O$ in water and were standardised complexometrically [20]. Tris (i.e., tris(hydroxymethyl)aminomethane) + nitric acid solutions with 0.05 mol l^{-1} ionic strength at pH 7.5 were applied as buffer solutions in the studies of complexation with glycine. KOH solutions were used for PMA neutralisation. KNO_3 0.01 mol l^{-1} was employed as the supporting electrolyte. Ultrapure water (Milli-Q plus 185 system, Millipore) was used in all experiments.

3.2. Apparatus

Conductimetric titrations of PMA solutions were performed by means of a conductimeter Orion 120 connected to a conductimetric cell 99-01-01 (cell constant 1.03 cm^{-1}).

Differential pulse polarography (DPP), reverse pulse polarography (RPP), differential pulse anodic stripping voltammetry (DPASV) and constant-current stripping chronopotentiometry (SCP) measurements were performed in an Autolab System PGSTAT20 (EcoChemie, The Netherlands) attached to a Metrohm 663 VA Stand (Metrohm, Switzerland) and a personal computer with GPES4 data acquisition software (EcoChemie). The

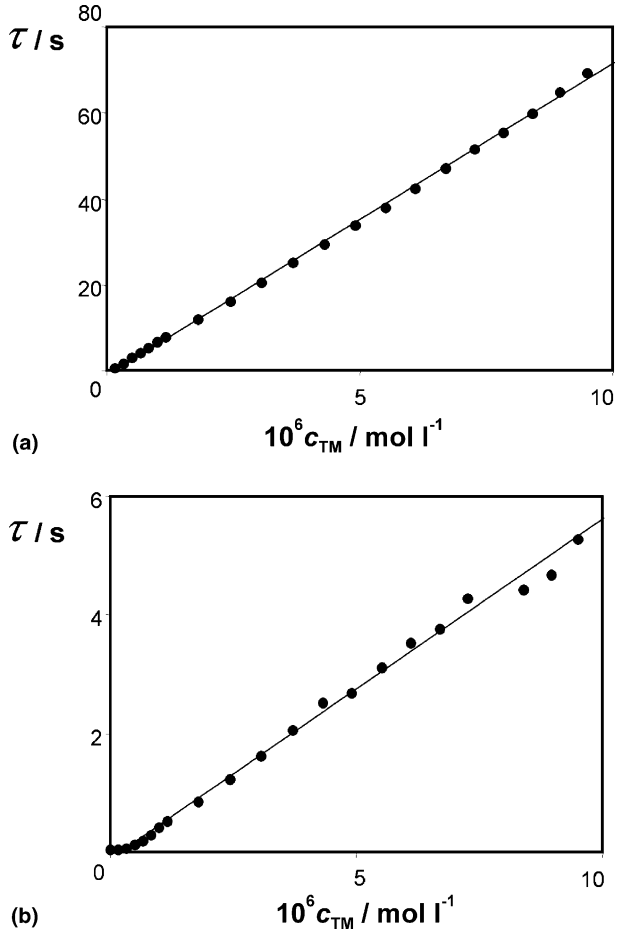

Fig. 2. Confirmation of the total depletion SCP stripping regime in MFE-RDE from the transition times (τ) measured for a solution containing Cd(II) and 0.01 mol l^{-1} of KNO_3 using a deposition time of 120 s: (a) τ vs. c_{TM} plot using an oxidation current $I_{ox} = 10^{-6}$ A; (b) τ vs. c_{TM} plot using an oxidation current $I_{ox} = 10^{-9}$ A.

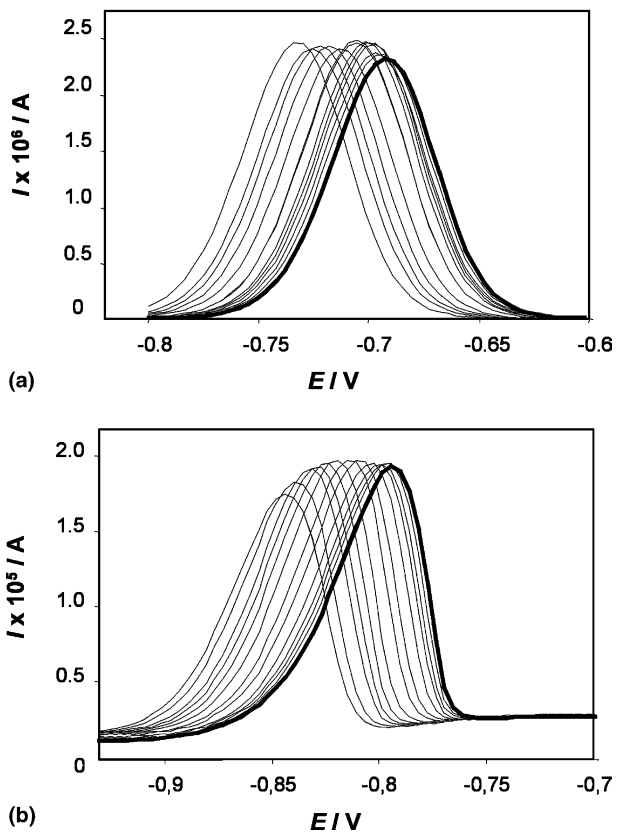

Fig. 3. Voltammograms measured by ASV in a HMDE (a) and in a MFE-RDE (b) during the titration of a solution containing 10^{-6} mol l^{-1} of Cd(II) with glycine at pH 7.5 and ionic strength 0.05 mol l^{-1} using a deposition time of 120 s. The initial signals measured in the absence of glycine are denoted with a thicker line.

system was also connected to a Metrohm 665 Dosimat for the addition of solutions and to an Orion SA 720 pH-meter for monitoring the pH value during the experiments. All the measurements were carried out in a glass cell at constant room temperature (25 °C) under a purified nitrogen atmosphere (Air Liquide).

The reference electrode (to which all potentials are referred) and the auxiliary electrode were Ag|AgCl|KCl (3 mol l^{-1}) and glassy carbon, respectively. In some experiments, the working electrode used was a multimode electrode Metrohm producing drops of ca. 0.5 mm^2 surface that could work as an HMDE or as a static mercury drop electrode (SMDE). In other cases, a mercury film deposited on a glassy carbon rotating disk electrode (Metrohm) of 2 mm diameter (MFE-RDE) was used (see below).

Unless otherwise indicated, pulse times of 40 ms, drop times of 0.8 s and scan rates of 5 mV s^{-1} were used in the polarographic techniques (DPP and RPP). Pulse amplitudes of 50 mV were applied in DPP and DPASV stripping scans. In both SCP and DPASV a deposition potential of −0.95 V was applied for a time ranging from 30 to 120 s. In the case of the HMDE, a rest period of 30 s was performed between the deposition and the stripping steps, which was not necessary in MFE. The usual rotating speed of MFE-RDE was 1500 rpm.

3.3. Preparation of the mercury film on the MFE-RDE

Prior to the deposition of the film, the glassy carbon disk was polished using a suspension of alumina particles of 300 nm diameter. Then, the electrode was attached to the stand (together with the reference and auxiliary electrodes) and immersed into 20 ml of a solution containing 200 mg l^{-1} of $HgCl_2$ and 0.1 mol l^{-1} of HCl. After deaeration of the solution for 10 min, a deposition potential of −0.5 V was applied for 2 min with solution stirring, followed by a rest period (without stirring) of 30 s. Then, both deposition and resting periods were repeated at −0.7, −0.8 and −0.9 V and, finally, three further times at −0.9 V. Once the mercury film had been deposited, the three electrodes were rinsed with water and the mercury solution could be replaced in the cell by that which was to be measured. This procedure, which partially modifies a previous methodology [21] has proven to produce mercury films that can be used over one day without noticeable degradation.

3.4. Voltammetric and chronopotentiometric titrations

Each titration started by placing in the cell, a volume of 25 ml of a solution containing Cd^{2+}-ion and 0.01 mol l^{-1} of KNO_3 (in the case of the Cd–PMA system) or

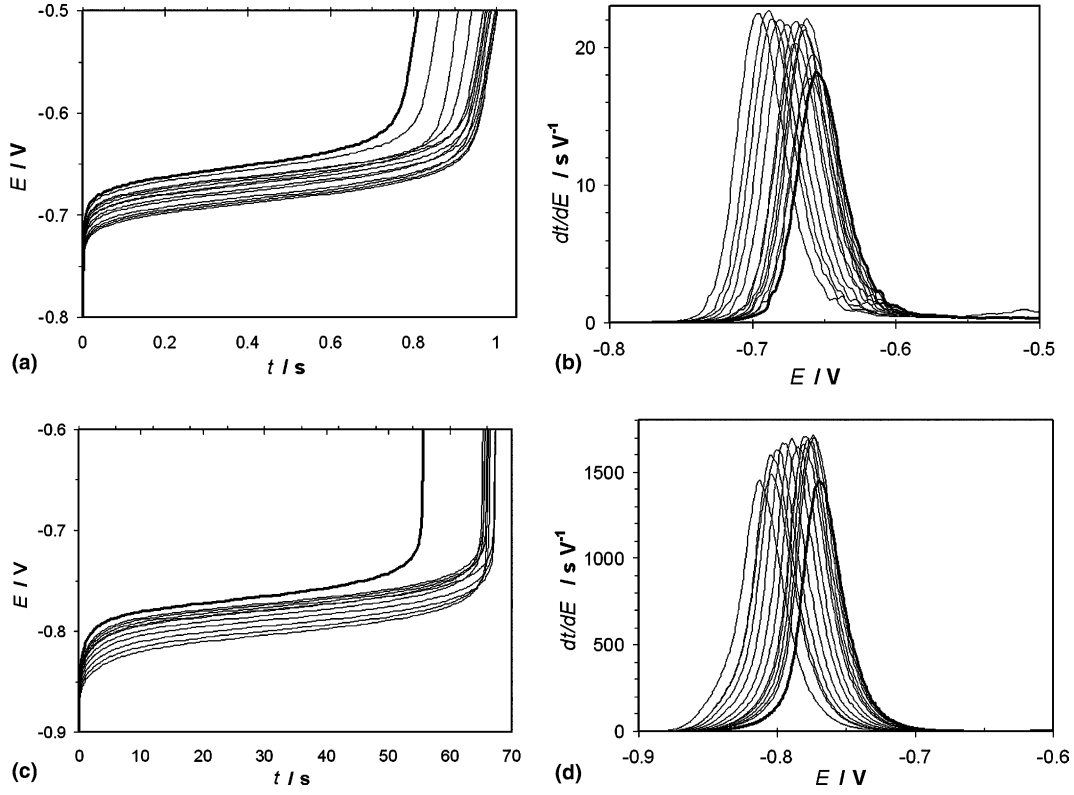

Fig. 4. SCP signals measured in a HMDE (a, b) and in a MFE-RDE (c, d) during the titration of a solution containing 10^{-6} mol l^{-1} of Cd(II) with glycine at pH 7.5 and ionic strength 0.05 mol l^{-1} using a deposition time of 120 s and $I_{ox} = 10^{-6}$ A. (a) and (c) show the original chronopotentiograms and (b) and (d) the corresponding derivatives of time with respect to potential. The initial signals measured in the absence of glycine are denoted with a thicker line.

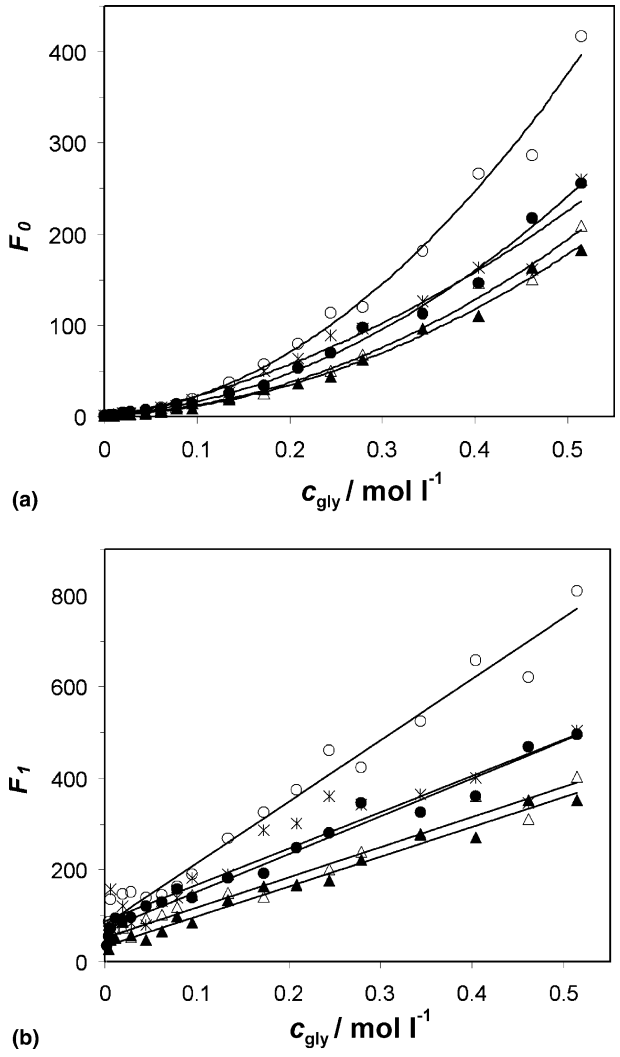

Fig. 5. Leden functions of order 0 (a) and 1 (b) obtained from the signals shown in Fig. 4 and from an additional titration by DPP. They are plotted as functions of the glycine concentration and compared with the curves fitted using Eqs. (21)–(23) (solid lines). DPP in SMDE (∗), ASV in HMDE (△), ASV in MFE-RDE (○), SCP in HMDE at $I_{ox} = 10^{-9}$ A (total depletion regime) (▲), SCP in MFE-RDE at $I_{ox} = 10^{-9}$ A (●).

0.05 mol l^{-1} Tris buffer at pH 7.5 (in the case of the Cd–glycine system). Then, the sample was deaerated with pure nitrogen for 10 min and a scan was recorded. Further, aliquots of glycine or PMA solutions were added and the respective curves were recorded. In the case of SCP, the transition time was measured as the area under the baseline-corrected dt/dE plot, which according to previous work [9], minimises the contribution of capacitive currents and other secondary effects. All solutions were deaerated and mechanically stirred for 1 min after each addition. In order to prevent changes in ionic strength, the solution to be added contained the same concentration of KNO_3 or Tris as that in the cell. In the case of PMA titrations, the pH of the solution prior to PMA additions was adjusted to 6–7 adding small volumes of a KOH solution to prevent significant changes in the degree of dissociation of PMA [18].

4. Results and discussion

4.1. Stripping regime in constant-current SCP

As a first step, the influence of the SCP oxidative current on the stripping regime in both HMDE and MFE-RDE electrodes was studied. In the case of the HMDE, according to Town and van Leeuwen [9], the presence of three characteristic regions was confirmed: high currents ensure semi-infinite linear diffusion, low currents produce total depletion and too low currents suffer from interference of dissolved oxygen. Fig. 1(a) shows the $\log\tau$ vs. $\log I_{ox}$ plot as compared to the theoretical lines from Eq. (10), with slope −2 for semi-infinite linear diffusion and −1 for total depletion. Figs. 1(b) and (c) show that the stripping regime in HMDE can be also confirmed by the linearity of the τ vs. c_{TM}^2 and τ vs. c_{TM} plots for linear diffusion (high currents) and total depletion (low currents), respectively. In MFE-RDE, the total depletion regime predominates in a wide range of oxidation currents, which can be confirmed by the linearity of the τ vs. c_{TM} plots shown in Fig. 2.

4.2. Study of the Cd^{2+}–glycine system as a model of simple labile complexes without electrodic adsorption

ASV and SCP measurements have been carried out during the titration of solutions containing 10^{-6} mol l^{-1}

Table 1
Stability constants determined for the Cd(II)–glycine system at pH 7.5 and an ionic strength of 0.05 mol l^{-1} using different techniques and electrodes

Method	$\log\beta_1$	$\log\beta_2$
DPP in SMDE	4.20 (0.08)	7.42 (0.04)
ASV in HMDE	3.97 (0.07)	7.34 (0.02)
ASV in MFE-RDE	4.17 (0.07)	7.65 (0.02)
SCP in HMDE, $I_{ox} = 10^{-6}$ A	3.8 (0.1)	7.34 (0.02)
SCP in MFE-RDE, $I_{ox} = 10^{-6}$ A	4.10 (0.05)	7.44 (0.02)
Potentiometry at ionic strength 0 mol l^{-1} [22]	4.14	7.60
Potentiometry at ionic strength 0.1 mol l^{-1} [22]	4.22 ± 0.05	7.69 ± 0.04

They are compared with potentiometric values from [22]. The standard deviations obtained in the fitting of the conditional stability constants are denoted by parenthesis.

of Cd(II) with glycine at pH 7.5. Fig. 3 compares the ASV voltammograms measured using the HMDE and MFE-RDE. In both cases, the addition of the ligand produces a shift of the signal to more negative potentials and very small changes in the peak height. This is consistent with Eqs. (19) and (20), taking into account the small size of the ligand. Fig. 4 shows the SCP chronopotentiograms obtained in the same kind of titration using a MFE-RDE, which ensures a stripping regime of total depletion, and using a HMDE with high oxidation currents, which produces a linear diffusion regime. In both cases, and in both t vs. E and dt/dE vs. E plots, a similar trend to that observed by ASV is noticed: waves or peaks change their height/area ratios slightly and they move progressively towards more negative potentials.

Fig. 5 shows the Leden function of order 0 computed from Eqs. (20) (ASV data), (21) (SCP data using HMDE) and (22) (SCP data using MFE-RDE) and also the corresponding functions of order 1 (Eq. (23)). Despite the expected low influence in the final result, the small variations of the size of the signals have been taken into account keeping the term ϕ in the equations above. In ASV, ϕ is computed as the ratio of peak heights, considering the use of a DP oxidative scan. In SCP, ϕ is assumed to be the ratio of the areas under the baseline-corrected peaks in the dt/dE vs. E plot, as recommended for the elimination of capacitive currents [9]. The linearity of the Leden functions of order 1 suggests the presence of two successive complexes: ML and ML_2.

Table 1 contains the values of the stability constants adjusted from these plots and corrected for side-reactions of glycine protonation in the form:

$$\log \beta_1 = \log \beta'_1 + \log \alpha_L, \tag{24}$$

$$\log \beta_2 = \log \beta'_2 + 2 \log \alpha_L, \tag{25}$$

where β_1, β_2 are the overall stability constants of ML and ML_2 complexes, respectively, β'_1, β'_2 are the corresponding conditional stability constants (these are adjusted from F_1 under the conditions of the experiment) and α_L is the side reaction coefficient for glycine, given by

$$\alpha_L = 1 + [H^+]/K_{a2} + [H^+]^2/(K_{a1}K_{a2}). \tag{26}$$

The values of the acidity constants of glycine, $pK_{a1} = 2.35$ and $pK_{a2} = 9.76$, have been taken from the literature [22].

Table 1 shows that the values found for both stability constants using ASV and SCP in a MFE-RDE are quite similar to each other and reasonably close to the values obtained by DPP and by potentiometry [22]. The ASV and SCP measurements using the HMDE provide sta-

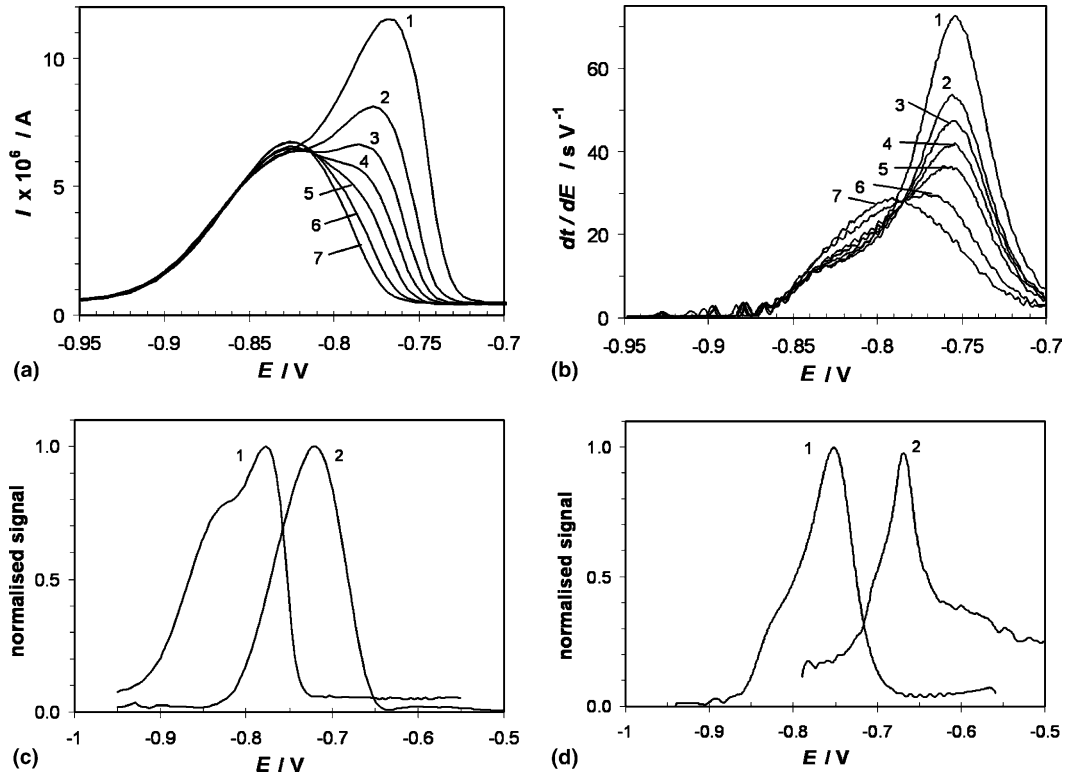

Fig. 6. Signal splitting effects observed during the titration of a solution containing 10^{-6} mol l^{-1} of Cd(II) and 0.01 mol l^{-1} of KNO_3 with a PMA solution at a degree of dissociation $\alpha_d = 0.7$ and pH 7.2 using a deposition time of 120 s. Influence of the ligand excess: signals obtained in a MFE-RDE by ASV (a) and constant-current SCP at $I_{ox} = 10^{-6}$ A (b) at ligand-to-metal ratio 98 (1), 126 (2), 153 (3), 180 (4), 207 (5), 260 (6) and 338 (7). Effect of the technique and the kind of electrode: ASV (c) or SCP (d) measurements in MFE-RDE (1) or HMDE (2) at a metal-to-ligand ratio of 153.

bility constants not too different, but somewhat lower than such values.

4.3. Study of the Cd^{2+}–PMA system as a model of macromolecular labile complexes with electrodic adsorption

The Cd^{2+}–PMA system presents an important induced adsorption of the metal onto the electrode, as proved by the presence of maxima in normal pulse polarograms [23]. This presence has been confirmed under the conditions of the present study (data not shown).

ASV and SCP measurements have been carried out during the titration of solutions containing 10^{-6} mol l^{-1} of Cd(II) with PMA with a degree of neutralisation of 0.7 at pH 7.2. In preliminary experiments it was found that, under certain conditions, ASV and SCP signals could be split into two partly overlapping peaks. Fig. 6 contains some examples of such splitting. This phenomenon can be observed even in the absence of electrodic adsorption and is explained in terms of a lack of excess of the ligand in the vicinity of the electrode surface during the stripping step [9]. The peak at more negative potentials would correspond to the metal oxidised to form a complex with the ligand in solution and the peak at more positive potentials (very close to that of the free metal in the absence of the ligand) would be produced by the oxidised metal that cannot be complexed because of the local deficiency of ligand. In Fig. 6, this is confirmed by the fact that PMA additions decrease the weight of the signal at more positive potentials (that of the unclomplexed metal). Additional experiments have proved that the increase of the total metal concentration or the deposition time increase the importance of that peak, also in agreement with such an explanation.

The signal splitting is more important for the MFE-RDE than for the HMDE, as depicted in Fig. 6. This is quite logical, considering that the oxidation in a MFE is more effective than in a HMDE because the reduced metal atoms practically do not have to diffuse in the mercury to be oxidised on the surface. Thus, a higher local excess of oxidised metal can be formed, as the oxidation becomes mass-transfer controlled, favouring signal splitting in MFE as compared to HMDE. When comparing the results of ASV and SCP, it is not clear which technique is most affected by this problem, since it depends essentially on the time taken by the stripping process (determined among other factors by the scan rate in ASV and the oxidation current in SCP). Moreover, it was found that the application of solution stirring during the stripping step produces a decrease of the signal splitting, probably because of the improvement of the slow mass transport of the macromolecular ligand to the electrode.

In spite of previous work that ensures a minimum effect of signal splitting in SCP when τ is measured as the area under the dt/dE curve [24], for comparison purposes the above-mentioned titrations were repeated under electrochemical conditions that ensured the absence of such a phenomenon (higher ligand excess and solution stirring during the stripping step in RDE-MFE). In the case of SCP at MFE-RDE, experiments were done at two levels of oxidation current and stirring rate during the stripping step in order to explore the influence of such parameters on the results. Moreover, a titration at a higher concentration level of the metal was made by RPP, a technique that has proved to be quite insensitive to electrodic adsorption when limiting currents are considered [25] (half-wave potentials, however, can be affected by that). Figs. 7 and 8 show the voltammograms and chronopotentiograms, respectively, measured in these experiments, and Fig. 9 shows the corresponding ϕ vs. c_L^* and F_0 vs. c_L^* plots computed in the same way as for the Cd–glycine system. The fitting of Eqs. (19), (21), (22) to these data produces the values of the stability constant K shown in Table 2. In the case of ϕ data, the value of $p = 2/3$ has been applied in the

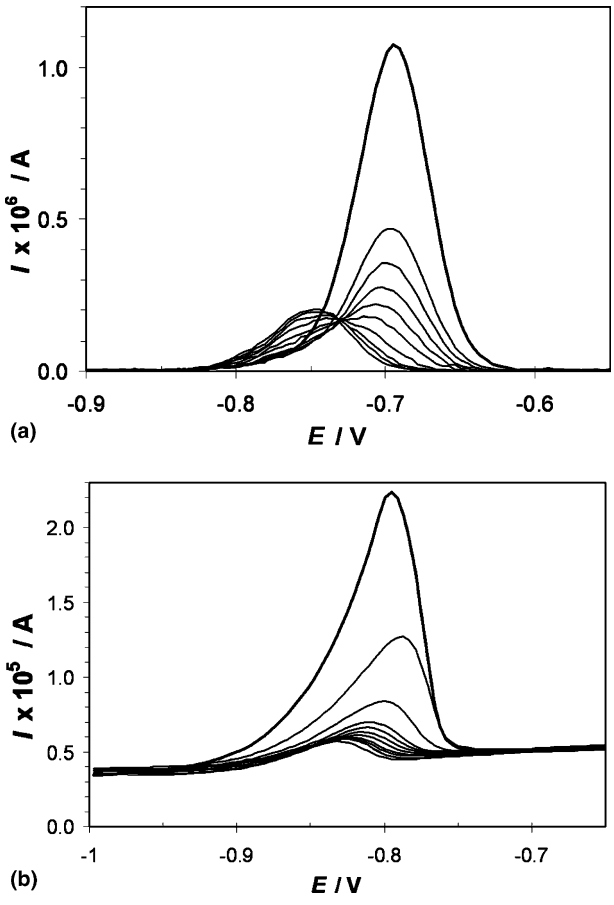

Fig. 7. Voltammograms measured by ASV in a HMDE (a) and in a MFE-RDE (b) during the titration of a solution containing 10^{-6} mol l^{-1} of Cd(II) and 0.01 mol l^{-1} of KNO_3 with a PMA solution at a degree of dissociation $\alpha_d = 0.7$ and pH 7.2 (ligand-to-metal ratio from 0 to 370) using a deposition time of 120 s and, for RDE, solution stirring during the stripping step (500 rpm). The initial signals measured in the absence of PMA are denoted with a thicker line.

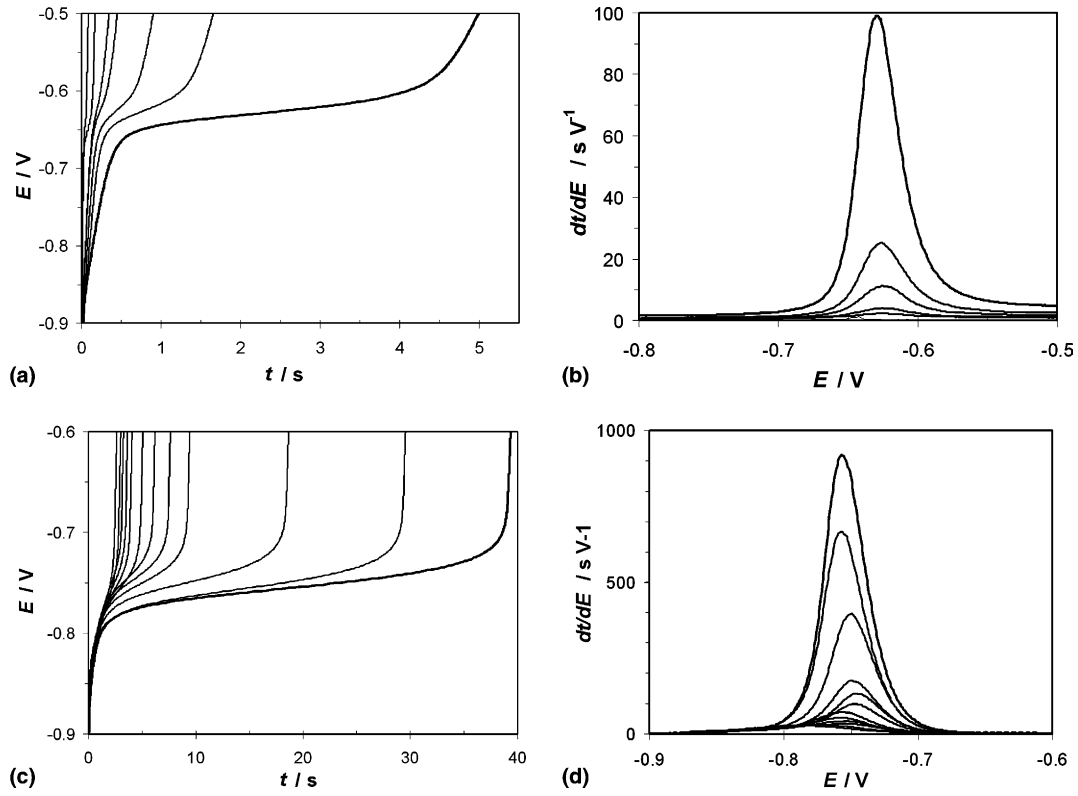

Fig. 8. Chronopotentiograms measured by SCP in a HMDE at $I_{ox} = 10^{-9}$ A (a, b) and in a MFE-RDE at $I_{ox} = 10^{-6}$ A (c, d) during the titration of a solution containing 10^{-6} mol l^{-1} of Cd(II) and 0.01 mol l^{-1} of KNO_3 with a PMA solution at a degree of dissociation $\alpha_d = 0.7$ and pH 7.2 (ligand-to-metal ratio from 0 to 370) using a deposition time of 120 s and, for RDE, solution stirring during the stripping step (500 rpm). (a) and (c) show the original chronopotentiograms and (b) and (d) the corresponding derivatives of time with respect to potential. The initial signals measured in the absence of PMA are denoted with a thicker line.

fitting of Eq. (19) to both ASV and SCP (total depletion) titration curves, and the value of $\varepsilon = 0.004$, optimised by fitting the RPP titration curves, has been fixed in all cases (the value of the diffusion coefficient provided by BDH is quite imprecise and does not take into account conformational changes).

The analysis of Table 2, despite the notorious dispersion of some results, suggests a reasonable agreement of the log K values determined from ϕ data in most experiments (especially when ε is fixed), and larger discrepancies in the values computed from Leden functions, i.e., considering potential shifts. This means, on the one hand, that the capabilities of SCP in the minimisation of adsorption are comparable to these of ASV with both HMDE and MFE electrodes and, on the other hand, that the potential shifts in ASV and SCP can be seriously affected by adsorption. Nevertheless, in the case of SCP, the "anomalous" behaviour of potential shifts can also be due to other reasons. It must be noted that the peak potential in SCP is affected by many experimental variables as, for instance, the deposition time [24,26]. In this sense, further tests with ultramicroelectrodes should be done, since, according to Town and van Leeuwen [27], they can significantly reduce the peak potential variability.

Finally, the comparison of the log K values obtained from SCP titrations in MFE-RDE under different experimental conditions shows that the best results (these closer to ASV and RPP values) were obtained using relatively high oxidation currents (10^{-6} A) and low stirring rates during the stripping step (500 rpm). This seems to be related to the interference of dissolved oxygen: stirring favours the transport of oxygen towards the electrode and low currents increase the duration of the stripping. Then, oxygen arrives faster to the electrode surface and has more time to chemically oxidise a part of the reduced metal, which decreases the transition time.

5. Conclusions

The facts described so far suggest us the following conclusions:

Constant-current-SCP appears to be a valuable alternative to the more widespread ASV, as suggested by the results obtained by both techniques on Cd–glycine and Cd–PMA systems. In the study of the first system, data are computed exclusively from potential shifts. Thus, the agreement between ASV and SCP results suggests that the peak potential in the SCP analysis of

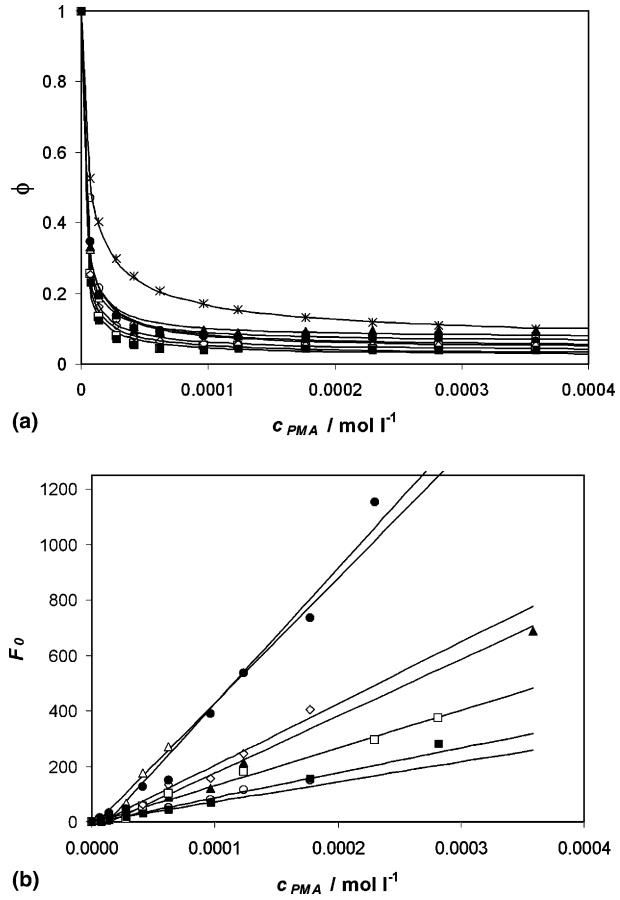

Fig. 9. Plots of ϕ and F_0 functions vs. the concentration of PMA obtained from the ASV and SCP signals shown in Figs. 7 and 8 plus those coming from an additional titration by RPP. Solid lines denote the curves fitted using Eqs. (19)–(23). RPP in SMDE (∗), ASV in HMDE (△), ASV in MFE-RDE (○), SCP in HMDE $I_{ox} = 10^{-9}$ A (▲), SCP in MFE-RDE $I_{ox} = 10^{-6}$ A, 500 rpm (●), SCP in MFE-RDE $I_{ox} = 10^{-6}$ A, 2500 rpm (□), SCP in MFE-RDE $I_{ox} = 10^{-9}$ A, 500 rpm (◇), SCP in MFE-RDE $I_{ox} = 10^{-9}$ A, 2500 rpm (■).

non-adsorbing labile complexes could be employed in the DeFord–Hume method according to Eqs. (21) or (22). In the study of Cd–PMA system, there is an acceptable agreement between ASV and SCP data obtained from stripping currents and transition times, whereas results obtained from potential shifts are quite different. This confirms, as in previous work, the unreliable character of ASV and SCP peak potentials in macromolecular systems including electrodic adsoption. Furthermore, it must be pointed out that, in the present study, SCP results are no better than those of ASV, which suggests further tests with systems suffering from stronger electrodic adsorption in order to confirm whether SCP is less adsorption-sensitive than ASV.

The application of SCP in HMDE presents the advantage of a great experimental simplicity and reproducibility. However, it suffers from the nondefinition of the hydrodynamic conditions during the deposition step (which requires, as in HMDE-ASV, the use of an empirical parameter p) and the dependence of the stripping regime on the oxidative current (large currents ensure semi-infinite linear diffusion but yield too short transition times, whereas small ones ensure total depletion but also incur important interferences from dissolved oxygen). Moreover, for a drop area of 0.5 mm^2, the contribution of sphericity can be non-negligible, especially when working close to linear diffusion conditions.

As compared to the HMDE case, the use of SCP on MFE-RDE implies more difficulties in the preparation and use of the electrode but, in contrast, it provides important advantages. First, the hydrodynamic conditions allow the application of the Levich equation (which ensures a p parameter equal to 2/3) and, second, the total depletion regime (with a linear relationship between transition time and concentration) holds in a wide range of oxidation currents.

An important interferent in SCP is the dissolved oxygen, which cannot be totally removed from the cell. This oxygen seems to oxidise a portion of the metal reduced in the amalgam chemically, which competes with the electrochemical oxidation by the constant current and causes a decrease in the transition time. This problem can be minimised by combination of relatively

Table 2
Values of the ratios between diffusion coefficients (ε) and the stability constant (K) determined for the Cd(II)–PMA system at $\alpha_n = 0.7$, pH 7.2 and ionic strength 0.01 mol l^{-1} in KNO_3 by using different techniques and electrodes

Method	Fixed p	ε	$\log K(\phi)$	$\log K(\phi)$ fixed $\varepsilon = 0.004$	$\log K(F)$
RPP in SMDE	1/2	0.004 (0.001)	5.60 (0.01)	5.60 (0.01)	–
ASV in HMDE	2/3	0.008 (0.001)	5.84 (0.02)	5.83 (0.02)	6.65 (0.04)
ASV in MFE-RDE	2/3	0.015 (0.002)	5.95 (0.04)	5.80 (0.05)	5.95 (0.01)
SCP in HMDE, $I_{ox} = 10^{-9}$ A (total depletion)	2/3	0.010 (0.003)	5.84 (0.03)	5.80 (0.03)	6.69 (0.01)
SCP in MFE-RDE, $I_{ox} = 10^{-6}$ A, 500 rpm	2/3	0.020 (0.003)	5.89 (0.04)	5.79 (0.05)	6.29 (0.01)
SCP in MFE-RDE, $I_{ox} = 10^{-6}$ A, 2500 rpm	2/3	0.004 (0.002)	6.10 (0.05)	6.09 (0.04)	6.13 (0.02)
SCP in MFE-RDE, $I_{ox} = 10^{-9}$ A, 500 rpm	2/3	0.006 (0.001)	6.05 (0.02)	6.02 (0.02)	6.35 (0.03)
SCP in MFE-RDE, $I_{ox} = 10^{-9}$ A, 2500 rpm	2/3	0.003 (0.002)	6.16 (0.04)	6.17 (0.04)	5.99 (0.02)

In the table, $\log K(\phi)$ indicates data computed from Eq. (19) with a fixed value of p and adjustable or fixed ε (which is indicated) and $\log K(F)$ denotes data computed from Eqs. (21)–(23). The standard deviations obtained in the fitting of the different parameters are denoted by parenthesis.

large oxidation currents (producing not too long transition times) and low stirring rates (in order to make difficult the transport of oxygen to the electrode). In the case of MFE-RDE, good results have been obtained using current inside the range 10^{-9}–10^{-6} A and a rotation speed of 500 rpm.

When working with macromolecular ligands that are not in a large excess with respect to the metal ion, a double peak can be observed in both ASV and SCP. This is due to the lack of enough ligand to complex all the metal ions that are released by the oxidation of the amalgam. This problem is especially important in MFE-RDE. In order to minimise the appearance of double peaks, the ligand excess or the rotation rate of the electrode can be increased to make the signal of complexed metal predominant. Also, by increasing the deposition time, or without electrode rotation during the stripping step, the signal of the uncomplexed oxidised metal can be maximised. In this last situation, however, the DeFord–Hume approach for the analysis of potentials does not seem to be reliable. Anyway, working under total depletion conditions and computing stability constants exclusively from transition times measured as the area under the dt/dE plot should greatly minimise the problem of double peaks.

Acknowledgements

The authors gratefully acknowledge financial support from the Spanish Ministry of Science and Technology (Project BQU2000-0642-C03-01) and from the Generalitat de Catalunya (2001SGR-00056 Project). They also acknowledge Herman P. van Leeuwen (Iberdrola Visiting Professor for Science and Technology at the University of Barcelona for 6 months) and Raewyn Town for useful discussions and for being initiated into their pioneering work on speciation by SCP. Núria Serrano acknowledges the University of Barcelona for a Ph.D. grant.

References

[1] F. Vydra, K. Stulik, E. Julakova, Electrochemical Stripping Analysis, Ellis Horwood, Chichester, 1976.
[2] J. Wang, Stripping Analysis: Principles, Instrumentation and Applications, VCH, Deerfield Beach, 1985.
[3] M. Esteban, E. Casassas, Trends Anal. Chem. 13 (1994) 110.
[4] A.J. Bard, L.R. Faulkner, Electrochemical Methods. Fundamentals and Applications, second ed., Wiley, New York, 2001.
[5] J.M. Estela, C. Tomás, A. Cladera, V. Cerdà, Crit. Rev. Anal. Chem. 25 (1995) 91.
[6] D. Jagner, A. Graneli, Anal. Chim. Acta 83 (1976) 19.
[7] D. Jagner, Analyst 107 (1982) 593.
[8] M.L. Gozzo, L. Colacicco, C. Callà, G. Barbaresi, R. Parroni, B. Giardina, S. Lippa, Clin. Chim. Acta 285 (1999) 53.
[9] R.M. Town, H.P. van Leeuwen, J. Electroanal. Chem. 509 (2001) 58.
[10] R.M. Town, H.P. van Leeuwen, J. Electroanal. Chem. 523 (2002) 1.
[11] H.G. de Jong, H.P. van Leeuwen, K. Holub, J. Electroanal. Chem. 234 (1987) 1.
[12] H.G. de Jong, H.P. van Leeuwen, J. Electroanal. Chem. 234 (1987) 17.
[13] H.G. de Jong, H.P. van Leeuwen, J. Electroanal. Chem. 235 (1987) 1.
[14] M. Esteban, H.G. de Jong, H.P. van Leeuwen, Int. J. Environ. Anal. Chem. 38 (1990) 75.
[15] J.M. Díaz-Cruz, C. Ariño, M. Esteban, E. Casassas, J. Electroanal. Chem. 333 (1992) 33.
[16] D.D. DeFord, D.N. Hume, J. Am. Chem. Soc. 73 (1951) 5321.
[17] D.R. Crow, Polarography of Metal Complexes, Academic Press, London, 1969.
[18] J.M. Díaz-Cruz, M. Esteban, M.A.G.T. van den Hoop, H.P. van Leeuwen, Anal. Chim. Acta 264 (1992) 163.
[19] R.F.M.J. Cleven, Ph.D. Thesis, Agricultural University, Wageningen, 1984.
[20] A.I. Vogel, Textbook of Quantitative Chemical Analysis, fifthe ed., Longman, London, 1989.
[21] D. Jagner, M. Josefson, S. Westerlund, K. Årén, Anal. Chem. 53 (1981) 1406.
[22] A.E. Martell, R.M. Smith, Critical Stability Constants, Amino-acids, vol. 1, Plenum Press, New York, 1976.
[23] J. Puy, F. Mas, J.M. Díaz-Cruz, M. Esteban, E. Casassas, Anal. Chim. Acta 268 (1992) 261.
[24] R.M. Town, H.P. van Leeuwen, J. Electroanal. Chem. 535 (2002) 11.
[25] J. Galceran, D. Reñé, J. Salvador, J. Puy, M. Esteban, F. Mas, J. Electroanal. Chem. 375 (1994) 307.
[26] R.M. Town, H.P. van Leeuwen, J. Electroanal. Chem. 535 (2002) 1.
[27] R.M. Town, H.P. van Leeuwen, J. Electroanal. Chem. 523 (2002) 16.

8.2 Suitability of stripping chronopotentiometry for heavy metal speciation using hygrogen peroxyde as oxidant: application to the Cd(II)-EDTA-PMA system

N. Serrano, M.M. Gómez-Boadas, J.M. Díaz-Cruz, F. Berbel, C. Ariño, M. Esteban.

Electroanalysis 17 **(2005)** 2201-2207

Full Paper

Suitability of Stripping Chronopotentiometry for Heavy Metal Speciation Using Hydrogen Peroxide as Oxidant: Application to the Cd(II)-EDTA-PMA System

Núria Serrano, Maria del Mar Gómez-Boadas, José Manuel Díaz-Cruz, Francisco Berbel, Cristina Ariño, Miquel Esteban*

Departament de Química Analítica, Facultat de Química, Universitat de Barcelona, Av. Diagonal 647, E-08028 Barcelona, Spain
*e-mail: josemanuel.diaz@ub.edu

Received: May 10, 2005
Accepted: July 15, 2005

Abstract
The possibilities of stripping chronopotentiometry (SCP) for heavy metal speciation have been tested in the modality of chemical oxidation using the model systems Cd(II)-polyacrylic acid (PMA), Cd(II)-EDTA and Cd(II)-PMA-EDTA. The use of 0.03% H_2O_2 as a chemical oxidant provides reliable results from transition times, but peak potentials are dramatically affected by the presence of this reagent. The study suggests that chemical-oxidation SCP can be a technique complementary to other stripping modalities in the study of inert and macromolecular labile metal complexes.

Keywords: Stripping chronopotentiometry (SCP), Potentiometric stripping analysis (PSA), Heavy metal speciation, Oxygen peroxide, Cadmium

DOI: 10.1002/elan.200503350

1. Introduction

Stripping techniques are useful tools for the analysis of heavy metal ions in environmental and biological samples [1, 2]. The most widespread modality is anodic stripping voltammetry (ASV), which is based on the reduction of the metal ion to form an amalgam in a mercury electrode (deposition step), a resting period to achieve an homogeneous distribution of the metal inside the mercury and, finally, the metal reoxidation during an anodic potential scan where the current is registered as a function of potential (stripping step). However, many problems have been reported in their application, mainly related to the adsorption of different species onto the electrode.

Stripping Chronopotentiometry (SCP), also named Potentiometric Stripping Analysis (PSA) [3, 4], is usually performed on mercury electrodes and includes a deposition step identical to that of ASV and a stripping step where the accumulated metal is reoxidized by the action of a chemical oxidant or by imposing a constant current. Both SCP modalities measure the evolution of the potential as a function of time and use the transition time (that between two consecutive potential jumps) as the main analytical parameter. SCP has been extensively applied to the determination of total amounts of heavy metals in biological samples, since it has been empirically proved to be less sensitive to the presence of organic matter than ASV. However, few attempts have been made to exploit the interesting features of SCP in the field of heavy metal speciation.

Recently, Town and van Leeuwen successfully applied constant-current SCP (CCSCP) in a hanging mercury drop electrode (HMDE) to heavy metal speciation [5–9]. They also developed a SCP modality at scanned deposition potential (SSCP) which appears to be especially useful in the presence of electrodic adsorption, electrochemical irreversibility and/or heterogeneous complexation [10, 11]. A further work [12] showed the usefulness of the mercury film rotating disk electrode (MFE-RDE) in the application of CCSCP to heavy metal speciation.

As a complement of such studies, the present work tests the possibilities of the SCP modality based on chemical oxidation for heavy metal speciation. This SCP mode, as compared to CCSCP, appears to be more problematic, but it has also potential advantages: it is available in practically all commercial potentiostats and is less sensitive to the interference of dissolved oxygen. Although acceptable results had already been obtained in quite simple systems using the widespread oxidant Hg(II) [13], our main challenge is to find a suitable chemical oxidant that does not modify metal speciation in a significant way. This is why Hg(II) or the less popular Fe(III) or Ce(IV) [14, 15] have not been considered (Hg-, Fe- and Ce-ions can displace the analyzed metal from their complexes). Taking into account the promising results obtained by Soares et al. [16] using $KMnO_4$ in the SCP study of some Pb(II) complexes, the research of additional suitable oxidants has been focused in another "anionic" reagent such as $K_2Cr_2O_7$, already used for nonspeciation studies [17], and also in "non metallic" oxidants like O_2 or H_2O_2. It must

be noted that in the case of $K_2Cr_2O_7$ (in a similar way as for permanganate), the eventual interference of Cr(III)-ions resulting from dichromate reduction should not be discarded. As a first approach to heavy metal speciation, the model system Cd(II)-EDTA-polymethacrylate (PMA) has been considered, which yields a mixture of a practically inert complex (Cd(II)-EDTA) free from electrodic adsorption plus a labile macromolecular complex (Cd(II)-PMA) which tends to adsorb onto the electrode surface [18].

2. Theory

Let us consider a heavy metal ion M which can be bound in solution to a ligand L and reversibly reduced in a mercury electrode:

$$\begin{array}{c} \mathrm{M} + m\mathrm{L} \underset{\beta_m}{\rightleftharpoons} \mathrm{ML}_m \\ ne^- \uparrow\downarrow \\ \mathrm{M(Hg)} \end{array} \quad (1)$$

In this scheme, electrical charges have been omitted for the sake of simplicity and β_m denotes the overall complexation constant for the species ML_m:

$$\beta_m = c^*_{\mathrm{ML}m}/c^*_{\mathrm{M}}\ (c^*_{\mathrm{L}})^m \quad (2)$$

where c^*_i stands for the bulk concentration of i species.

When using a HMDE, in both ASV and SCP the concentration $c_{\mathrm{M(Hg)}}$ of reduced M in the amalgam at the end of the deposition step is given by [19]:

$$c_{\mathrm{M(Hg)}} = k\ t_{\mathrm{d}}\ \bar{D}^p\ c^*_{\mathrm{M,lab}} \quad (3)$$

where k is a constant depending on several experimental parameters, t_d is the deposition time, $c^*_{M,lab}$ is the total concentration of metal in free plus labile forms, p is a parameter related to the hydrodynamic conditions (quite close to 2/3 in practice) and $\bar{D}$ is the average diffusion coefficient of the metal in solution. When association–dissociation equilibria are slow as compared to the measurement time (inert situation) $c^*_{M,lab}$ and $\bar{D}$ equal the concentration and the diffusion coefficient of the free metal ion, c^*_M and D_M, respectively. When complexation equilibria are fast (labile situation) $c^*_{M,lab}$ equals the total concentration of metal c^*_{TM} and $\bar{D}$ can be computed as a weighted average of the diffusion coefficients of the different metal species [20–22]:

$$\bar{D} = (c^*_{\mathrm{M}}/c^*_{\mathrm{TM}})\ \mathrm{D_M} + \Sigma_m\ (c^*_{\mathrm{ML}m}/c^*_{\mathrm{TM}})\ D_{\mathrm{ML}m} \quad (4)$$

with D_i denoting the diffusion coefficient of the species i.

In SCP the stripping step consists of a smoothed change in the potential as the metal is being stripped to the solution delimited by two sharp potential changes. The transition time τ between both potential jumps for the case of chemical stripping can be roughly described by the equation [4, 23]:

$$\tau = k'\ t_{\mathrm{d}}\ c_{\mathrm{M,lab}}/c^*_{\mathrm{ox}} \quad (5)$$

where k' is again a constant and c^*_{ox} is the bulk concentration of the chemical oxidant.

In the voltammetric study of metal complexes the usual strategy is based on the comparison of the currents and peak potentials measured for the metal in the presence and in the absence of the ligand [20–22]. Thus, in the case of ASV, a normalized current ϕ_{ASV} can be defined, according to Equations 3–6, as:

$$\begin{aligned}\phi_{\mathrm{ASV}} &= I_{\mathrm{ASV}}(\text{with L})/I_{\mathrm{ASV}}(\text{without L}) = \\ &= c_{\mathrm{M(Hg)}}(\text{with L})/c_{\mathrm{M(Hg)}}(\text{without L}) = (\bar{D}/D_{\mathrm{M}})^p\end{aligned} \quad (6)$$

When SCP is used, an analogous normalized parameter ϕ_{SCP} can be defined as a ratio between transition times. Thus, according to Equation 5, such parameter can also be related to the ratio between diffusion coefficients:

$$\begin{aligned}\phi_{\mathrm{SCP}} &= \tau(\text{with L})/\tau(\text{without L}) = \\ &= c_{\mathrm{M(Hg)}}(\text{with L})/c_{\mathrm{M(Hg)}}(\text{without L}) = (\bar{D}/D_{\mathrm{M}})^p\end{aligned} \quad (7)$$

Then, it is expected that ϕ_{SCP} values verify the same relationship as ϕ_{ASV} values with respect to the ligand concentration. When labile complexes are formed with low-size ligands, ϕ_{SCP} should remain very close to 1. If complexes are inert, ϕ_{SCP} should be equal to the free metal fraction:

$$\phi_{\mathrm{SCP}}(\text{inert complexes}) = c^*_{\mathrm{M}}/c^*_{\mathrm{TM}} \quad (8)$$

If the complexes are macromolecular and labile, Equation 4 holds and, in the case of 1:1 stoichiometry, ϕ values should verify the equation by de Jong et al. [20–22]:

$$\begin{aligned}&\phi_{\mathrm{SCP}}(\text{macromolecular labile complexes}) = \\ &= (1 + \varepsilon\ K\ c^*_{\mathrm{TL}})^p/(1 + K\ c^*_{\mathrm{TL}})^p\end{aligned} \quad (9)$$

where K is the stability constant of the 1:1 complex and ε is the ratio between the diffusion coefficients of the complex and the free metal ion ($= D_{ML}/D_M$).

Concerning to potentials, it has been postulated the validity of the DeFord–Hume method [24] for ASV data according to the expression:

$$F_0 = \exp\ (-nF/RT\ \Delta E_{\mathrm{ASV}} - \ln\ \phi_{\mathrm{ASV}}) = 1 + \Sigma_i\ \beta_i\ (c^*_{\mathrm{L}})^i \quad (10)$$

where F_0 is the Leden function of zero order and ΔE_{ASV} is the potential shift (usually negative) caused by the addition of the ligand to the free metal ion. Further experimental work confirmed empirically the validity of such approach in the absence of electrodic adsorption [25]. By analogy with the ASV case, we postulate the applicability of Equation 10 to the peak potential shifts (ΔE_{SCP}) found in dt/dE vs. E plots substituting ϕ_{ASV} by ϕ_{SCP}, in a similar way as for constant–current SCP under total depletion regime [12]:

$$F_0 = \exp\ (-nF/RT\ \Delta E_{\mathrm{SCP}} - \ln\ \phi_{\mathrm{SCP}}) = 1 + \Sigma_i\ \beta_i\ (c^*_{\mathrm{L}})^i \quad (11)$$

When a 1:1 labile macromolecular complex and a more stable 1:1 inert complex coexist, the following equations

have been deduced and experimentally verified for polarographic measurements [26]:

$$\phi = \left(\frac{1+\varepsilon K_{\mathrm{lab}}\, c^*_{\mathrm{TLlab}}}{1+K_{\mathrm{lab}}\, c^*_{\mathrm{TLlab}}}\right)^{p} \frac{1}{2K_{\mathrm{in}}\, c^*_{\mathrm{TM}}} \{-(1+K_{\mathrm{lab}}\, c^*_{\mathrm{TLlab}} + K_{\mathrm{in}}(c^*_{\mathrm{TLin}} - c^*_{\mathrm{TM}})) + [(1+K_{\mathrm{lab}}\, c^*_{\mathrm{TLlab}} + K_{\mathrm{in}}(c^*_{\mathrm{TLin}} - c^*_{\mathrm{TM}}))^2 + 4K_{\mathrm{in}}\, c_{\mathrm{TLin}}(1+K_{\mathrm{lab}} c_{\mathrm{TLlab}})]^{1/2}\} \quad (12)$$

$$F_0 = 2\,K_{\mathrm{in}}\, c^*_{\mathrm{TM}}\big(1+K_{\mathrm{lab}}\, c^*_{\mathrm{TLlab}}\big)/ \{-\big(1+K_{\mathrm{lab}}\, c^*_{\mathrm{TLlab}} + K_{\mathrm{in}}\big(c^*_{\mathrm{TLin}} - c^*_{\mathrm{TM}}\big)\big) + \big[\big(1+K_{\mathrm{lab}}\, c^*_{\mathrm{TLlab}} + K_{\mathrm{in}}\big(c^*_{\mathrm{TLin}} - c^*_{\mathrm{TM}}\big)\big)^2 + 4\,K_{\mathrm{in}}\, c^*_{\mathrm{TM}}\big(1+K_{\mathrm{lab}}\, c^*_{\mathrm{TLlab}}\big)\big]^{1/2} \quad (13)$$

with $p = 1/2$, K_{lab} and K_{in} being the corresponding stability constants for the labile and inert complexes, c^*_{TLlab} and c^*_{TLin} as the total concentration of each kind of ligand, c^*_{TL} as the sum $c^*_{\mathrm{TLlab}} + c^*_{\mathrm{TLin}}$ and ε denoting the ratio between the diffusion coefficients of the labile complex and the free metal ion. In the present work we postulate the validity of Equations 12 and 13 with the value $p = 2/3$ for ASV and (chemical-oxidation) SCP measurements.

3. Experimental

3.1. Reagents

Cd(II) stock solutions 10^{-2} mol L^{-1} were prepared from $Cd(NO_3)_2 \cdot 4H_2O$ and standardized complexometrically [27]. Stock solutions of the ligands were prepared from the disodium salt of ethylenediaminotetraacetic acid, EDTA, ($C_{10}H_{14}N_2Na_2O_8 \cdot 2H_2O$) by Merck and a solution of 20% of polymethacrylic acid (PMA) by BDH. They were further standardized by complexometric [27] or conductometric acid–base titration, respectively. The rest of reagents used were analytical grade. Potassium hydroxide (Merck) was used for the partial neutralization of PMA solutions, potassium nitrate (Merck) was employed as the supporting electrolyte, hydrogen peroxide (30% solution, Panreac) and potassium dichromate (Panreac) were tested as suitable oxidants and mercury(II) chloride (Merck) was employed to form the mercury film on the glassy carbon rotating disk electrode. Ultrapure water (Milli-Q plus 185 system, Millipore) was used in all experiments.

3.2. Apparatus

Differential pulse anodic stripping voltammetry (DPASV) and stripping chronopotentiometry (SCP) measurements were performed in an Autolab System PGSTAT20 (EcoChemie, The Netherlands) attached to a Metrohm 663 VA Stand (Metrohm, Switzerland) and a personal computer with GPES4 data acquisition software (EcoChemie). The system was also connected to a Crison micropH 2000 pH-meter for monitoring the pH value during the experiments. All the measurements were carried out in a glass cell at constant room temperature (25 °C) under a purified nitrogen atmosphere (Air Liquide). Additions of solutions were carried out by means of micropipettes Nichiryo.

In all cases the reference electrode, to which all potentials are referred, was Ag | AgCl | KCl (3 mol L^{-1}) and the counter electrode was a glassy carbon electrode. In some experiments, the working electrode used was a multimode electrode Metrohm producing drops of ca. 0.5 mm^2 surface that could work as an HMDE. In other experiments, a mercury film deposited on a glassy carbon rotating disk electrode (Metrohm) of 2 mm diameter (MFE-RDE) was used (see below).

Pulse amplitudes of 50 mV and pulse times of 50 ms were applied in (DP)ASV stripping scans. In both SCP and ASV a deposition potential of −0.95 V was applied during 90 s in the case of HMDE and 50 s in the case of MFE-RDE. Equilibration periods of 30 and 5 s were applied for HMDE and MFE-RDE, respectively. The usual rotating speed of MFE-RDE was 1500 rpm.

Conductometric titrations of PMA solutions were carried out by means of a conductometer Orion 120 attached to a cell with constant 1.03 cm^{-1} and to an automatic burette 665 Dosimat Metrohm for the addition of KOH standard solution.

3.3. Preparation of the Mercury Film on the MFE-RDE

Prior to the deposition of the film, the glassy carbon disk was polished using a suspension of alumina particles of 300 nm diameter. Then, the electrode was attached to the stand and immersed into 20 ml of a solution containing 200 mg L^{-1} of $HgCl_2$ and 0.1 mol L^{-1} of HCl. After deaeration of the solution for 10 min, a deposition potential of −0.5 V was applied for 2 min with solution stirring, followed by a rest period (without stirring) of 30 s. Then, both deposition and resting periods were repeated at −0.6, −0.7, −0.8 and −0.9 V and, finally, three further times at −0.9 V. Once the mercury film had been deposited, the three electrodes were rinsed with water and the mercury solution could be replaced in the cell by that which was to be measured. This procedure, which partially modifies a previous methodology [28] has proven to produce mercury films that can be used over one day without degradation.

3.4. Voltammetric and Chronopotentiometric Titrations

Each titration started by placing in the cell 25 ml of a solution containing 1.0×10^{-6} mol L^{-1} of Cd(II) and 0.01 mol L^{-1} of KNO_3 and, for SCP measurements, the

corresponding concentration of the chemical oxidant ($K_2Cr_2O_7$ or H_2O_2). Then, the sample was deaerated with pure nitrogen for 20 min and a scan was recorded in order to determine the current and the peak potential in the absence of ligands. Further, aliquots of a solution containing EDTA (at pH 8.0), PMA partially neutralized with KOH (at pH 8.0, which produces deprotonation of 80% of carboxylic groups) or a mixture of both (also at pH 8.0) were added and the respective curves were recorded. In the case of SCP, the transition time was measured as the area under the baseline-corrected dt/dE plot, which minimizes the contribution of capacitive currents and other secondary effects [5]. All solutions were deaerated and stirred for 1 min after each addition. In some SCP experiments where oxygen was used as chemical oxidant, the sample was not deaerated and a flow of air was passing through the solution during a controlled time after each SCP measurement. The pH of the solutions prior to ligand titration was adjusted to 7–8 adding small volumes of a KOH solution. In order to prevent changes in ionic strength, the solution to be added contained the same concentration of KNO_3 as that in the cell.

4. Results and Discussion

4.1. Selection of a Proper Chemical Oxidant Using Cd(II) and Cd(II)-PMA Systems

The ideal oxidant for SCP heavy metal speciation should be enough effective to dissolve the metal from the amalgam but still relatively weak (or slow) in order to avoid a significant oxidation of the complexing agents present in the solution. Moreover, it should not produce cations that could displace heavy metal ions from their complexes in the sample.

In principle, the easiest way to achieve these goals would be to use the dissolved oxygen already existing in the nondeaerated sample. However, some tentative experiments with Cd(II) solutions in KNO_3 medium showed a very poor reproducibility of SCP signals that could be attributed to unpredictable variations in the (quite low) concentration of dissolved oxygen which, according to Equation 5, strongly influences transition times. Such variations are, in fact, a balance between the oxygen consumed in the stripping step and the oxygen incoming from the air. Several attempts were made passing a continuous flow of air through the solution before each measurement, but a satisfactory reproducibility could not be achieved.

In contrast, a good reproducibility was observed when using $K_2Cr_2O_7$ or H_2O_2 in SCP measurements of Cd(II) + KNO_3 solutions in a wide range of oxidant concentrations. Then, in order to test the possible influence of both reagents on heavy metal speciation, several titrations of Cd(II) with PMA were carried out by SCP using different concentrations of each chemical oxidant and the results were compared to those collected in ASV titrations carried out under the same conditions but, obviously, in the absence of the oxidant. These experiments showed that the use of moderate concentrations of H_2O_2, around 0.03%, in SCP produces ϕ vs. c^*_{TL} plots similar to these obtained by ASV that can be fitted to Equation 9 to produce log K and ε values quite coincident to the corresponding ASV values (Fig. 1 and Table 1). However, as discussed later, potential shifts were quite disperse and this hindered the calculation of log K using Equation 11. In the case of $K_2Cr_2O_7$, it was not possible to find oxidant concentrations suitable to produce regular-shaped ϕ vs. c^*_{TL} nor F_0 vs. c^*_{TL} curves to fit Equations 5 and 11. As Figure 1 shows, a typical ϕ vs. c^*_{TL} plot obtained with dichromate decreases more slowly with c^*_{TL} than the ones measured by ASV and H_2O_2-SCP (quite coincident with each other) and for large concentrations approaches zero and not the limiting value ε^p predicted by Equation 5. This distorted shape makes impossible the fitting of the mentioned equation to obtain reliable values for log K and ε and suggests that the presence of dichromate significantly affects the complexation equilibria between Cd(II) and PMA. Then, it was concluded that the use of 0.03% of H_2O_2 as a chemical oxidant was the best choice to test the possibilities of SCP in more complex systems.

4.2. Application of SCP with H_2O_2 to the System Cd(II) + EDTA + PMA

After passing the test with a typical labile macromolecular complex like Cd(II)-PMA, a further step in the study of the applicability of H_2O_2-SCP to heavy metal speciation should include a more involved system like Cd(II)-EDTA-PMA, that is expected to contain a mixture of an inert complex (Cd(II)-EDTA) and a labile macromolecular complex (Cd(II)-PMA).

In fact, the long time scale of SCP measurements (of the order of the deposition time) makes difficult to ensure the inert behavior of the complex along the titration. Previous investigations on the Cd(II)-EDTA system reported that the contribution of the kinetic current due to complex dissociation can be important in polarography [29, 30] and, especially, in stripping voltammetry [31]. The complex dissociation takes place through a protonated form:

$$CdHEDTA^- \underset{k_a}{\overset{k_d}{\rightleftharpoons}} Cd^{2+} + HEDTA^{3-} \qquad (14)$$

where k_a, k_d are the association and dissociation rate constants, respectively. For these constants, Kim and Birke [29] determined the values $k_d = 16.8\ s^{-1}$ and $k_a = 8.1 \times 10^9\ L\ mol^{-1}\ s^{-1}$. Using these values and taking the deposition time (90 s) as the time scale t of the measurements, it is possible to make a rough prediction of the kinetic behavior by applying the lability criterion by de Jong et al. [20–22]. In a first step, the product $k_d\,t$ (ca. 1500, quite higher than 1) suggests that the kinetic regime would be closer to the dynamic situation than to the static one. In a second step, the lability criterion compares the kinetic flux coming from complex dissociation (J_{kin}) with the diffusional flux of the free metal (J_{dif}):

$$J_{kin}/J_{dif} = k_d/(k_a\, c^*_{TL})^{1/2}\, (D_{ML}/D_M)^{-1/2}\, t^{1/2} \quad (15)$$

where c^*_{TL} is the total bulk concentration of the ligand (mostly in the form $HEDTA^{3-}$ at pH values close to 8) and D_{ML}, D_M are the diffusion coefficients of the complex and the free metal ion (very similar). In our particular case, and for $c^*_{TL} = 10^{-6}$ mol L^{-1} (10^{-9} mol cm^{-3}) the computation of the ratio between fluxes yields a value of ca. 50, which is too small to ensure lability but too large to produce an inert behavior. Thus, a nonlabile or quasi-inert complex is expected whose dissociation can be enough important during the deposition step to produce a noticeable increase of the stripping signals and a shift to more negative potentials. However, we should not forget that the criterion holds for a large ligand excess (which is not always fulfilled in this work) and semi-infinite linear diffusion (when the regime of the deposition process is closer to convective diffusion).

After several experiments with the Cd(II)-EDTA system, it was found that at pH values close to 8.0 the influence of the complex dissociation on the stripping signal was quite small, as proved by the little shift in the potential of the free metal peak (in most of cases, smaller than 5 mV). It is possible that pH values higher than 8.0 would still produce lower dissociation effects, but they were not considered to prevent the formation of Cd(II) hydroxycomplexes.

Figure 2 summarizes the ϕ titration curves measured by HMDE-ASV (a), HMDE-SCP (b) and MFE-SCP (c) after successive additions into a Cd(II) solution of the ligands EDTA and PMA separately and both together at pH 8.0. The experimental points obtained for the Cd(II)-PMA system are compared to the curve fitted from Eqn. 9, showing a good agreement. The points measured for the Cd(II)-EDTA system are compared to the predictions made for a conditional stability constant $\log K' = 14.2$ at pH 8.0 [32].

As Figure 2 shows, there is a good agreement in the beginning of the titration but some deviations appear when approaching the 1:1 Cd/EDTA ratio (in the graph $c_{TL} = 2.08 \times 10^{-5}$ mol L^{-1} in terms of the total ligand concentration in the EDTA/PMA mixture). This suggests a progressive dissociation of the inert complex as the ligand concentration increases, which is supported by a significant shift of the peak of the free metal in the ending part of the titration (Fig. 3a). This is in apparent contradiction with the lability criterion above, which predicts an increase of the inert character as the ligand concentration increases, but may be explained considering that most of the titration is carried out

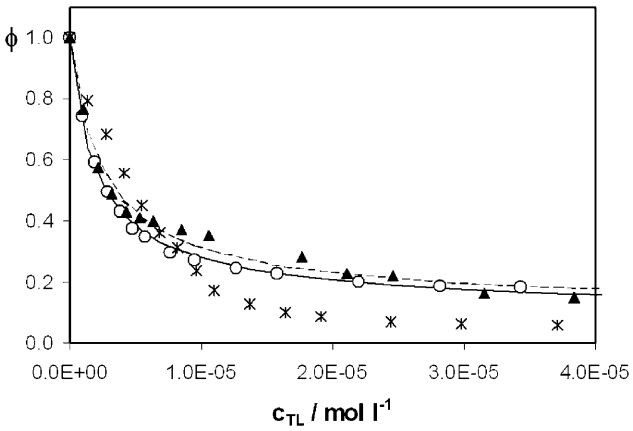

Fig. 1. Normalized signals (ϕ) as a function of total ligand concentration obtained in titrations of 1×10^{-6} mol L^{-1} Cd(II) solutions with PMA at pH 8.0 in the presence of KNO_3 0.01 mol L^{-1} by means of ASV (○), SCP in HMDE with $K_2Cr_2O_7$ 1×10^{-5} mol L^{-1} (*) and SCP in HMDE with H_2O_2 0.03% (▲). Lines denote the fitted curves according to Equation 9.

in excess of Cd(II) with respect to EDTA. Then, the lower proportion of the complex as compared to the free metal can make negligible the contribution of the complex dissociation to the current as compared to the (convective) diffusion of the free metal ion. When EDTA additions lead to an excess of both ligand and complex with respect to the free metal, the kinetic contribution starts to be significant and agrees with the predictions of the lability criterion in the case of ligand excess.

Finally, the data measured for the system Cd(II)-PMA-EDTA are compared to the predictions of Equation 12 using the values of ε and $\log K$(Cd-EDTA), $\log K$(Cd-PMA) previously determined. For all three stripping modalities, a good agreement can be observed during most of the titration and only small deviations can be detected in the same regions where the Cd(II)-EDTA complex do not behave as a totally inert system.

The evolution of the peak potentials is summarized in Figure 3. In ASV, the presence of EDTA practically does not change the peak position until the last additions, where the negative potential shift suggests noticeable kinetic effects. In contrast, the presence of PMA alone or mixed with EDTA causes an important potential shift towards more negative potentials. From a qualitative point of view, this fact agrees with the theoretical predictions. However, the fitting of Eq. (10) produces a too high $\log K$ value (Table 1),

Table 1. Stability constants ($\log K$) and ratio between diffusion coefficients (ε) computed from ϕ and F_0 data for the Cd(II)-PMA system at pH 8.0 (dissociation degree close to 0.8) in the presence of KNO_3 0.01 mol L^{-1} using different stripping techniques. The corresponding standard deviations are denoted by parenthesis.

Technique	ε	$\log K$ (ϕ)	$\log K$ (F_0)
ASV-HMDE	0.032 (0.004)	5.87 (0.02)	6.38 (0.01)
SCP-HMDE using 0.03% H_2O_2	0.03 (0.01)	5.76 (0.03)	–
SCP-MFE using 0.03% H_2O_2	0.05 (0.01)	5.82 (0.03)	–

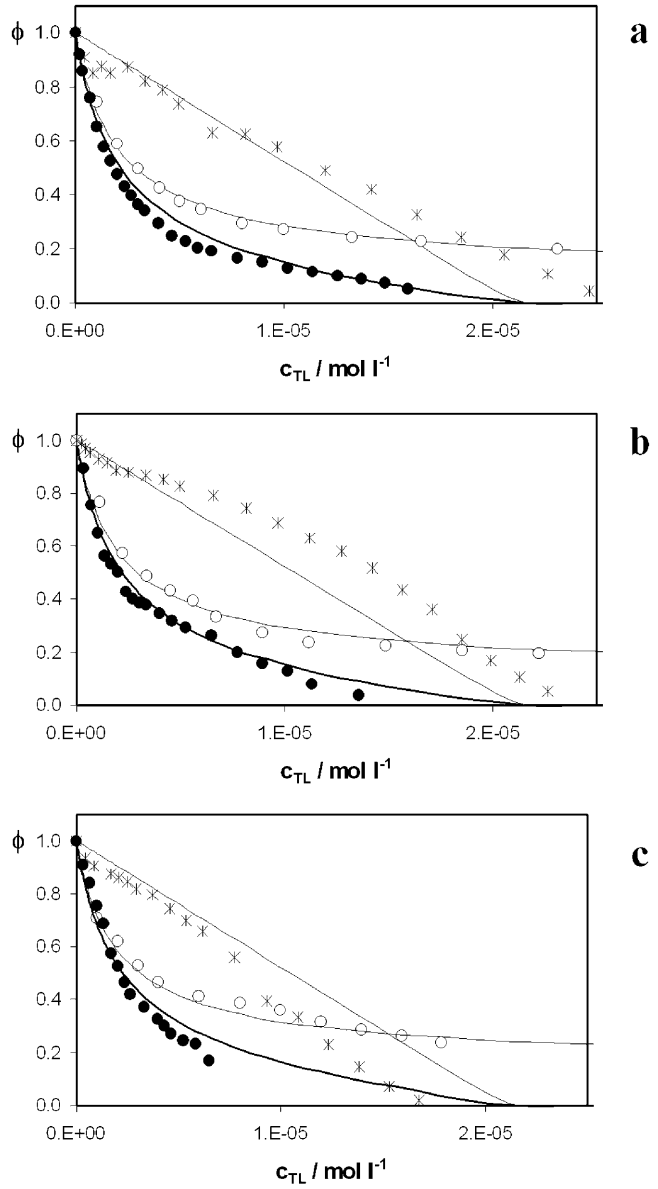

Fig. 2. Normalized signals (ϕ) as a function of total ligand concentration obtained in titrations of 1×10^{-6} mol L^{-1} Cd(II) solutions with EDTA (*), PMA (○) and a mixture of 4.8% of EDTA and 95.2% of PMA (●) in the presence of KNO_3 0.01 mol L^{-1} at pH 8.0. Measurements were made by ASV (a), SCP in HMDE with 0.03% H_2O_2 (b) and SCP in MFE-RDE with 0.03% H_2O_2 (c). Lines denote the fitted curves according to Equations 8, 9, and 12. For comparison purposes, in the case of EDTA or PMA alone c_{TL} has been computed as the total concentration of the mixture of ligands (4.8/95.2) necessary to provide the actual concentration of PMA or EDTA.

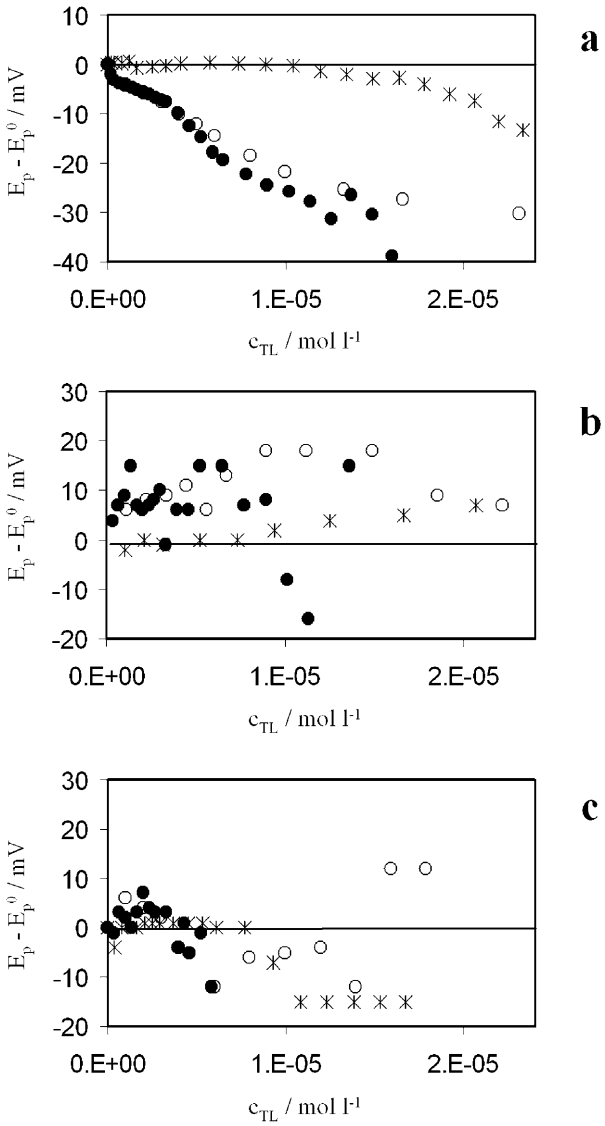

Fig. 3. Potential shifts as functions of the total ligand concentration obtained in titrations of 1×10^{-6} mol L^{-1} Cd(II) solutions with EDTA (*), PMA (○) and a mixture of 4.8% of EDTA and 95.2% of PMA (●) in the presence of KNO_3 0.01 mol L^{-1} at pH 8.0. Measurements were carried out by of ASV (a), SCP in HMDE with 0.03% of H_2O_2 (b), and SCP in MFE-RDE with 0.03% of H_2O_2 (c).

which is surely due to the well known problem of electrodic adsorption of the Cd(II)-PMA complex [18]. In a similar way as for reverse pulse polarography [33], the influence of electrodic adsorption on ASV currents seems to be much less important than in ASV potentials.

In the case of SCP measurements there is not a well-defined evolution of the peak potentials in any of the systems considered: quite often positive shifts are registered and, in general, there is a large dispersion of the potential shifts around zero or a value close to zero. This may be due to the contribution of the redox couple associated to hydrogen peroxyde to the electrode potential during the metal reoxidation. Anyway, this undefinition makes impossible the use of SCP peak potentials for equilibrium calculations under the conditions of the present study.

5. Conclusions

The SCP modality which uses a chemical oxidant can be applied to heavy metal speciation if a proper reagent is

selected to ensure the metal reoxidation without disturbing the chemical equilibria of the metal ion in the sample. In the present work, this goal has been achieved for the three model systems Cd(II)-PMA, Cd(II)-EDTA and Cd(II)-PMA-EDTA by using 0.03% H_2O_2 as the chemical oxidant and by considering only the normalized area of the signals. In contrast, peak potentials appeared to be strongly affected by the presence of the chemical oxidant, so that they remained useless. This suggests that the use of H_2O_2-SCP should be restricted to inert or macromolecular labile systems where complexation can be monitories exclusively from the (important) decrease in signal areas. Another suitable application can be SSCP, where the characteristic curves containing information about metal speciation are built exclusively with SCP areas at different (scanned) deposition potentials.

In comparison with ASV, H_2O_2-SCP should be less sensitive to electrodic adsorption. Nevertheless, it must be noted that in the particular case of the Cd(II)-PMA system both techniques appeared to be equally good. Thus, it could happen that real differences are noticed only for much stronger adsorbing complexes.

In comparison with constant-current SCP (CCSCP), H_2O_2-SCP suffers from the risk of sample contamination by H_2O_2 impurities, the eventual oxidation of species in solution and the limited possibilities of playing with the duration of the stripping step (which in constant-current SCP can be easily done by varying the oxidation current among different orders of magnitude). As the main advantages, H_2O_2-SCP requires simpler (and cheaper) electroanalytical equipment than CCSCP, so that it is available in most commercial potentiostats, Additionally, it should be less sensitive to the interference of dissolved oxygen (its concentration will be much smaller than that of H_2O_2, which means a negligible contribution to chemical oxidation).

Finally, when compared to the previous results with $KMnO_4$ [16], the use of H_2O_2 as oxidative reagent seems to introduce stronger perturbations in the potential data. However, H_2O_2 has the advantages of not introducing additional metallic species like Mn(II), Mn(III) or Mn(IV) and of a quite lower oxidation power, which reduces the risk of oxidizing ligands present in the sample.

To summarize the previous considerations, we can conclude that chemical-oxidation SCP does not seem to be a powerful alternative to ASV or CCSCP in the field of heavy metal speciation. Anyway, it may be a complementary technique to overcome some of the limitations of ASV and CCSCP, especially if proper oxidative reagents, equally good or better than $KMnO_4$ or H_2O_2, are investigated.

6. Acknowledgements

The authors gratefully acknowledge financial support from the Spanish Ministry of Science and Technology (Project BQU2003-07587-C02-01) and from the Generalitat de Catalunya (2001SGR-00056 Project). Núria Serrano acknowledges the University of Barcelona for a Ph.D. grant.

7. References

[1] J. Wang, *Stripping Analysis: Principles, Instrumentation and Applications*, VCH, Deerfield Beach **1985.**
[2] M. Esteban, E. Casassas, Trends Anal. Chem. **1994**, *13*, 110.
[3] D. Jagner, A. Graneli, Anal. Chim. Acta **1976**, *83*, 19.
[4] J. M. Estela, C. Tomás, A. Cladera, V. Cerdà, *Crit. Rev. Anal. Chem.* **1995**, *25*, 91.
[5] R. M. Town, H. P. van Leeuwen, *J. Electroanal. Chem.* **2001**, *509*, 58.
[6] R. M. Town, H. P. van Leeuwen, *J. Electroanal. Chem.* **2002**, *523*, 1.
[7] R. M. Town, H. P. van Leeuwen, *J. Electroanal. Chem.* **2002**, *523*, 16.
[8] R. M. Town, H. P. van Leeuwen, *J. Electroanal. Chem.* **2002**, *535*, 1.
[9] R. M. Town, H. P. van Leeuwen, *J. Electroanal. Chem.* **2002**, *535*, 11.
[10] R. M. Town, H. P. van Leeuwen, *Environ Sci. Technol.* **2003**, *37*, 3945.
[11] R. M. Town, H. P. van Leeuwen, *Electroanalysis* **2004**, *16*, 458.
[12] N. Serrano, J. M. Díaz-Cruz, C. Ariño, M. Esteban, *J. Electroanal. Chem.* **2003**, *560*, 105.
[13] C. Labar, *Electrochim. Acta* **1993**, *38*, 807.
[14] C. Labar, R. Müller, L. Lamberts, *Electrochim. Acta* **1991**, *36*, 2103.
[15] X. Yuan-Hong, C. Tuen-Chi, M. Jin-Yuan, *Anal. Chim. Acta* **1989**, *222*, 263.
[16] H. M. V. M. Soares, A. A. N. Almeida, M. P. O. Castro, S. C. Pinho, M. T. S. D. Vasconcelos, *Analyst* **1998**, *123*, 1377.
[17] M. Fayyad, M. Tutunji, Z. Taha, *Anal. Lett.* **1988**, *21*, 1425.
[18] J. Puy, F. Mas, J. M. Díaz-Cruz, M. Esteban, E. Casassas, *Anal. Chim. Acta* **1992**, *268*, 261.
[19] M. Esteban, H. G. de Jong and H. P. van Leeuwen, *Int. J. Environ Anal. Chem.* **1990**, *38*, 75.
[20] H. G. de Jong, H. P. van Leeuwen, K. Holub, *J. Electroanal. Chem.* **1987**, *234*, 1.
[21] H. G. de Jong, H. P. van Leeuwen, *J. Electroanal. Chem.* **1987**, *234*, 17.
[22] H. G. de Jong and H. P. van Leeuwen, *J. Electroanal. Chem.* **1987**, *235*, 1.
[23] T. C. Chau, D. Y. Li, Y. L. Wu, *Talanta* **1982**, *29*, 1083.
[24] D. D. DeFord and D. N. Hume, *J. Am. Chem. Soc.* **1951**, *73*, 5321.
[25] J. M. Díaz-Cruz, M. Esteban, M. A.G. T. van den Hoop and H. P. van Leeuwen, *Anal. Chim. Acta* **1992**, *264*, 163.
[26] C. de Haro, F. Berbel, J. M. Díaz-Cruz, C. Ariño, M. Esteban, *J. Electroanal. Chem.* **1999**, *462*, 157.
[27] A. I. Vogel, *Textbook of Quantitative Chemical Analysis*, 5th ed., Longman, London **1989.**
[28] D. Jagner, M. Josefson, S. Westerlund, K. Årén, *Anal. Chem.* **1981**, *53*, 1406.
[29] M. H. Kim, R. L. Birke, *Anal. Chem.* **1983**, *55*, 1735.
[30] J. Gálvez, C. Serna, A. Molina, H. P. van Leeuwen, *J. Electroanal. Chem.* **1984**, *167*, 15.
[31] M. S. Shuman, G. P. Woodward Jr., *Anal. Chem.* **1973**, *45*, 2032.
[32] A. E. Martell, R. M. Smith, Critical *Stability Constants*, Vol. 1: *Amino Acids*, Plenum Press, New York **1974.**
[33] J. Galceran, D. Reñé, J. Salvador, J. Puy, M. Esteban, F. Mas, *J. Electroanal. Chem.* **1994**, *375*, 307.

8.3 Stripping chronopotentiometry and stripping voltammetry of mixtures of heavy metal ions producing close signals: the Cd(II)-Pb(II)-phthalate system

N. Serrano, J.M. Díaz-Cruz, C. Ariño, M. Esteban.

Electroanalysis 18 **(2006)** 955-964

Full Paper

Stripping Chronopotentiometry and Stripping Voltammetry of Mixtures of Heavy Metal Ions Producing Close Signals: The Cd(II)-Pb(II)-Phthalate System

Núria Serrano, *José Manuel Díaz-Cruz*,* *Cristina Ariño*, *Miquel Esteban*

Departament de Química Analítica, Facultat de Química, Universitat de Barcelona, Martí i Franquès 1-11, E-08028, Barcelona, Spain
*e-mail: josemanuel.diaz@ub.edu

Received: January 09, 2006
Accepted: March 08, 2006

Abstract
The effects of the proximity of the signals of two heavy metal ions in stripping voltammetry (SV) and constant-current stripping chronopotentiometry (SCP) is studied at mercury drop (HMDE) and mercury film (MFE) electrodes. For this purpose, the Cd(II)-Pb(II)-phthalate system is used, taking advantage of the approaching of the signals corresponding to Cd(II)-phthalate and Pb(II)-phthalate labile complexes as phthalate is added to mixtures of Cd(II) and Pb(II)-ions. The results are compared with those obtained by differential pulse polarography (DPP) and by stripping measurements on the Pb(II)-phthalate system alone, showing discrepancies in SCP data under nondepletive conditions and negligible differences in the other cases.

Keywords: Stripping chronopotentiometry (SCP), Anodic stripping voltammetry (ASV), Mercury film electrode (MFE), Hanging mercury drop electrode (HMDE), Multianalyte system, Heavy metal speciation

DOI: 10.1002/elan.200603492

1. Introduction

Stripping techniques are very effective in decreasing the detection limits of some elements by means of the combination of a deposition step where the analyte is accumulated onto the electrode and a stripping step where it is totally or partially dissolved from the electrode to the solution. The excellent detection limits achieved and the sensitivity to different chemical species have transformed these techniques into powerful tools for the analysis of heavy metal ions in environmental and biological samples [1, 2].

For heavy metal ions, the most widely used stripping technique is stripping voltammetry (SV), especially in the anodic stripping modality (ASV). It consists of the reduction of the metal ion to form an amalgam in a mercury electrode (deposition step) and the subsequent metal reoxidation by means of an anodic potential scan (stripping step). Then, the evolution of current as a function of potential is measured. Usually, an equilibration period between deposition and stripping steps is required to ensure a homogeneous distribution of the metal inside the mercury. Despite the widespread character of ASV, many problems have been reported in their application to samples containing organic matter, mainly due to adsorption of species onto the electrode.

Stripping chronopotentiometry (SCP), also known as potentiometric stripping analysis (PSA), was introduced by Jagner and Graneli as an alternative to ASV [3, 4]. It is usually performed on mercury electrodes and includes the same deposition and equilibration steps as in ASV and a stripping step where the accumulated metal is reoxidized by a chemical oxidant or by imposing a constant current. Both SCP modalities register the evolution of the potential with time and use the transition time between potential jumps as the analytical parameter. The empirical evidence that SCP is less sensitive to the presence of organic matter than ASV has stimulated its application for determining total amounts of heavy metals in foods, beverages and biological samples [4]. However, SCP has remained practically unused in the field of heavy metal speciation until the recent works by Town and van Leeuwen [5–9], who obtained valuable information from the SCP analysis of different metal complexes at a hanging mercury drop electrode (HMDE) and some ultramicroelectrodes (UME). The same authors have further developed a promising modality of the technique at scanned deposition potential (SSCP), which appears to be especially useful in the presence of electrodic adsorption, electrochemical irreversibility and/or heterogeneous complexation [10, 11]. A complementary work using mercury film rotating disk electrode (MFE-RDE) has also shown the interesting features of this electrode in metal speciation by SCP [12].

In this context, the present work considers a problem that can be encountered in the analysis of natural samples containing a mixture of different heavy metal complexes.

That is the simultaneous presence of two metal ions producing stripping signals so close that it is not possible to select an intermediate deposition potential enough negative to ensure the mass-transport controlled reduction of the more electropositive ion. Under these conditions, some problems arise which are characteristic of multimetal systems: the formation of intermetallic compounds and the ongoing reduction of the less electropositive metals during the stripping step (when the more electropositive metals are being reoxidized, the potential can be still sufficiently negative to carry on with the reduction of the less electropositive metals). In the case of constant current SCP, electroless oxidation can also take place: the (negative) reduction current due to ongoing reduction of the less electropositive metals can enhance the (positive) reoxidation current of the metal so that the overall stripping current remains constant. These phenomena have been analyzed by Town and van Leeuwen using SSCP for the case of Cd(II) in the presence of Zn(II)- and Cu(II)-ions in noncomplexing media, which produced quite well separated signals [13]. Among other considerations, they remark that these phenomena can be enhanced at increasing proportions of the more electropositive metal, that electroless oxidation has less impact at large oxidation currents and using UME, and that ongoing reduction of the less electropositive metals can be avoided by choice of a less negative deposition potential for their study. Nevertheless, when the signals of two metals are too close, it is not possible to select a proper deposition potential in the middle of both processes. Thus, the purpose of the present work is to evaluate empirically the impact of some of the above mentioned phenomena on the experimental results obtained on the model system Cd(II)-Pb(II)-phthalate by ASV and SCP at HMDE and MFE-RDE electrodes as compared to a simpler, nonstripping technique like differential pulse polarography (DPP). Additional stripping experiments have been carried out for the Pb(II)-phthalate systems in the absence of cadmium. As lead and cadmium do not form intermetallic compounds [14], the study will be mainly concerned with electroless oxidation/reduction reactions and ongoing reduction processes.

2. Theory

The situation of a metal ion M which can be complexed in solution by a ligand L and reversibly reduced at a mercury electrode can be summarized as:

$$\begin{array}{ccc} \mathrm{M} + m\,\mathrm{L} & \rightleftharpoons & \mathrm{ML}_m \\ n\mathrm{e}^- \uparrow\downarrow & & \\ \mathrm{M(Hg)} & & \end{array} \qquad (1)$$

where the electrical charges have been omitted for the sake of simplicity. The overall complexation constant for the species ML_m is denoted by β_m

$$\beta_m = c_{\mathrm{ML}m}{}^*/c_{\mathrm{M}}{}^* \; (c_L^*)^m \qquad (2)$$

where $c_i{}^*$ stands for the bulk concentration of species i.

In both ASV and SCP of labile complex systems, the concentration $c_{M(Hg)}$ of reduced M in the amalgam at the end of the deposition step is given by [5–7, 12]:

$$c_{\mathrm{M(Hg)}} = k\bar{D}^{\mathrm{p}} c_{\mathrm{TM}}{}^* \qquad (3)$$

where k is a constant depending on experimental conditions such as the deposition time or the stirring rate, $c_{TM}{}^*$ is the total concentration of metal, p is a parameter related to the hydrodynamic conditions (close to 2/3 in practice) and $\bar{D}$ is the average diffusion coefficient of the metal in solution. According to the model by de Jong et al. [15–17], $\bar{D}$ can be computed as a weighted average of the diffusion coefficients of the different metal species:

$$\bar{D} = (c_{\mathrm{M}}{}^*/c_{\mathrm{TM}}{}^*)\; D_{\mathrm{M}} + \Sigma_m \; (c_{\mathrm{ML}m}{}^*/c_{\mathrm{TM}}{}^*)\; D_{\mathrm{ML}m} \qquad (4)$$

with D_i denoting the diffusion coefficient of species i. Thus, for a system with ML and ML_2 complexes, Equation 4 becomes:

$$\bar{D} = D_M \left[\frac{1 + \varepsilon_1 \beta_1 \, c_L^* + \; \varepsilon_2 \beta_2 \, (c_L^*)^2}{1 + \beta_1 \, c_L^* + \beta_2 \, (c_L^*)^2} \right] \qquad (5)$$

where $\varepsilon_1 = D_{\mathrm{ML}}/D_{\mathrm{M}}$ and $\varepsilon_2 = D_{\mathrm{ML2}}/D_{\mathrm{M}}$.

As for the stripping step, in the case of ASV on MFE-RDE, a numerical solution has been found for the peak current I_{ASV} [18]:

$$I_{\mathrm{ASV}} = (n^2 F^2 v l A c_{\mathrm{M(Hg)}})/(2.7\; RT) \qquad (6)$$

with v the scan rate, l the film thickness and A the film surface. When ASV is carried out at a HMDE, several approaches have been proposed that, in general terms, predict a linear relationship between I_{ASV} and $c_{M(Hg)}$.

The stripping process in SCP takes place between two sudden potential changes: in the first one, the potential moves (according to a capacitive process) from the deposition value to that governed by the electrochemical equilibrium between M(Hg) and M; in the second one (again a capacitive process), the potential moves to new values given by a different redox couple, once the concentration of reduced metal on the electrode surface has virtually decreased to zero. Along the time comprised between both potential jumps, the potential smoothly changes as the metal is being stripped to the solution. Such time is termed transition time τ, and is the analytical parameter in SCP. In order to minimize the contribution of the capacitive current, τ is usually measured as a peak area in a derivative dt/dE vs. E plot [5]. When the constant current modality is used, two limiting situations are possible. For thick mercury films and large oxidation currents, the metal depletion from the mercury only affects the most external

layer of the electrode and the semi-infinite linear diffusion regime applies. Then, the Sand equation can be invoked to obtain [5]:

$$\tau^{1/2} = nFA\ D_{M(Hg)}{}^{1/2}\ \pi^{1/2}\ c_{M(Hg)}/(2\ I_{ox}) \quad (7)$$

with $D_{M(Hg)}$ denoting the diffusion coefficient of the reduced metal inside the mercury and I_{ox} the constant oxidation current. In contrast, the use of thin mercury films and small values of I_{ox} leads to the total depletion regime, which implies reoxidation of all the metal previously reduced to M(Hg). Then, equations for total electrolysis can be applied to obtain [5]:

$$\tau = nFAlc_{M(Hg)}/I_{ox} \quad (8)$$

In the voltammetric study of metal complexes the usual strategy is based on the comparison of the currents and peak potentials measured for the same total concentration of the metal in the presence and in the absence of the ligand. In the case of a transient voltammetric technique like DPP, a normalized current ϕ_{DPP} can be defined in the form [15–17]:

$$\phi_{DPP} = I_{DPP}\ (\text{with L})/I_{DPP}\ (\text{without L}) = (\bar{D}/D_M)^{1/2} \quad (9)$$

For the considered 1:1 and 1:2 stoichiometries (Equation 5), this expression can be transformed into the equation:

$$\phi_{DPP} = \left(\frac{\bar{D}}{D_M}\right)^{1/2} = \left(\frac{1+\varepsilon_1\beta_1 c_L^* + \varepsilon_2\beta_2 (c_L^*)^2}{1+\beta_1 c_L^* + \beta_2 (c_L^*)^2}\right)^{1/2} \quad (10)$$

Taking into account Equations 3–6, analogous expressions can be used for ASV by replacing 1/2 by 2/3:

$$\phi_{ASV} = I_{ASV}(\text{with L})/I_{ASV}(\text{without L}) = c_{M(Hg)}(\text{with L})/c_{M(Hg)}\ (\text{without L}) = (\bar{D}/D_M)^{2/3} \quad (11)$$

$$\phi_{ASV} = \left(\frac{\bar{D}}{D_M}\right)^{2/3} = \left(\frac{1+\varepsilon_1\beta_1 c_L^* + \varepsilon_2\beta_2 (c_L^*)^2}{1+\beta_1 c_L^* + \beta_2 (c_L^*)^2}\right)^{2/3} \quad (12)$$

When constant-current SCP is used, an analogous parameter ϕ_{SCP} can be defined as a ratio between transition times:

$$\phi_{SCP} = \tau\ (\text{with L})/\tau\ (\text{without L}) \quad (13)$$

In SCP, however, the relationship between ϕ and the diffusion coefficient ratio strongly depends on the stripping regime. For semi-infinite linear diffusion or total depletion, combination of Equations 3–5 with 7 and 8, respectively, produces:

$$\phi_{SCP}^{\text{linear diffusion}} = \left(\frac{c_{M(Hg)}(\text{with } L)}{c_{M(Hg)}(\text{without } L)}\right)^2 = \left(\frac{\bar{D}}{D_M}\right)^{4/3} = \left(\frac{1+\varepsilon_1\beta_1 c_L^* + \varepsilon_2\beta_2 (c_L^*)^2}{1+\beta_1 c_L^* + \beta_2 (c_L^*)^2}\right)^{4/3} \quad (14a)$$

$$\phi_{SCP}^{\text{total depletion}} = \left(\frac{c_{M(Hg)}(\text{with } L)}{c_{M(Hg)}(\text{without } L)}\right) = \left(\frac{\bar{D}}{D_M}\right)^{2/3} = \left(\frac{1+\varepsilon_1\beta_1 c_L^* + \varepsilon_2\beta_2 (c_L^*)^2}{1+\beta_1 c_L^* + \beta_2 (c_L^*)^2}\right)^{2/3} \quad (14b)$$

As for characteristic potentials, ASV follows the DeFord–Hume expression [19, 20]:

$$F_0 = \exp\ (-nF/RT\ \Delta E_{ASV} - \ln\ \phi_{ASV}) = 1 + \Sigma_i\ \beta_i\ (c_L^*)^i \quad (15)$$

where F_0 is the Leden function of zero order and ΔE_{ASV} is the potential shift caused by the addition of the ligand to the free metal ion.

By analogy with ASV, it has been empirically verified that Equation 15 also holds for the peak potential shifts (ΔE_{SCP}) found in dt/dE vs. E plots replacing ϕ_{ASV} by (i) $\phi_{SCP}{}^{1/2}$, in the case of semi-infinite linear diffusion (HMDE at high stripping currents), or by (ii) ϕ_{SCP}, in the case of total depletion (HMDE at low stripping currents and MFE-RDE) [12]:

$$F_0 = \exp\ (-n\text{F/R}T\ \Delta E_{SCP,\text{linear diffusion}} - 1/2\ \ln\ \phi_{SCP,\text{linear diffusion}}) = 1 + \Sigma_i\ \beta_i\ (c_L^*)^i \quad (16a)$$

$$F_0 = \exp\ (-n\text{F/R}T\ \Delta E_{SCP,\text{total depletion}} - \ln\ \phi_{SCP,\text{total depletion}}) = 1 + \Sigma_i\ \beta_i\ (c_L^*)^i \quad (16b)$$

It must be pointed out that in the case of total depletion there are some theoretical considerations which justify the validity of such approach, especially in the presence of a large excess of ligand over the metal and under conditions which render the characteristic SCP parameters (E_p and τ) independent of the deposition time [9].

3. Experimental

3.1. Reagents

All reagents used were Merck analytical grade. Solutions of phthalate were prepared from potassium hydrogenphthalate and partially neutralized with KOH until pH 5.5. Cd(II) and Pb(II) stock solutions 10^{-2} mol L^{-1} were prepared from $Cd(NO_3)_2\ .4H_2O$ and $Pb(NO_3)_2$ respectively and standardized complexometrically [22]. KNO_3 0.01 mol L^{-1} was employed as the supporting electrolyte. Ultrapure water (Milli-Q plus 185 system, Millipore) was used in all experiments. According to the literature [20], diffusion coefficients of Cd(II)- and Pb(II)-ions are 0.72×10^{-5} and 0.95×10^{-5} $cm^2\ s^{-1}$, respectively.

3.2. Apparatus

Differential pulse polarography (DPP), differential pulse anodic stripping voltammetry (DPASV) and constant-

current stripping chronopotentiometry (SCP) measurements were performed in an Autolab System PGSTAT20 (EcoChemie, The Netherlands) attached to a Metrohm 663 VA Stand (Metrohm, Switzerland) and a personal computer with GPES4 data acquisition software (EcoChemie). The system was also connected to a Metrohm 665 Dosimat for the addition of solutions and to an Orion SA 720 pH-meter for monitoring the pH value during the experiments. All the measurements were carried out in a glass cell at constant room temperature (25 °C) under a purified nitrogen atmosphere (Air Liquide).

In all cases the reference electrode, to which all potentials are referred, was Ag | AgCl | KCl (3 mol L^{-1}) and the counter electrode was a glassy carbon electrode. In some

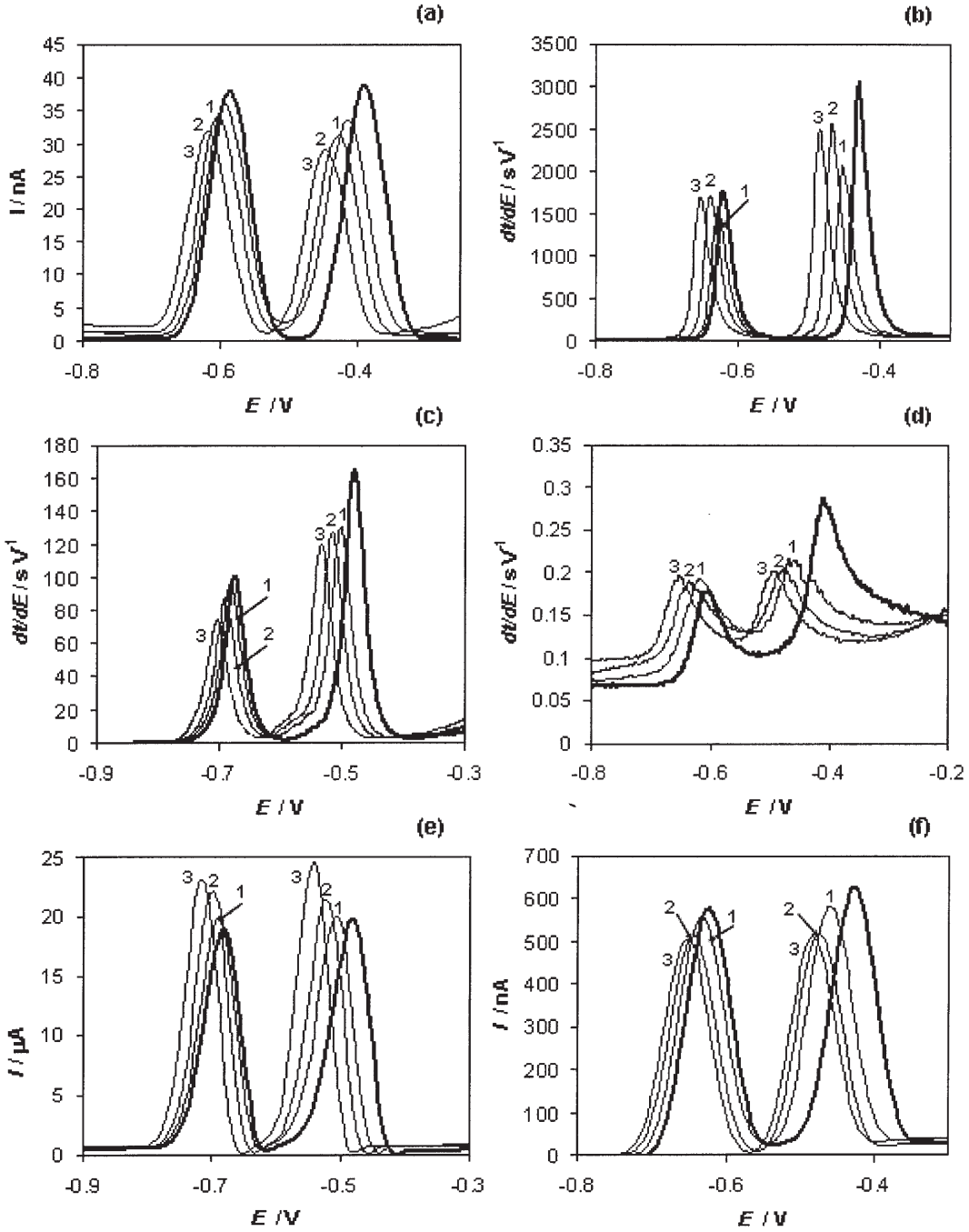

Fig. 1. Typical signals obtained by DPP in SMDE (a), SCP in HMDE at $I_{ox} = 10^{-9}$ A (b), SCP in RDE-MFE at $I_{ox} = 10^{-6}$ A (c), SCP in HMDE at $I_{ox} = 10^{-6}$ A (d), ASV in RDE-MFE (e), ASV in HMDE (f) for the system Cd(II)-Pb(II)-phthalate containing 1.0×10^{-6} mol L^{-1} of Cd(II) and Pb(II) in stripping techniques and 5.0×10^{-6} mol L^{-1} of each ion in DPP at pH 5.5 and 0.01 mol L^{-1} in KNO_3. Thicker lines denote voltammograms or chronopotentiograms in the absence of ligand. Signals denoted as 1, 2, and 3 were measured at ligand concentrations of 1.4×10^{-3}, 4.3×10^{-3}, and 1.5×10^{-2} mol L^{-1}, respectively.

experiments, the working electrode used was a multimode electrode Metrohm producing drops of ca. 0.5 mm^2 surface that could work as an HMDE or as a static mercury drop electrode (SMDE). In other experiments, a mercury film deposited on a glassy carbon rotating disk electrode (Metrohm) of 2 mm diameter (MFE-RDE) was used (see below).

Drop times of 0.8 s, pulse times of 40 ms and scan rates of 5 mV s^{-1} were used in all polarographic measurements, when not otherwise indicated. Pulse amplitudes of 50 mV were applied in DPP and DPASV stripping scans. In both SCP and DPASV a deposition potential of -0.85 V was applied during 60 s with solution stirring (HMDE) or electrode rotation (MFE). Some preliminary tests at different deposition times showed that 60 s was a good compromise which avoids amalgam saturation and provides reliable potential shifts according to the requirements of reference [9]. In the case of the HMDE, a rest period of 30 s was performed between the deposition and the stripping steps at the same deposition potential but in the absence of stirring. This was not necessary in MFE. The rotating speed of MFE-RDE was 1500 rpm.

3.3. Preparation of the Mercury Film on the MFE-RDE

Prior to the deposition of the film, the glassy carbon disk was polished using a suspension of alumina particles of 300 nm diameter. Then, the electrode was attached to the stand (together with the reference and auxiliary electrodes) and immersed into 20 mL of a solution containing 200 mg L^{-1} of $HgCl_2$ and 0.1 mol L^{-1} of HCl. After deaeration of the

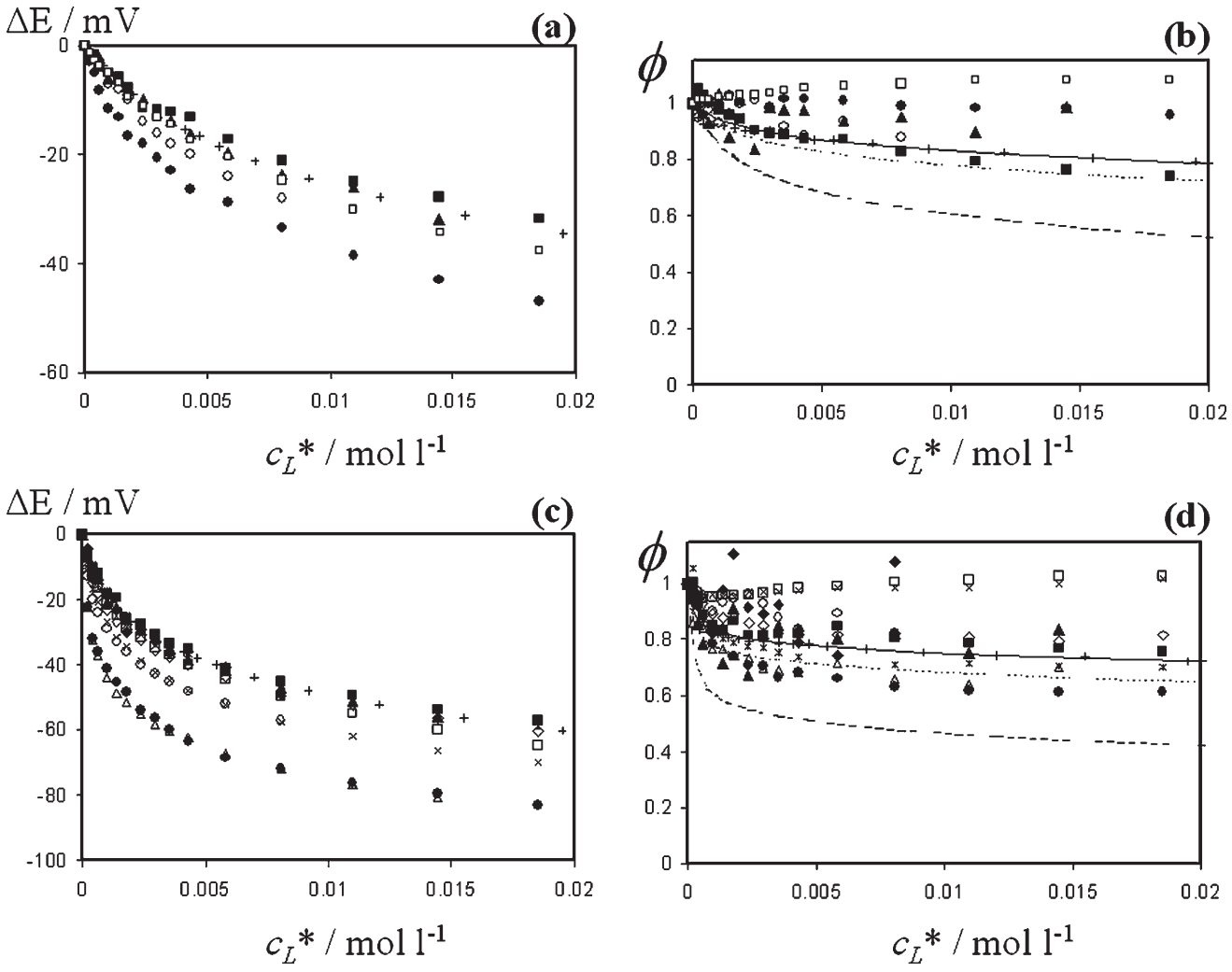

Fig. 2. Potential shifts ΔE (a, c) and normalized currents ϕ (b, d) measured for Cd(II) (a, b) and Pb(II) (c, d) ions as functions of the total ligand concentration in the bulk c_L^* along the titration of a mixture of both metals with phthalate solution under the conditions described in Figure 1. Lines reproduce the curve fitted to DPP data using Equation 10 (—) and the simulated curves for stripping measurements according to Equations 12, 14a, and 14b for an exponential parameter 2/3 (·····) or 4/3 (– – – –). DPP (+), ASV in HMDE (○), ASV in MFE-RDE (□), SCP in HMDE with $I_s = 10^{-6}$ A (●), SCP in HMDE with $I_s = 10^{-9}$ A (▲), SCP in MFE-RDE with $I_s = 10^{-6}$ A (■), ASV in HMDE for Pb(II) only (◇) , ASV in MFE-RDE for Pb(II) only (×) , SCP in HMDE for Pb(II) only with $I_s = 10^{-6}$ A (△), SCP in HMDE for Pb(II) only with $I_s = 10^{-9}$ A (◆), SCP in MFE-RDE for Pb(II) only (∗).

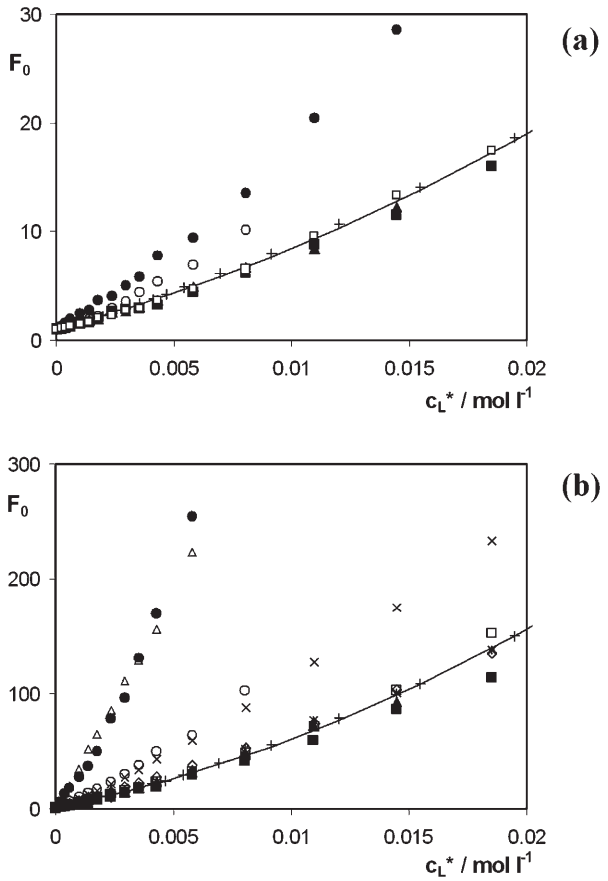

Fig. 3. Computed values of the Leden function of zero order (F_0) obtained from the signals of Cd(II) (a) and Pb(II) (b) versus the total concentration of phthalate (c_L^*) in the stripping experiments shown in Figures 1 and 2. Solid lines reproduce the curve fitted to the DPP data. DPP (+), ASV in HMDE (○), ASV in MFE-RDE (□), SCP in HMDE with $I_s = 10^{-6}$ A (●), SCP in HMDE with $I_s = 10^{-9}$ A (▲), SCP in MFE-RDE with $I_s = 10^{-6}$ A (■), ASV in HMDE for Pb(II) only (◇) , ASV in MFE-RDE for Pb(II) only (×) , SCP in HMDE for Pb(II) only with $I_s = 10^{-6}$ A (△), SCP in HMDE for Pb(II) only with Is = 10^{-9} A (◆), SCP in MFE-RDE for Pb(II) only (∗).

solution for 10 min, a deposition potential of −0.5 V was applied for 2 min with solution stirring, followed by a rest period (without stirring) of 30 s. Then, both deposition and resting periods were repeated at −0.6, −0.7, −0.8 and −0.9 V and, finally, three further times at −0.9 V. Once the mercury film was deposited, the three electrodes were rinsed with water and the mercury solution was replaced in the cell by that to be measured. This procedure, which partially modifies a previous methodology [23] has proven to produce mercury films that can be used over one day without noticeable degradation.

3.4. Voltammetric and Chronopotentiometric Titrations

Each titration started by placing in the cell 25 mL of a solution containing Cd^{2+} and/or Pb^{2+} ions and 0.01 mol L^{-1} of KNO_3. Then, the sample was deaerated with pure nitrogen for 10 min and a scan was recorded. Further, aliquots of phthalate were added and the respective curves were recorded. In the study about cadmium-to-lead ratio, additions of a Pb(II) solution were made to both a solution containing Cd(II) or just the supporting electrolyte. In the case of SCP, the transition time was measured as the area under the baseline-corrected dt/dE plot which, according to previous work [5], minimizes the contribution of capacitive currents and other secondary effects. All solutions were deaerated and mechanically stirred for 1 min after each addition. The initial pH of the metal solution was near to 5.5 in all experiments and the further additions of "self-buffered" phthalate solution ensured pH values very close to 5.50, as proved by the pH monitoring along the whole titration. Comparison of Cd(II) and Pb(II) signals registered at pH 5.5 and at more acidic pH proved that undesired phenomena like metal hydrolysis or losses by metal adsorption onto cell walls were not significant.

4. Results and Discussion

Figure 1 compares the evolution of the signals obtained by different techniques and electrodes along the titration of a solution containing Pb(II)-ions or a mixture of Cd(II)- and Pb(II)-ions with a large excess of phthalate at pH 5.5. Figure 2 shows the evolution of peak potentials and peak currents (i.e, ΔE vs. c_L^* and ϕ vs. c_L^* plots, respectively). The qualitative behavior is similar in all techniques: the signals of both metals decrease slightly and progressively shift towards more negative potentials. This is consistent with the expected formation of electrochemically labile complexes with diffusion coefficients smaller but still similar to those of free metal ions. Anyway, the most interesting feature is that the higher stability of Pb(II) complexes causes larger potential shifts than in the case of Cd(II), which produces a progressive decreasing of the separation between the two signals as the phthalate concentration increases (usually, from 200 to 160 mV). This behavior may hinder independent stripping measurements for each metal ion if there is not a suitable deposition potential between both peaks to provide mass transport-controlled deposition of lead without noticeable reduction of cadmium. In this situation, the analysis of both metals has to be restricted to the same stripping run, with a possible increase of cadmium-lead interferences that will be evaluated in the present work.

For this purpose, it is useful to compare with the DPP titration set which is, obviously, free from these effects related to deposition and stripping. Figure 2 shows that the potential shifts measured by stripping techniques are quite consistent and similar to DPP data, except for SCP under linear diffusion conditions (HMDE, $I_{ox} = 10^{-6}$ A), which presents larger ΔE values. As for the normalized currents (ϕ), they are more disperse, inside the range between the DPP values and 1. The fitting of Equation 10 to the DPP ϕ vs. c_L^* curves with simultaneous optimization of β_1, β_2, ε_1 and ε_2 does not produce reliable results and the same is true when applying Equations 12 and 14 to the other curves. This may

Table 1. Stability constants determined for the Cd(II)-phthalate and Pb(II)-phthalate systems in cadmium-lead mixtures (1×10^{-6} mol L^{-1} of each metal-ion in stripping experiments and 5×10^{-6} mol L^{-1} in DPP) and for Pb(II) alone at pH 5.5 and 0.01 mol L^{-1} KNO_3 using different techniques and electrodes. The standard deviations obtained in the fitting and some literature data are also shown.

Method	Cd(II)-phthalate				Pb(II)-phthalate			
	$\log \beta_1$	S.D.	$\log \beta_2$	S.D	$\log \beta_1$	S.D.	$\log \beta_2$	S.D.
DPP SMDE (Cd + Pb)	2.94	0.01	4.58	0.01	3.79	0.01	5.64	0.01
ASV HMDE (Cd + Pb)	3.08	0.03	5.03	0.07	4.07	0.01	5.75	0.03
ASV HMDE (Pb only)					3.93	0.01	5.37	0.01
SCP HMDE 10^{-6} A (Cd + Pb)	3.28	0.02	5.03	0.02	4.72	0.02	6.36	0.08
SCP HMDE 10^{-6} A (Pb only)					4.69	0.01	6.41	0.03
SCP HMDE 10^{-9} A (Cd + Pb)	2.91	0.03	4.72	0.08	3.80	0.03	5.70	0.05
SCP HMDE 10^{-9} A (Pb only)					3.74	0.05	5.85	0.11
ASV MFE-RDE (Cd + Pb)	2.96	0.01	4.64	0.01	3.76	0.01	5.74	0.01
ASV MFE-RDE (Pb only)					4.15	0.02	5.63	0.02
SCP MFE-RDE 10^{-6} A (Cd + Pb)	2.89	0.02	4.60	0.02	3.81	0.01	5.40	0.02
SCP MFE-RDE 10^{-6} A (Pb only)					3.91	0.02	5.46	0.04
Literature data at 0.1 mol L^{-1} of ionic strength [24]	2.78 [a]		4.76 [a]		3.40 [b]		–	
Previous literature data corrected to 0.01 mol L^{-1} of ionic strength by Davies equation	3.28		5.26		3.90			
Literature data at 1 mol L^{-1} of ionic strength	1.86 [c]		2.88 [c]		2.78 [c]		4.01 [c]	

[a] Reference [25], $NaNO_3$ 0.1 mol L^{-1} 25 °C.
[b] Reference [26], KNO_3 0.1 mol L^{-1} 25 °C.
[c] Reference [27],1 mol L^{-1} 25 °C.

be due to the low decrease of currents along the titration (low sensitivity) and to the excessive number of parameters which interact with each other during the optimization. As discussed later, the fitting significantly improves when the stability constants are fixed using the values computed from F_0 vs. c_L^* curves.

The calculation of the Leden function F_0 (Fig. 3) combines the contributions of both potentials and currents and defines three main groups of data: i) SCP measurements for Pb(II) and Cd(II) + Pb(II) samples in HMDE at $I_{ox} = 10^{-6}$ A, which produce F_0 values quite higher than those obtained by DPP; ii) some ASV measurements yielding slightly higher F_0 values as compared to DPP; and iii) the rest of stripping measurements (a large majority), that are very similar to the DPP case. Figure 3 shows the fitting of Equation 15 to the F_0 vs. c_L^* data measured by DPP for Cd(II)- and Pb(II)-ions. In both cases a good fitting is obtained using a second degree polynomial, which confirms the presence of ML and ML_2 complexes and allows the evaluation of the corresponding stability constants β_1 and β_2 (Table 1). In a similar way, all F_0 vs. c_L^* titration curves measured by stripping techniques can be fitted to a second degree polynomial using Equations 16a and 16b, which produces the set of stability constants shown in Table 1 together with DPP results and some data from Literature. It must be pointed out that the values in Table 1 have been corrected for the protonation of phthalate at pH 5.5 by means of the values of the protonation constants (determined at zero ionic strength) $\log \beta_{p1} = 5.41$ and $\log \beta_{p2} = 8.36$ [27]. These values have been extrapolated to ionic strength 0.01 mol L^{-1} by using the Davies equation, thus yielding $\log \beta_{p1} = 5.23$ and $\log \beta_{p2} = 8.09$, which produces a side reaction coefficient $\log \alpha = 0.19$ at pH 5.5. Using this correction, the stability constants determined in this work are not too far from the literature data, despite the differences in ionic strength. It must be noted that the larger phthalate additions (up to 0.02 mol L^{-1}) substantially modify the ionic strength at the end of some titrations, which would impact on the β_2 values.

As mentioned before, the values of the stability constants computed from F_0 can be used to fix them in the fitting of Equation 10 to DPP current data. In this way, reliable estimations are obtained for the relative diffusion coefficients of the different complexes: ε_1(Cd-phthalate) = 0.71 (0.01); ε_2(Cd-phthalate) = 0.44 (0.03); ε_1(Pb-phthalate) = 0.65 (0.02); ε_2(Pb-phthalate) = 0.37 (0.05); where standard deviations are given in parentheses. The corresponding fitted curves are shown in Figure 2b (Cd) and Figure 2d (Pb). These values have been substituted in Equations 14a and 14b in order to simulate the expected ϕ vs. c_L^* curves of the stripping measurements, which also appear in Figure 2. It can be noticed that practically all stripping currents are higher than the theoretical prediction (in some cases relatively close but in others quite higher). In the case of Pb(II), this could be explained in terms of ongoing reduction of Pb(II) during the time taken by Cd(II) to be oxidized, which would produce an additional amount of reduced Pb and, thus, an increase of its oxidation signal. In SCP measurements, electroless effects could also be involved: the ongoing reduction of Pb(II) would produce a negative current that would force an increase of the effective oxidation current to maintain the overall stripping current constant, which would cause a decrease in the transition time of Cd(II). However, Cd(II) signals are not too low, but slightly too high, which suggests that electroless effects may be small. Additionally, the influence of these normalized current (not very far from 1) in the F_0 function is much less important than the determinant influence of potential shifts: the comparison of Figures 2a and 2c with Figures 3a and 3b

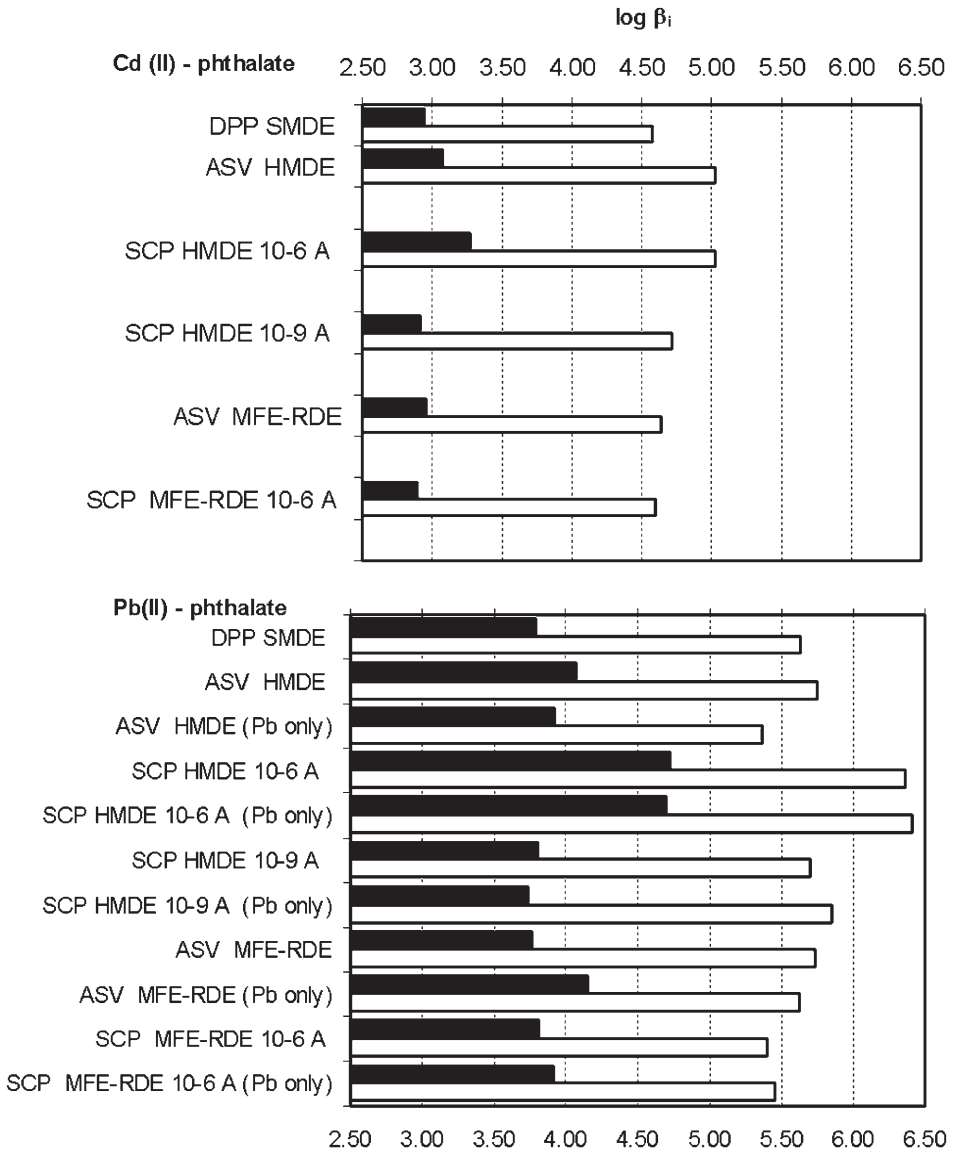

Fig. 4. Comparison of the stability constants β_1 (black bars) and β_2 (white bars) of the Cd(II)- and Pb(II)- phthalate complexes obtained by different techniques.

shows that the three groups of curves (very similar, slightly different and quite different from DPP) are identical in the two kinds of plots.

Figure 4 compares the log β values in Table 1. From this graph, it is clear that SCP at HMDE with $I_{ox} = 10^{-6}$ A produces systematically higher values of all constants (either for cadmium or lead complexes). Moreover, in the case of lead these values are practically independent of the presence of cadmium. These facts suggest that the disagreement could be more related to the stripping regime itself (linear diffusion) than to the simultaneous presence of cadmium and lead. In fact, the high oxidation current applied produces very short transition times, which increases the error. On the other hand, it is not sure that a purely linear diffusion holds along the full titration. In contrast, the values obtained for the other techniques are quite consistent: the differences between the higher and the lower

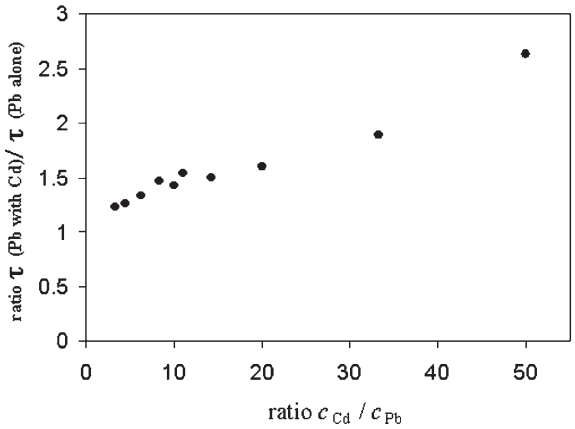

Fig. 5. Ratio between the transition times measured for Pb(II)-ion along the titrations of i) a 10^{-6} mol L^{-1} Cd(II) solution and ii) a KNO_3 blank with a Pb(II) solution as function of the ratio between the concentrations of Cd(II) and Pb(II).

constants are always lower than 0.5 logarithmic units. This means that the possible perturbations during the stripping step due to the proximity of cadmium and lead signals do not significantly affect the calculation of stability constants by means of the Leden function analysis. Taking into account that the slight deviations from the expected behavior were mainly noticed in current data, it would be interesting to perform a further study with macromolecular complexes with much lower diffusion coefficients in order to test whether in this case such deviations are sufficiently dramatic to seriously affect the calculation of stability constants.

In order to investigate the influence of the ratio between the concentrations of Cd(II) and Pb(II) on the above-discussed results, additional experiments were done. Figure 5 shows the result of the titration with Pb(II) of a blank solution and a sample containing 1×10^{-6} mol L^{-1} of Cd(II). It can be seen that the presence of Cd(II) enhances the signal of Pb(II) in a proportion which increases at increasing the Cd(II)-to-Pb(II) ratio. As expected, such enhancement is small at ratios close to 1, but can be important under large excess of Cd(II). It must be noted that the increase of the Pb(II) signal does not produce any noticeable change in the signal of Cd(II) (not shown), which suggests that this can be essentially due to the ongoing lead reduction more than to electroless effects. Other experiments consisted of SCP titrations at HMDE ($I_{ox} = 10^{-6}$ A) of Cd(II)-Pb(II) mixtures with phthalate at higher proportions of Cd(II) (2:1 and 10:1). Figure 6 shows that for the case of Pb(II), results are quite

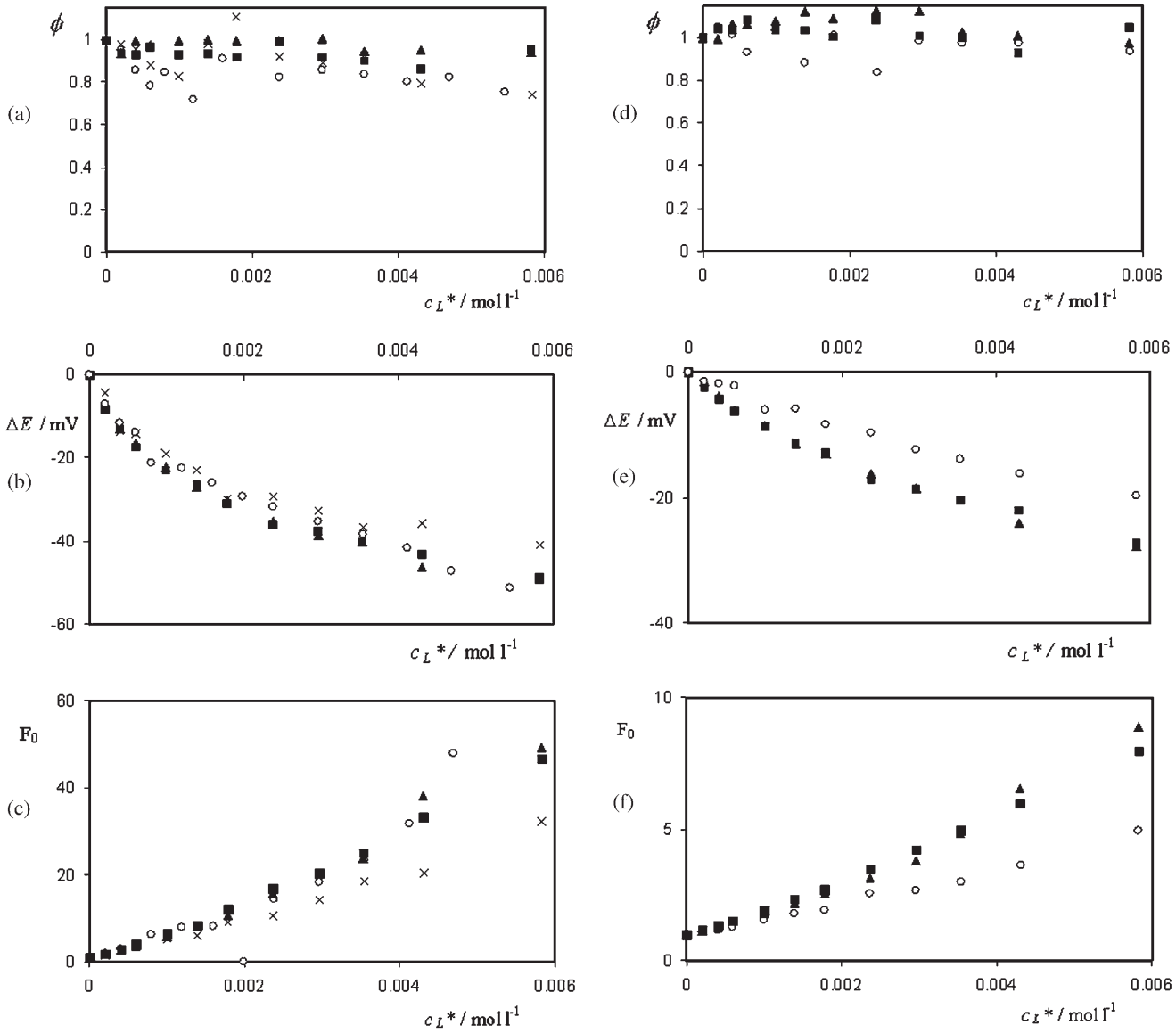

Fig. 6. Normalized transition times ϕ (a, d), potential shifts ΔE (b, e) and values of the Leden function F_0 (c, f) measured by SCP (at HMDE with $I = 10^{-9}$ A) for Pb(II) (a, b, c) and Cd(II) (d, e, f) in the presence of different concentrations of Cd(II)-ion as functions of the total phthalate concentration c_L^* under the conditions described in Figure 1. Pb(II) 1×10^{-6} mol L^{-1} (×); Pb(II) 1×10^{-6} mol L^{-1} + Cd(II) 1×10^{-6} mol L^{-1} (○); Pb(II) 5×10^{-7} mol L^{-1} + Cd(II) 1×10^{-6} mol L^{-1} (■); Pb(II) 5×10^{-7} mol L^{-1} + Cd(II) 5×10^{-6} mol L^{-1} (▲).

Table 2. Stability constants determined by SCP at a HMDE using 10^{-9} A of constant oxidation current for the Cd(II)-phthalate and Pb(II)-phthalate systems in cadmium-lead mixtures of different ratios at pH 5.5 and 0.01 mol L^{-1} KNO_3. The standard deviations obtained in the fitting are also shown.

Solution	Ratio Cd:Pb	Cd(II)-phthalate				Pb(II)-phthalate			
		$\log \beta_1$	S.D.	$\log \beta_2$	S.D.	$\log \beta_1$	S.D.	$\log \beta_2$	S.D.
Pb^{2+} 1×10^{-6} mol L^{-1}	0:1					3.74	0.05	5.85	0.11
Pb^{2+} 1×10^{-6} mol L^{-1} + Cd^{2+} 1×10^{-6} mol L^{-1}	1:1	2.91	0.03	4.72	0.08	3.80	0.03	5.70	0.05
Pb^{2+} 5×10^{-7} mol L^{-1} + Cd^{2+} 1×10^{-6} mol L^{-1}	2:1	3.15	0.01	5.09	0.01	3.97	0.01	5.89	0.02
Pb^{2+} 5×10^{-7} mol L^{-1} + Cd^{2+} 5×10^{-6} mol L^{-1}	10:1	3.17	0.03	5.12	0.04	3.94	0.04	6.06	0.04

similar to previous ones and only a slight increase of the ϕ and ΔE values at increasing proportion of Cd(II) can be noticed. The corresponding plots for Cd(II) exhibit a similar trend. Table 2 summarizes the stability constants determined for both metal ions in these titrations and compares them with the values previously determined at Cd(II)-to-Pb(II) ratios of 0:1 and 1:1. The inspection of the table suggests a slight increase of the stability constants at increasing proportions of Cd(II) but still inside the range of variability of the results obtained by different techniques. This means that the described perturbations in the presence of Cd(II) have a low impact on the stability constant calculation (possibly because of the normalization through ϕ), so that it is possible to obtain acceptable results even in the presence of a large excess of Cd(II).

5. Conclusions

The proximity of the signals can be a problem in the stripping analysis of mixtures of complexes of different heavy metal ions. If the signals are excessively close, it is not possible to find an intermediate deposition potential to perform a separated stripping analysis of the most electropositive metal and, as a consequence, its signal can be affected by the evolution of the preceding one. However, experiments on the Cd(II)-Pb(II)-phthalate system show that the possible interactions between the reoxidation processes of both metal ions only cause small deviations in the currents and have practically no effects on the calculation of stability constants from the Leden function F_0. The exception is SCP measurements under linear diffusion regime, which produce too high values for the stability constants.

6. Acknowledgements

The authors gratefully acknowledge financial support from the Spanish Ministry of Science and Technology (Project BQU2003-07587-C02-01) and from the Generalitat de Catalunya (2001SGR-00056 Project). Núria Serrano acknowledges the University of Barcelona for a Ph.D. grant.

7. References

[1] J. Wang, *Stripping Analysis: Principles, Instrumentation and Applications*, VCH, Deerfield Beach **1985.**
[2] M. Esteban, E. Casassas, *Trends Anal. Chem.* **1994**, *13*, 110.
[3] D. Jagner, A. Graneli, *Anal. Chim. Acta* **1976**, *83*, 19.
[4] J. M. Estela, C. Tomás, A. Cladera, V. Cerdà, *Crit. Rev. Anal. Chem.* **1995**, *25*, 91.
[5] R. M. Town, H. P. van Leeuwen *J. Electroanal. Chem.* **2001**, *509*, 58.
[6] R. M. Town, H. P. van Leeuwen, *J. Electroanal. Chem.* **2002**, *523*, 1.
[7] R. M. Town, H. P. van Leeuwen, *J. Electroanal. Chem.* **2002**, *523*, 16.
[8] R. M. Town, H. P. van Leeuwen, *J. Electroanal. Chem.* **2002**, *535*. 1.
[9] R. M. Town, H. P. van Leeuwen, *J. Electroanal. Chem.* **2002**, *535*, 11.
[10] R. M. Town, H. P. van Leeuwen, *Environ. Sci. Technol.* **2003**, *37*, 3945.
[11] R. M. Town, H. P. van Leeuwen, *Electroanalysis* **2004**, *16*, 458.
[12] N. Serrano, J. M. Díaz-Cruz, C. Ariño, M. Esteban, *J. Electroanal. Chem.* **2003**, *560*, 105.
[13] R. M. Town, H. P. van Leeuwen, *J. Electroanal. Chem.* **2004**, *573*, 147.
[14] R. Neeb, *Inverse Polarographie und Voltammetrie*, Verlag Chemie, Weinheim **1969.**
[15] H. G. de Jong, H. P. van Leeuwen, K. Holub, *J. Electroanal. Chem.* **1987**, *234*, 1.
[16] H. G. de Jong, H. P. van Leeuwen, *J. Electroanal. Chem.* **1987**, *234*, 17.
[17] H. G. de Jong, H. P. van Leeuwen, *J. Electroanal. Chem.* **1987**, *235*, 1.
[18] A. J. Bard, L. R. Faulkner, *Electrochemical Methods: Fundamentals and Applications*, 2nd ed., Wiley, New York, **2001.**
[19] D. D. DeFord, D. N. Hume, *J. Am. Chem. Soc.* **1951**, *73*, 5321.
[20] D. R. Crow, *Polarography of Metal Complexes*, Academic Press, London **1969.**
[21] J. Heyrovsky, J. Kůta, *Principles of Polarography*, Academic Press, New York **1966.**
[22] A. I. Vogel, *Textbook of Quantitative Chemical Analysis*, 5th ed., Longman, London **1989.**
[23] D. Jagner, M. Josefson, S. Westerlund, K. Årén, *Anal. Chem.* **1981**, *53*, 1406.
[24] IUPAC Stability Constants Database. Academic Software, **2001.**
[25] P. Amico, R. P. Bonomo, R. Cali, V. Cucinotta, P. G. Daniele, G. Ostacoli, E. Rizzarelli *Inorg. Chem*. **1989**, *28*, 3555.
[26] J. Ambrose, A. Covington, H. Thirsk, *Trans. Faraday Soc.* **1969**, *65*, 1897.
[27] A. E. Martell, R. M. Smith, *Critical Stability Constants*, Vol. 5, First Supplement, Plenum Press, New York **1982.**

DISCUSSIÓ DELS RESULTATS

Estimació del règim de redissolució i selecció d'un agent oxidant

L'etapa de reoxidació en la cronopotenciometria té lloc mitjançant l'ús d'un agent oxidant en solució o mitjançant l'aplicació d'una intensitat anòdica constant. Per tant, primerament es va fer una estimació del règim de redissolució existent en la cronopotenciometria de redissolució (SCP) a intensitat constant, el qual depenent de la intensitat d'oxidació i del tipus d'elèctrode, pot ser pròxim a la difusió lineal semi-infinita o a la redissolució total. Igualment, es va procedir a la recerca d'un oxidant químic òptim per emprar en les mesures per SCP amb agent oxidant.

En el treball 8.1 s'ha estimat i confirmat, d'acord amb la bibliografia [48], que per a un elèctrode de gotes de mercuri, intensitats d'oxidació petites produeixen un règim de redissolució total, mentre que per a intensitats d'oxidació grans el règim que es té és de difusió lineal semi-infinita. En la figura 1a del treball 8.1 es mostra l'estimació del règim de redissolució en un HMDE, mitjançant la representació logarítmica de la intensitat d'oxidació en funció del temps de transició. Es pot veure que per a intensitats d'oxidació més grans de $6\ 10^{-7}$ A, el valor del pendent de la representació logarítmica és –2 (equació 2.9), fet que indica que existeix un règim de difusió lineal semi-infinita, mentre que per a intensitats inferiors a $6\ 10^{-7}$ A, el valor –1 del pendent fa referència a un règim de redissolució total (equació 2.9).

En les representacions de la figura 1b i 1c del treball 8.1 es poden veure més clarament els dos règims de reoxidació definits anteriorment. En la figura 1b del treball 8.1 la representació de la concentració de metall al quadrat en funció del temps de transició, la qual mostra una relació lineal, indica condicions de difusió lineal semi-infinita (equació 2.7). En la figura 1c del treball 8.1, la representació mostra la dependència lineal que es dóna entre la concentració de metall i el temps de transició, fet que indica un règim de redissolució total (equació 2.8).

Això es pot justificar considerant que com més petita és la intensitat d'oxidació, més triga el procés de redissolució, la qual cosa permet que un major percentatge del metall amalgamat pugui arribar a la superfície de l'elèctrode, des de l'interior, per a oxidar-se.

Emprant un MF-RDE, el transport ràpid de metall en la fina pel·lícula durant la redissolució suposa que les mesures es realitzen sota condicions de redissolució total. L'estimació del règim de redissolució ha mostrat (figura 2a i 2b del treball 8.1), com s'esperava, que per a una intensitat d'oxidació de 10^{-6} A, la relació τ *vs.* c_{TM} és lineal (equació 2.8), el mateix que succeeix per a una intensitat d'oxidació de 10^{-9} A. Per tant es pot dir que en un ampli interval d'intensitats d'oxidació (entre 10^{-6} A i 10^{-9} A), el règim és de redissolució total.

En la modalitat de SCP amb agent oxidant, normalment s'usa l'ió Hg(II) [104, 105], però aquest té tendència a complexar-se amb els lligands que s'utilitzen, motiu pel qual en el treball 8.2 es busca un oxidant alternatiu que alteri el mínim el sistema en estudi. En la bibliografia es troben descrits altres oxidants usats en SCP com el $KMnO_4$ [106], el $K_2Cr_2O_7$ [107], el Ce(III) [108], el Fe(III) [108] i l'O_2 entre d'altres.

El Ce(III) i el Fe(III) s'han descartat per la mateixa raó que el Hg(II) i l'O_2 també es va rebutjar per la dificultat de mantenir constant la seva concentració en el decurs de les valoracions.

Per provar l'eficàcia del $K_2Cr_2O_7$ com a agent oxidant es van fer unes mesures inicials amb una solució de Cd(II) i es van obtenir bons resultats, però al fer la valoració emprant un lligand macromolecular com el PMA els resultats no van ser tan satisfactoris. Les raons d'aquest comportament del dicromat no són del tot clares, però es podria relacionar amb el considerable poder oxidant del Cr(VI), que podria oxidar la superfície del mercuri en presència d'un agent complexant com el PMA i dificultar el bescanvi d'electrons.
Finalment es va provar amb una solució de H_2O_2 al 0.03 % i es va considerar com l'agent oxidant òptim, ja que els resultats que s'obtenien eren bons tant per les mesures de Cd(II) sense lligand, com per les valoracions de Cd(II) amb PMA.

Cas de la formació de complexos làbils senzills: sistema Cd(II)-glicina

En el treball 8.1 els estudis sobre el sistema Cd(II)-glicina (model de sistema amb complexos làbils senzills sense adsorció electròdica) confirmen que la cronopotenciometria de redissolució (SCP) a intensitat constant és una opció valuosa en comparació a la molt més usual voltamperometria de redissolució anòdica (ASV),

proporcionant resultats perfectament comparables als de les tècniques polarogràfiques, com la polarografia diferencial d'impulsos (DPP). Tanmateix, en els experiments portats a terme, ASV també proporciona resultats acceptables.

L'estudi de les corbes voltamperomètriques i cronopotenciomètriques amb HMDE i MF-GCRDE mostren un desplaçament dels senyals cap a valors de potencial més negatius, respecte el senyal del metall en absència de lligand, a mesura que augmenta la concentració de glicina. Les variacions en la intensitat de pic, com era d'esperar, no són significatives. Aquest comportament indica que en l'escala de temps d'aquestes tècniques els complexos formats són làbils electroquímicament, i per altra banda, tal i com era d'esperar pel cas de complexos amb lligand senzill, que els coeficients de difusió de l'ió metàl·lic i dels diferents complexos són força semblants.

Les representacions de les funcions de Leden d'ordre zero (F_0) en funció de la concentració de glicina (figura 5a del treball 8.1), calculades a partir de les dades experimentals obtingudes per DPP (SMDE), ASV (HMDE i MF-GCRDE) i SCP (HMDE i MF-GCRDE), s'ajusten a un polinomi de grau dos, indicant la presència dels complexos ML i ML_2. A partir de la funció de Leden d'ordre zero (F_0) s'avalua la funció de Leden de primer ordre (F_1) (figura 5b del treball 8.1), obtenint-se per a les diferents tècniques una representació en forma de línia recta, que confirma la presència en el medi d'únicament dos complexos.

A partir dels ajustos polinomials de les funcions F_0 i F_1, equacions (2.14, 2.15 i 2.19), es calculen els valors de les constants de complexació globals per al sistema Cd(II)-glicina (taula 8.1).

La bona concordança de les dades cronopotenciomètriques amb els resultats polarogràfics suggereix que a la pràctica la metodologia de DeFord-Hume [33, 34] és perfectament aplicable a les mesures per SCP, la qual cosa no era tan evident des del punt de vista teòric.

Cas de la formació de complexos làbils macromoleculars: sistema Cd(II)-PMA

El sistema Cd(II)-PMA (treball 8.1) s'ha estudiat com a model de complexos làbils macromoleculars amb adsorció, emprant la cronopotenciometria de redissolució a

intensitat constant com una alternativa a la voltamperometria de redissolució anòdica que com ja s'ha dit es veu més afectada per l'adsorció de les diferents espècies en l'elèctrode.

En les valoracions realitzades primerament per ASV i per SCP amb HMDE i MF-GCRDE, es va trobar el problema, ja conegut, de la saturació de lligand. Aquest problema sorgeix quan es treballa amb lligands macromoleculars que no es troben en gran excés respecte l'io metàl·lic, produint-se un desdoblament dels senyals (figura 6 del treball 8.1) si a l'etapa de redissolució no hi ha prou lligand a la superfície de l'elèctrode per complexar l'io metàl·lic que s'hi va generant per oxidació de l'amalgama. Aquest problema és més important a ASV que a SCP, especialment quan s'utilitza MF-GCRDE. Per minimitzar l'aparició de dobles pics es pot potenciar el senyal del metall complexat augmentant l'excés de lligand o la rotació de l'elèctrode durant la redissolució o es pot potenciar el senyal del metall que es reoxida però que no es complexa augmentant el temps de deposició o treballant sense agitació. En aquest últim cas, però, l'aplicabilitat del mètode de DeFord-Hume és discutible. De tota manera, des del punt de vista de la quantificació, quan es detecta el problema dels dobles pics, la utilització d'àrees sembla molt més recomanable que la mesura d'alçades.

Els voltamperogrames i els cronopotenciogrames obtinguts en les condicions òptimes que minimitzen el problema de la saturació del lligand, mostren un desplaçament dels senyals cap a valors de potencial més negatius, respecte el senyal del metall en absència de lligand, a mesura que augmenta la concentració de PMA. En aquest cas el PMA és un lligand macromolecular, i això provoca variacions importants en la intensitat de pic. Aquests comportaments indiquen, la presència de complexos làbils, i per altra banda, que els coeficients de difusió de l'ió metàl·lic i del complex no són iguals, fet característic quan es té un lligand macromolecular.

Sobre els voltamperogrames i cronopotenciogrames obtinguts per les diferents tècniques i elèctrodes, prèviament suavitzats, es mesuren els potencials de pic (E_p) i les àrees dels pics en absència i presència de lligand. Es construeixen les corbes F_0 *vs.* c_L^* (figura 9b del treball 8.1), les quals s'ajusten a una recta (equacions 2.30, 2.31 i 2.32), per tal d'obtenir els valors de la constant K (taula 8.1). La construcció de les corbes ϕ *vs.* c_L^*

(figura 9a del treball 8.1) permet ajustar l'equació (2.29) a les dades experimentals mitjançant l'optimització simultània dels paràmetres p, ε i K, o bé l'optimització per a valors fixos d'un o de diferents paràmetres (taula 8.1).

Els resultats cronopotenciomètrics obtinguts dels ajustos de les corbes ϕ *vs*. c_L^* són perfectament comparables als polarogràfics, el que demostra que la metodologia de de Jong *et al*. és també perfectament aplicable a les mesures per SCP.

Cas de la formació d'una mescla de complex inert i complex làbil macromolecular: sistema Cd(II)-EDTA-PMA

En les aigües naturals es poden trobar una gran varietat de lligands. Per tant, seria de gran utilitat disposar de models de complexació que permetin l'estudi de sistemes que continguin simultàniament diferents tipus de lligands.

En el treball 8.2 s'ha emprat la cronopotenciometria de redissolució amb oxidant químic per l'estudi del sistema format per dos tipus de lligands, l'EDTA que forma complexos inerts i el PMA que com ja s'ha vist anteriorment és un lligand macromolecular que forma complexos làbils amb el metall. Si es compleixen les hipòtesis 1-6 de l'apartat 2.4, el model té una solució anàloga a la del cas de la complexació làbil macromolecular resolt per de Jong *et al*. [35-37].

La labilitat dels complexos és un concepte que depèn del temps de mesura (t_m) de cada tècnica. Es pot considerar que t_m està relacionat amb el temps que disposa un complex ML per difondre cap a l'elèctrode, dissociar-se i reduir-se. Per tant, un complex ML donat pot presentar un comportament làbil per una tècnica amb un t_m llarg (per exemple, ASV) i un comportament inert per una altra amb un t_m més curt (per exemple, DPP).

S'ha comprovat que el complex Cd-EDTA presenta un comportament pràcticament inert a pH 8, ja que el potencial de pic varia < 5mV fins a assolir la proporció 1:1 i la funció ϕ varia linealment amb la concentració de lligand fins a una relació Cd-EDTA 1:1.

La construcció de les corbes ϕ *vs*. c_L^* per a les valoracions voltamperomètriques i cronopotenciomètriques (utilitzant H_2O_2 al 0.03% com a agent oxidant) amb HMDE i

MF-GCRDE, realitzades pels sistemes Cd-EDTA, Cd-PMA i Cd-EDTA-PMA, mostra (figura 2 del treball 8.2) que el sistema Cd-EDTA s'ajusta bé al començament de la corba teòrica mentre que a relacions pròximes a 1:1 Cd/EDTA, presenta una certa desviació que podria ser deguda a una petita pèrdua del caràcter inert (lleugera dissociació del complex). Pel sistema Cd-PMA i pel sistema mescla Cd-EDTA-PMA, les corbes experimentals mostren una concordança força bona amb les teòriques, el que permet l'ajust de les equacions teòriques a les dades experimentals i obtenir els valors de ε i K (taula 8.1).

Cas de sistemes multi-metall: sistema Cd(II)-Pb(II)-ftalat

En mostres biològiques i medis naturals, nombrosos metalls pesants es troben presents simultàniament en proporcions variables. En el treball 8.3 s'ha procedit a l'estudi voltamperomètric i cronopotenciomètric amb intensitat constant amb un HMDE i un MF-GCRDE, del sistema Cd(II)-Pb(II)-ftalat com a model de sistema multi-metall.

Quan diferents metalls pesants es troben presents en una mostra és necessari considerar les possibles interferències que poden sorgir en la seva preconcentració conjunta en l'elèctrode (per exemple, la formació de complexos intermetàl·lics) i en l'etapa de reoxidació (per exemple, un element pot afectar a la manera de reoxidar-se d'un altre, i/o la capacitat de diferenciar els senyals de diferents elements). Alguns d'aquests problemes es podrien eliminar seleccionant un potencial de deposició intermedi, però en el cas del sistema Cd(II)-Pb(II)-ftalat l'acostament progressiu dels senyals corresponents als complexos làbils Cd(II)-ftalat i Pb(II)-ftalat a mesura que el ftalat s'afegeix a la solució d'ions Cd(II) i Pb(II), impossibilita l'elecció d'aquest potencial intermedi.

Com que s'ha comprovat a la bibliografia que el Cd(II) i el Pb(II) no formen complexos intermetàl·lics [109], l'estudi en el treball 8.3 del sistema Cd(II)-Pb(II)-ftalat s'ha centrat en els altres problemes propis dels sistemes multi-metall: la reducció addicional (*ongoing reduction*) i l'oxidació addicional (*electroless oxidation*).

Els senyals de les valoracions voltamperomètriques i cronopotenciomètriques amb intensitat constant amb HMDE i MF-GCRDE obtinguts pel sistema Cd(II)-Pb(II)-ftalat (figura 1 del treball 8.3) mostren una lleugera disminució en la intensitat de pic i un

desplaçament cap a valors de potencial més negatius a mesura que augmenta la concentració de ftalat. Aquest comportament és consistent amb la formació de complexos electroquímicament làbils amb coeficients de difusió lleugerament més petits als dels ions metàl·lics. En les diferents valoracions s'observa que els desplaçaments de potencial, respecte el senyal del metall en absència de lligand, en el cas del Pb(II) són més grans que en el cas del Cd(II) degut a la major estabilitat del complex Pb(II)-ftalat, fet que produeix la disminució progressiva de la separació entre els dos senyals a mesura que augmenta la concentració de ftalat en el medi.

Les representacions de les corbes ϕ *vs.* c_L^* del Cd(II) (figura 2b del treball 8.3) i del Pb(II) (figura 2d del treball 8.3) mostren valors de les intensitats de redissolució superiors als predits teòricament. En el cas del Pb(II) aquest comportament es pot explicar per la reducció addicional que experimenta el Pb(II) durant el temps que triga el Cd(II) en reoxidar-se. En el cas de les mesures per SCP també es podrien veure influenciades per l'efecte de l'oxidació addicional, però aquest no seria molt important ja que els senyals corresponents al Cd(II) haurien de ser força més baixos del que en realitat són.

L'ajust a un polinomi de grau dos de les representacions de les funcions de Leden d'ordre zero (F_0) del Cd(II) i del Pb(II) en funció de la concentració de ftalat (figura 3 del treball 8.3) indica la presència dels complexos ML i ML_2 i permet obtenir les constants d'estabilitat β_1 i β_2 (taula 8.1). Si es comparen els valors de les constants d'estabilitat obtinguts per les tècniques de redissolució amb els obtinguts en la valoració per DPP (lliure dels problemes de les etapes de deposició i reoxidació) es conclou que les possibles interaccions entre els processos de reoxidació d'ambdós ions metàl·lics pràcticament no afecten al càlcul de les constants d'estabilitat a partir de la funció de Leden F_0, ja que els valors de les β_n són molt propers, a excepció de les dades obtingudes per SCP amb HMDE en condicions de difusió lineal semi-infinita (I_{ox}: 10^{-6} A).

Taula 8.1. Resum dels sistemes M-lligand estudiats en el capítol 8.

Cd(II)-glicina pH 7.5 Força iònica 0.05 M	**HMDE/ SMDE**	**TÈCNICA**	**log β_1**		**log β_2**	
		DPP **DPASV** **CCSCP,** I_{ox}: 10^{-6}A	4.20 (0.08) 3.97 (0.07) 3.80 (0.1)		7.42 (0.04) 7.34 (0.02) 7.34 (0.02)	
	MF-GCRDE	**DPASV** **CCSCP,** I_{ox}: 10^{-6}A	4.17 (0.07) 4.10 (0.05)		7.65 (0.02) 7.44 (0.02)	
Cd(II)-PMA pH 7.2 Força iònica 0.01 M α_n: 0.7	**HMDE/ SMDE**	**TÈCNICA**	**p**	**ε**	**log K (ϕ)**	**log K (F_0)**
		RPP **DPASV** **CCSCP,** I_{ox}: 10^{-9}A	1/2 2/3 2/3	0.004 (0.001) 0.008 (0.001) 0.010 (0.003)	5.60 (0.01) 5.84 (0.02) 5.84 (0.03)	- 6.65 (0.04) 6.69 (0.01)
	MF-GCRDE	**DPASV** **CCSCP,** I_{ox}: 10^{-6}A, 500 rpm	2/3 2/3	0.015 (0.002) 0.020 (0.003)	5.95 (0.04) 5.89 (0.04)	5.95 (0.01) 6.29 (0.01)
Cd(II)-PMA pH 8.0 Força iònica 0.01 M α_n: 0.8	**HMDE**	**TÈCNICA**	**p**	**ε**	**log K (ϕ)**	**log K (F_0)**
		DPASV **SCP,** 0.03% H_2O_2	2/3 2/3	0.032 (0.004) 0.03 (0.01)	5.87 (0.02) 5.76 (0.03)	6.38 (0.01) -
	MF-GCRDE	**SCP,** 0.03% H_2O_2	2/3	0.05 (0.01)	5.82 (0.03)	-

			Cd(II)-ftalat ε_1 = 0.71 (0.01) ε_2 = 0.44 (0.03)		Pb(II)-ftalat ε_1 = 0.65 (0.02) ε_2 = 0.37 (0.05)	
		TÈCNICA	**log β_1**	**log β_2**	**log β_1**	**log β_2**
Cd(II)-Pb(II)-ftalat pH 5.5 Força iònica 0.01 M	**HMDE/ SMDE**	**DPP**	2.94 (0.01)	4.58 (0.01)	3.79 (0.01)	5.64 (0.01)
		DPASV	3.08 (0.03)	5.03 (0.07)	4.07 (0.01)	5.75 (0.03)
		CCSCP, I_{ox}: 10^{-6} A	3.28 (0.02)	5.03 (0.02)	4.72 (0.02)	6.36 (0.08)
		CCSCP, I_{ox}: 10^{-9} A	2.91 (0.03)	4.72 (0.08)	3.80 (0.03)	5.70 (0.05)
	MF-GCRDE	**DPASV**	2.96 (0.01)	4.64 (0.01)	3.76 (0.01)	5.74 (0.01)
		CCSCP, I_{ox}: 10^{-6}A	2.89 (0.02)	4.60 (0.02)	3.81 (0.01)	5.40 (0.02)

CAPÍTOL 9

Aplicació de la cronopotenciometria de redissolució per escombratge

CAPÍTOL 9. Aplicació de la cronopotenciometria de redissolució per escombratge a l'especiació de metalls pesants

Aquest capítol conté el treball on es presenta la metodologia SSCP-Analyzer desenvolupada per a l'anàlisi de les corbes SSCP i la seva aplicació en l'estudi de la complexació de sistemes relativament senzills com el Cd(II)-ftalat i Cd(II)-iodur. Malgrat que aquests sistemes ja han estat estudiats prèviament mitjançant diverses tècniques electroquímiques, s'ha de destacar que és la primera vegada que s'aplica aquest tractament numèric a unes dades obtingudes per SSCP per a l'estudi de l'especiació de metalls pesants.

Fins al moment, els estudis de complexació metàl·lica per ASV i SCP s'han fet a partir de l'anàlisi de les dades obtingudes de les valoracions on el lligand s'afegia al metall o viceversa. En el cas de la SSCP aquesta metodologia no és adequada, ja que el temps que es requereix per enregistrar en la seva totalitat una corba SSCP (obtinguda a partir de 20-40 mesures individuals per SCP a diferents potencials de deposició) és important i

no permet considerar un nombre elevat de relacions metall-lligand. D'altra banda, el propi senyal SSCP conté informació en un ampli ventall de relacions metall/lligand. És per això que en aquests estudis la informació es pot extreure d'un número reduït de corbes SSCP.

9.1 Full-wave analysis of stripping chronopotentiograms at scanned deposition potential (SSCP) as a tool for heavy metal speciation: theoretical development and application to Cd(II)-phthalate and Cd(II)-iodide systems

N. Serrano, J.M. Díaz-Cruz, C. Ariño, M. Esteban, J. Puy, E. Companys, J. Galceran, J. Cecilia

Journal of Electroanalytical Chemistry 600 **(2007)** 275-284

Available online at www.sciencedirect.com
ScienceDirect
Journal of Electroanalytical Chemistry 600 (2007) 275–284
Journal of Electroanalytical Chemistry
www.elsevier.com/locate/jelechem

Full-wave analysis of stripping chronopotentiograms at scanned deposition potential (SSCP) as a tool for heavy metal speciation: Theoretical development and application to Cd(II)-phthalate and Cd(II)-iodide systems

N. Serrano [a], J.M. Díaz-Cruz [a,*], C. Ariño [a], M. Esteban [a], J. Puy [b], E. Companys [b], J. Galceran [b], J. Cecilia [c]

[a] *Departament de Química Analítica, Universitat de Barcelona, Martí i Franqués 1, 08028 Barcelona, Spain*
[b] *Departament de Química, Universitat de Lleida, Rovira Roure 191, 25198 Lleida, Spain*
[c] *Departament de Matemàtica, Universitat de Lleida, Rovira Roure 191, 25198 Lleida, Spain*

Received 6 June 2006; received in revised form 19 September 2006; accepted 2 October 2006
Available online 13 November 2006

Abstract

A new mathematical treatment has been developed and implemented in an EXCEL spreadsheet in order to determine average equilibrium functions from the full set of data measured by scanning stripping chronopotentiometry (SSCP) in solutions containing different proportions of heavy metal ions and small-sized ligands. It has been applied to the experimental systems Cd(II)-phthalate and Cd(II)-iodide as models of complexation in the absence and in the presence of electrodic adsorption, respectively. The good agreement between the complexation parameters determined in this way, those predicted from literature data and those obtained using a cadmium ion selective electrode (ISE) confirms the validity of the proposed methodology and encourages its further refining for the analysis of macromolecular and heterogeneous systems.

Keywords: Metal speciation; Scanning stripping chronopotentiometry (SSCP); Full wave analysis; Cadmium; Phthalate; Iodide

1. Introduction

It has been recognised that stripping techniques are very effective in the analysis of heavy metal ions in environmental and biological samples [1–4] due to their excellent detection limits, which allows the study at the low concentrations existing in natural media. Stripping techniques applied to heavy metal ions combine a deposition step of metal reduction or adsorption with a stripping step where the accumulated metal is totally or partially dissolved from the electrode back into the solution or, in the case of adsorptive modalities, suffers an oxidation or reduction process from the adsorbed layer.

Stripping chronopotentiometry (SCP), also termed potentiometric stripping analysis (PSA) has been proposed by Jagner and Graneli [5,6] as an alternative to more conventional stripping techniques like anodic stripping voltammetry (ASV). In recent works [7–9] it has been demonstrated that SCP minimizes the problems caused by the adsorption of species onto the mercury electrode.

Constant-current SCP involves a deposition step where the metal is accumulated by reduction into the electrode and a stripping step where it is reoxidized by imposing a constant oxidising current. Then, SCP measures the evolution of the potential as a function of time and uses the transition time (τ), that between successive potential jumps, as the main analytical parameter.

There are some theoretical considerations and experimental experience on the use of constant-current SCP with

* Corresponding author. Tel.: +34 93 403 91 16; fax: +34 93 402 12 33.
E-mail address: josemanuel.diaz@ub.edu (J.M. Díaz-Cruz).

0022-0728/$ - see front matter © 2006 Elsevier B.V. All rights reserved.
doi:10.1016/j.jelechem.2006.10.007

Nomenclature

A	electrode surface area
ASV	anodic stripping voltammetry
β	overall stability constant
DEF	differential equilibrium functions
c_L	concentration of ligand
c_M	concentration of metal ion
c_{M^o}	concentration of reduced metal in the mercury drop
c^*_M	concentration of metal ion in the bulk solution
c_{ML}	concentration of complexed metal
c^*_{ML}	concentration of complexed metal in the bulk solution
$c^*_{T,M}$	total metal concentration in the bulk solution
δ	diffusion layer thickness
D	diffusion coefficient
E	potential
E_d	deposition potential
$E_{d,1/2,M}$	half-wave potential of the SSCP wave for a solution containing only metal
ε	ratio of the diffusion coefficients D_{ML}/D_M
E^0	standard potential of the redox system
F	Faraday constant
HMDE	hanging mercury drop electrode
I^*_d	limiting deposition current
I_s	SCP stripping current
ISE	ion selective electrode
K_c	average equilibrium function
L	ligand
M	free metal ion
ML	complexed metal ion
MFE	mercury film electrode
n	number of exchanged electrons
PSA	potentiometric stripping analysis
RDE	rotating disk electrode
SCP	stripping chronopotentiometry
SSCP	stripping chronopotentiometry at scanned deposition potential
SSV	scanned stripping voltammetry
t	time variable
T	Temperature
t_d	deposition time
τ	SCP transition (stripping) time
τ^*	SCP limiting τ value
τ^*_M	SCP limiting τ value for a solution containing only metal
$\tau_{d,M}$	characteristic time constant of the deposition process for a solution containing only metal
V	volume of the mercury electrode
x	spatial variable
ξ	dimensionless variable

hanging mercury drop electrode (HMDE) [7,10] and with rotating disk mercury film electrode (MFE-RDE) [11] for heavy metal speciation. In these works the effect of SCP oxidative current on the stripping regime in both HMDE and MFE-RDE electrodes was studied. In the case of HMDE [10,11] the presence of three characteristic regions was confirmed: high currents ensure semi-infinite linear diffusion, low currents produce total depletion and very low currents suffer from interference of dissolved oxygen. In MFE-RDE [11], the total depletion regime predominates in a wide range of oxidation currents. Despite the potential advantages of SCP, the potential-time characteristic of SCP is quite complicated and in some cases this renders the interpretation of metal complexation by SCP measurements rather difficult.

Stripping chronopotentiometry at scanned deposition potential (SSCP) has been introduced recently [12,13] as an alternative to scanned stripping voltammetry (SSV), a technique previously known as pseudopolarography, which consists in performing ASV measurements at different deposition potentials [14,15]. In the scanning modality, SSCP curves are constructed by plotting τ as a function of the deposition potential (E_d), which produces sigmoidal waves. It has been shown that, as it happens with ASV pseudopolarograms [14], the evolution of half-wave potentials of SSCP signals in the presence of complexing agents can be explained in terms of the classical DeFord–Hume method [16]. But if SSCP measurements are performed under depletive conditions (oxidation of all deposited metal), the results are expected to be much less affected by electrodic adsorption [7,8,17].

The usual way of investigating metal complexation by ASV or SCP is by means of titrations where the ligand is added to the metal or vice-versa. Then, an electrochemical measurement is carried out after every new addition. In the case of SSCP this can be done by fitting the evolution of the limiting current and half-wave potential with the added concentration to the DeFord–Hume or more sophisticated models. However, this method does not allow to consider a great number of metal-to-ligand ratios due to the large amount of time required to record a full SSCP wave (composed of 20–40 single SCP measurements at different E_d).

An alternative strategy would consist of the more comprehensive analysis of one single full SSCP wave, which effectively includes information at a wide range of metal-to-ligand ratios. This was considered in scanned stripping voltammetry and allowed the fitting of differential equilibrium functions (DEF) to explain the heterogeneous behaviour of humic acids [15]. The main goal of the present work is to investigate the possibility of a full-wave SSCP analysis of relatively simple systems (Cd(II)-phthalate and Cd(II)-iodide as models of small-sized labile complexes in the presence and in the absence of electrodic adsorption, respectively) as a first step to the application to more

complicated systems including macromolecular and heterogeneous complexes.

2. Mathematical model

2.1. Assumptions

Let us assume that

(i) The process of building up a M^o concentration inside the drop is much slower than the diffusion of the metal ion M from the solution to the electrode surface [12,18,19]. Thus, for the diffusion of M and ML, quasi-steady-state conditions apply all along the deposition period, bulk concentration values being maintained at a fixed distance $x = \delta$ (i.e., we assume planar finite diffusion). According to this assumption, the concentrations of M and ML at the electrode surface change with time, but concentration profiles in solution adapt instantaneously to steady state conditions compatible with the corresponding (time dependent) boundary concentrations.

(ii) Inside the electrode, there is a flat concentration profile of the reduced metal (due to its small volume and the fast diffusion/homogenization, see [12,18,19]) with increasing value along the deposition step.

(iii) The system $M + L \rightleftarrows ML$ is labile. This condition practically means that there is equilibrium between the metal and the complex concentrations at any relevant position in time and space, so that

$$K_c = \frac{c_{ML}(x,t)}{c_M(x,t)c_L(x,t)} \tag{1}$$

where K_c is the so-called average equilibrium function [20,21]. For simplicity and adapted to the particular experimental systems studied, we develop here the particular case of excess of ligand and sequential complexation of one metal with various ligands. In this context, c_{ML} indicates the total concentration of complexes having one metal and any number of ligand molecules.

(iv) The reduction/reoxidation process is reversible

$$c_{M^o}(0,t) = \exp\left(-\frac{nF}{RT}(E - E^0)\right)c_M(0,t) \tag{2}$$

where n is the number of exchanged electrons, F is the Faraday constant, T is the temperature, E is the potential, E^0 is the standard potential of the redox system, $c_{M^o}(0,t)$ is the concentration of reduced metal inside the mercury drop and $c_M(0,t)$ is the concentration of metal ion at the electrode surface in the solution.

(v) All the complexes share a common diffusion coefficient. We assume here that D_{ML} is the common diffusion coefficient to all the complexes. We call ε to its proportion to the free metal diffusion coefficient D_M

$$\varepsilon \equiv \frac{D_{ML}}{D_M} \tag{3}$$

2.2. Computing the bulk concentrations from the limiting stripping time (τ^*)

In the total depletion regime, the metal accumulated in the deposition step is completely reoxidized in a (measured) time τ by imposing a constant stripping current I_s. Thus, the total stripping charge, $I_s\tau$, can be related to the integral of the metal flux crossing the electrode surface during the deposition step. In diffusion limited conditions, labile complexation (i.e., $c_M(0,t) = c_{ML}(0,t) = 0$), assuming steady state in planar geometry and a common diffusion coefficient for all complexes, the metal flux is constant and given by $D_M\left(\frac{c^*_M + \varepsilon c^*_{ML}}{\delta}\right)$ so that a simple metal mass balance yields:

$$I_s\tau^* = nFAD_M\left(\frac{c^*_M + \varepsilon c^*_{ML}}{\delta}\right)t_d = I^*_d t_d \tag{4}$$

where I^*_d is the deposition current under diffusion limited conditions, τ^* is the corresponding stripping time, t_d is the deposition time and A is the area of the electrode.

Likewise, when only metal is present in the system

$$I_s\tau^*_M = nFAD_M\left(\frac{c^*_{T,M}}{\delta}\right)t_d \tag{5}$$

where τ^*_M indicates the stripping time in the system with the same amount of total metal but no ligand and under diffusion limited conditions.

Dividing (4) by (5) we have

$$c^*_M + \varepsilon c^*_{ML} = c^*_{T,M}\frac{\tau^*}{\tau^*_M} \tag{6}$$

which together with

$$c^*_M + c^*_{ML} = c^*_{T,M} \tag{7}$$

allows the determination of c^*_M and c^*_{ML} from the limiting stripping times of the SSCP waves (i.e., τ^* with and without ligand), provided the value of D_{ML} is known.

In fact, one could relax assumption (v) in 2.1 and consider a specific diffusion coefficient for each complex giving rise to dimensionless ratios ε_j. Then, Eq. (6) becomes

$$c^*_M + \sum_{j=1}^{n}\varepsilon_j c^*_{ML_j} = c^*_{T,M}\frac{\tau^*}{\tau^*_M} \tag{8}$$

This allows to interpret the common ε used in this work as a weighted average of the individual dimensionless diffusion coefficients, because, due to lability, even when we are not working with bulk concentrations

$$\varepsilon = \frac{\sum_{j=1}^{n}\varepsilon_j c_{ML_j}}{c_{ML}} = \frac{\sum_{j=1}^{n}\varepsilon_j c_{ML_j}}{\sum_{j=1}^{n} c_{ML_j}} = \frac{\sum_{j=1}^{n}\varepsilon_j\beta_j(c^*_L)^j}{\sum_{j=1}^{n}\beta_j(c^*_L)^j} \tag{9}$$

where β_j stands for the cumulative association constant giving rise to ML_j. For each SSCP series at a fixed ligand concentration (in excess), ε is a constant. The differences between ε of different series are considered negligible when compared with the inaccuracies associated to the stability

constant we are retrieving, so – in this preliminary work – we take a unique ε for all the complexes of a system.

2.3. Computing the concentrations at the electrode surface from the wave

2.3.1. Computing $c_M(0, t_d)$

The total metal accumulated in the deposition step, $I_s\tau$, can be related to the amount of reduced metal accumulated in the electrode, $nFVc_{M^o}$ (where V is the volume of the mercury electrode), and due to the reversibility of the system via Eq. (2), c_{M^o} can be related to $c_M(0,t_d)$:

$$I_s\tau = nFVc_{M^o} = nFV\exp\left(-\frac{nF}{RT}(E_d - E^0)\right)c_M(0,t_d) \quad (10)$$

where E_d stands for the deposition potential applied. Thus, for each couple $[E_d,\tau]$, Eq. (10) allows the calculation of $c_M(0,t_d)$. In order to minimize drift effects of the reference electrode, Eq. (10) can be written in terms of $E_{d,1/2,M}$, the half-wave potential of the SSCP wave for the system that contains only metal.

The SSCP wave for the system with only metal takes the form [12]:

$$\tau = \tau_{d,M}\frac{I_d^*}{I_s}\left(1 - \exp\left(-\frac{t_d}{\tau_{d,M}}\right)\right) \quad (11)$$

where

$$\tau_{d,M} = \frac{\delta V}{AD_M}\exp\left(-\frac{nF}{RT}(E_d - E^0)\right) \quad (12)$$

I_s and I_d^* are, respectively, the stripping and the deposition current in diffusion limited conditions.

Defining a dimensionless time $u = \frac{t_d}{\tau_{d,M}}$, the expression for the SSCP wave (11) combined with Eq. (4) takes the form:

$$\frac{\tau}{\tau^*} = \frac{\tau_{d,M}}{t_d}\left(1 - \exp\left(-\frac{t_d}{\tau_{d,M}}\right)\right) = \frac{(1-\exp(-u))}{u} \quad (13)$$

The condition of the half wave potential is $\frac{\tau}{\tau^*} = \frac{1}{2}$. Applied to (13) gives $u_{1/2} = 1.5936$ [9]. Using the definition of $\tau_{d,M}$, Eq. (12),

$$u_{1/2} = \frac{t_d}{\tau_{d,1/2,M}} = \frac{t_d AD_M}{\delta V}\exp\left(\frac{nF}{RT}(E_{d,1/2,M} - E^0)\right) \quad (14)$$

Isolating $c_M(0,t_d)$ in (10), replacing I_s from Eq. (4) for a case with just metal, and using (14), we obtain

$$c_M(0,t_d) = u_{1/2}c_{T,M}^*\frac{\tau}{\tau_M^*}\exp\left(\frac{nF}{RT}(E_d - E_{d,1/2,M})\right) \quad (15)$$

where τ_M^* is the limiting stripping time of the system with only metal present for $E_d \ll E^0$.

2.3.2. Computing $c_{ML}(0, t_d)$

For fully labile systems, the boundary condition at $x = 0$ can be written as

$$AD_M\left[\left(\frac{dc_M(x,t)}{dx}\right)_{x=0} + \varepsilon\left(\frac{dc_{ML}(x,t)}{dx}\right)_{x=0}\right] = V\left(\frac{dc_{M^o}(0,t)}{dt}\right) \quad (16)$$

As $c_M(x,t) + \varepsilon c_{ML}(x,t)$ has a linear concentration profile under steady state conditions, using (2) in the right hand side of (16), we have

$$AD_M\frac{c_M^* + \varepsilon c_{ML}^* - c_M(0,t) - \varepsilon c_{ML}(0,t)}{\delta} = V\exp\left(\frac{-nF}{RT}(E_d - E^0)\right)\left(\frac{dc_M(0,t)}{dt}\right) \quad (17)$$

which, using (14) becomes

$$\frac{t_d}{u_{1/2}}\exp\left(-\frac{nF}{RT}(E_d - E_{d,1/2,M})\right)\left(\frac{dc_M(0,t)}{dt}\right) = c_M^* + \varepsilon c_{ML}^* - c_M(0,t) - \varepsilon c_{ML}(0,t) \quad (18)$$

Eq. (18) is an algebraic equation for $c_{ML}(0,t_d)$ whose solution requires the knowledge of $\left(\frac{dc_M(0,t)}{dt}\right)$. However, in SSCP we only determine τ at the end of a fixed deposition time t_d. The key point to solve this problem comes from the use of a new dimensionless variable defined as

$$\xi = \frac{u_{1/2}t}{t_d}\exp\left(\frac{nF}{RT}(E_d - E_{d,1/2,M})\right) \quad (19)$$

Using this variable, Eq. (18) rewrites

$$\frac{dc_M(0,\xi)}{d\xi} = c_M^* + \varepsilon c_{ML}^* - c_M(0,\xi) - \varepsilon c_{ML}(0,\xi) \quad (20)$$

With the change of variables given by (19), time and potential influences are embedded in the new variable, ξ. As we are using different deposition potentials along the wave, we can numerically obtain the derivative of $c_M(0,\xi)$ with respect to ξ. With this derivative at hand, (20) allows the calculation of $c_{ML}(0,\xi)$ once $c_M^* + \varepsilon c_{ML}^*$ is known (for instance via Eq. (6)).

2.3.3. Computing K_c and checking consistency of results

The knowledge of a set of couples (E_d,τ) can yield $c_M(0,t_d)$ and $c_{ML}(0,t_d)$ via Eqs. (15) and (20) for the different deposition potentials along an SSCP wave. The computation of K_c (Eq. (1)), for each of these deposition potentials is then straightforward. As shown in the Results section, in the case of sequential complexation and excess of ligand, this K_c should remain essentially constant for a given concentration of ligand.

Notice that $c_M(0,t_d)$ and $c_{ML}(0,t_d)$ should tend to c_M^* and c_{ML}^* in the limit of less negative deposition potentials, i. e., at the potentials corresponding to the foot of the SSCP wave which corresponds to the conditions sought by the technique AGNES [19,22]. So, in this region, Eq. (15) reverts essentially to (10) with $c_M(0,t_d) = c_M^*$ and provides another independent way of obtaining c_M^* to that outlined around Eqs. (6) and (7), just using a quite apart region of the SSCP wave.

3. Experimental section

3.1. Reagents

All reagents used were Merck analytical grade. Solutions of phthalate were prepared from potassium hydrogenphthalate and partially neutralized with KOH until pH 5.5. KNO_3 0.01 mol L^{-1} was employed as the supporting electrolyte. Iodide solutions were prepared from potassium iodide and standardized according to Volhard method [23]. KNO_3 0.1 mol L^{-1} was applied as supporting electrolyte. Cd(II) stock solution of 1×10^{-2} mol L^{-1} was prepared from $Cd(NO_3)_2 \cdot 4H_2O$ and standardized complexometrically [23]. The diffusion coefficient of the uncomplexed metal ion is 0.72×10^{-5} cm^2 s^{-1} [24]. Ethylenediamine obtained from Aldrich (purity higher than 99%) was employed as complexing ligand for the calibration of cadmium ion selective electrode (Cd-ISE). Ultrapure water (Milli-Q plus 185 system, Millipore) was used in all experiments.

3.2. Apparatus and electrochemical parameters

Stripping chronopotentiometry at scanned deposition potential (SSCP) measurements were performed in an Autolab System PGSTAT12 (EcoChemie, The Netherlands) attached to a Metrohm 663 VA Stand (Metrohm, Switzerland) and a personal computer with GPES version 4.9 data acquisition software (EcoChemie). The system was also connected to a Metrohm 665 Dosimat for the addition of solutions and to an Orion SA 720 pH-meter for monitoring the pH value during the experiments. Calibration according to the literature [25] and measurements with cadmium ion selective electrode (Metrohm, Switzerland) were carried out with 809 Titrando (Metrohm, Switzerland) and a personal computer with Tiamo version 1.0 software. All the measurements were performed in a glass cell at constant room temperature (25 °C) under a purified nitrogen atmosphere (Air Liquide).

In all cases the reference electrode, to which all potentials are referred, was Ag|AgCl|KCl (3 mol L^{-1}) separated from the measurement solution by a liquid junction containing KNO_3 0.1 mol L^{-1} to prevent contamination of the sample by chloride ions. The counter electrode was a glassy carbon electrode. A hanging mercury drop electrode (HMDE) was used as a working electrode producing drops of ca. 0.5 mm^2 (which allows sphericity effects to be neglected).

In chronopotentiometric measurements deposition potentials between −0.88 and −0.58 V were applied during 90 s and a rest period of 5 s was performed at the same deposition potential between the deposition and the stripping steps. The SCP oxidising current, I_s, was 1×10^{-8} A, which corresponds to conditions approaching complete depletion ($I\tau$ constant) [10]. The transition time was measured as the area under the baseline-corrected dt/dE plot, which according to previous work [10], minimizes the contribution of capacitive currents and other secondary effects. The SSCP waves were constructed from a series of individual measurements of peak areas plotted as a function of the wide range of deposition potentials (E_d) applied.

3.3. Chronopotentiometric titration

Each titration started by placing in the cell a volume of 25 mL of a solution containing Cd(II)-ion and 0.01 mol L^{-1} of KNO_3 (in the case of the Cd-phthalate) or 0.1 mol L^{-1} of KNO_3 (in the case of the Cd-iodide). Then, the sample was deaerated with pure nitrogen for 30 min and for each point of the SSCP wave, the potential was held at the value chosen for the E_d for the duration of the deposition time (t_d) with solution stirring, followed by a rest period (without stirring), after which time the I_s was applied. Further, aliquots of phthalate or iodide were added and the respective curves were recorded. All solutions were deaerated and mechanically stirred for 30 s after each scan and for 3 min after each addition.

In order to prevent changes in ionic strength, the solution to be added contained the same concentration of KNO_3 as in the cell.

3.4. Calibration of Cd-ISE

The nominal measurable concentration range of the Cd-ISE was 10^{-1} to 10^{-7} mol L^{-1} but as shown in Fig. 1a, the calibration titration when Cd^{2+} is added to a KNO_3 solution reveals that Nernstian response is deteriorated below pCd ~5.

A previous work [25] has proved that the use of ethylenediaminetetraacetic acid (EDTA) or ethylenediamine (*en*) as complexing ligands increases the range in which the Cd-ISE has a Nernstian response.

In this work ethylenediamine (*en*) was selected as complexing ligand and the electrode behaviour was determined by measuring solutions containing different amounts of *en* (0.1 mol L^{-1}) with 1×10^{-3} mol L^{-1} $Cd(NO_3)_2$ in a range of free Cd from pCd 3 to pCd 10.3. These solutions were prepared the day before the measurement, so that, despite the slow kinetics between Cd^{2+} and *en*, the equilibrium state is reached.

Fig. 1b and c show the calibration curves obtained for cadmium ISE in *en* solutions at 0.01 mol L^{-1} and 0.1 mol L^{-1} of ionic strength, respectively. As shown, when a total cadmium concentration of 1×10^{-3} mol L^{-1} is used, the Cd-ISE has a Nernstian response in a wide range of free metal ion concentrations; but when the total concentration of the metal (free + complexed) decreases, the Nernstian response is deteriorated. As shown in Fig. 2 for 1×10^{-5} mol L^{-1} of total cadmium concentration, the Cd-ISE has a Nernstian behaviour until pCd ~ 9, but for a total concentration of 1×10^{-6} mol L^{-1} the Nernstian response of the Cadmium ISE is deteriorated below pCd ~ 7.

Thus, taking into account that in the study of our systems the total cadmium concentration is 1×10^{-6} mol L^{-1},

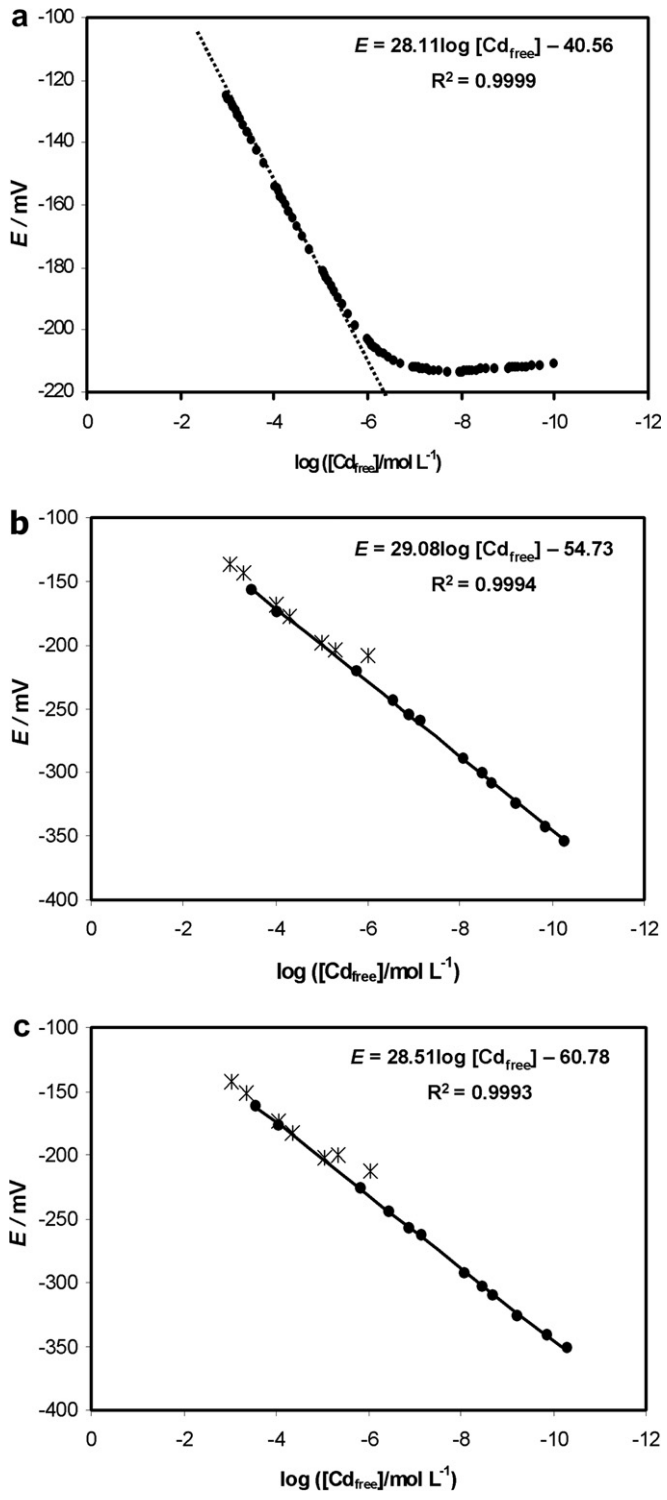

Fig. 1. Calibration curves for cadmium ISE. (a) Titration of 0.01 mol L^{-1} KNO_3 with Cd^{2+} solution. (b) and (c), calibration with a total cadmium concentration of 1×10^{-3} mol L^{-1} in the presence (–●–) and in the absence (–∗–) of different added volumes of *en* 0.1 mol L^{-1} at ionic strength 0.01 (b) and 0.1 (c) mol L^{-1} of KNO_3. Solid lines denote the corresponding calibration curves obtained by linear regression (equations are also shown).

measurements with Cd-ISE only will be possible for concentrations of free cadmium (c^*_{Cd}) higher than 1×10^{-7} mol L^{-1}.

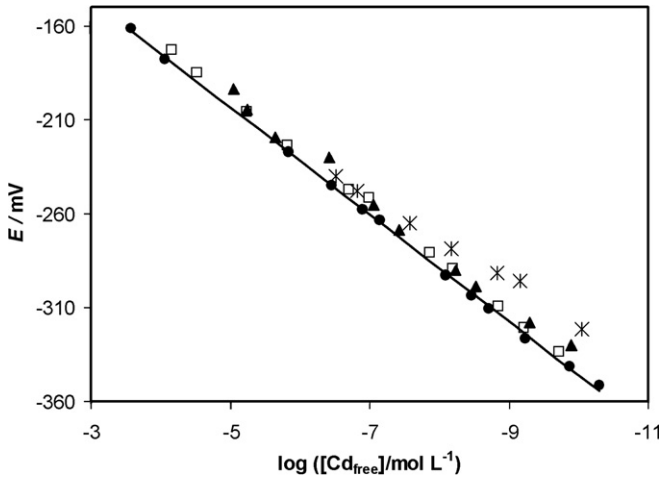

Fig. 2. Cadmium-ISE calibration curves for cadmium-*en* solutions containing different amounts of *en* (0.1 mol L^{-1}) into 1×10^{-3} mol L^{-1} (–●–), 1×10^{-4} mol L^{-1} (–□–), 1×10^{-5} mol L^{-1} (–▲–) and 1×10^{-6} mol L^{-1} (–∗–) of $Cd(NO_3)_2$ in the presence of 0.1 mol L^{-1} of KNO_3.

4. Results and discussion

4.1. Study of the Cd^{2+}-phthalate system as a model of small labile complexes without electrodic adsorption

Fig. 3 shows the SSCP curves obtained during the depletive chronopotentiometric titration of 10^{-6} mol L^{-1} Cd(II) solution with phthalate (free ligand concentrations 0, 1.22×10^{-3}, 5.89×10^{-3} and 2.15×10^{-2} mol L^{-1}) at pH 5.5 and ionic strength of 0.01 mol L^{-1} using a HMDE. The SSCP curves decrease in height and progressively shift towards more negative potentials with the addition of the ligand. This is consistent with the expected formation of electrochemically labile complexes of stoichiometry

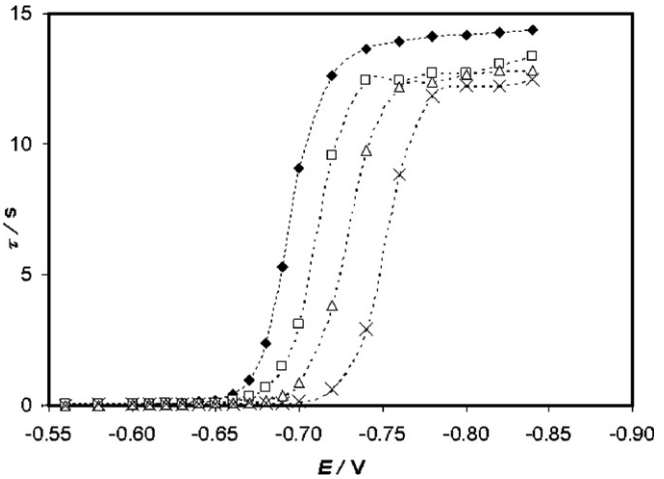

Fig. 3. Experimental SSCP waves measured with a HMDE for the Cd(II)-phthalate system at different phthalate concentrations. Curves were obtained using 1×10^{-6} mol L^{-1} Cd(II) in 0.01 mol L^{-1} KNO_3 (–◆–), and free phthalate concentration 1.22×10^{-3} (–□–), 5.89×10^{-3} (–△–) and 2.15×10^{-2} (–×–) mol L^{-1} at pH 5.5. Conditions: deposition time of 90 s, a rest time of 5 s and imposing $I_s = 10^{-8}$ A.

1:1 and 1:2 with diffusion coefficients smaller, but still relatively similar to those of free metal ions [7,16].

SSCP-Analyzer is a spreadsheet (available free of charge at http://web.udl.es/usuaris/q4088428/Publicacions/Publicacions.html) for the calculation of $c_M(0,t_d)$ via Eq. (10), $c_{ML}(0,t_d)$ via (20) and K_c via (1) from SSCP waves. The first step consists in introducing some parameters such as: deposition time (t_d), number of exchanged electrons (n), SSCP half wave potential in the absence of ligand ($E_{d,1/2,M}$), total ligand concentration ($c^*_{T,L}$), total metal concentration ($c^*_{T,M}$), diffusion coefficient of the metal ion (D_M), diffusion coefficient of the complex (D_{ML}), the maximum transition time in the SSCP wave in the presence of ligand (τ^*), the maximum transition time in the SSCP wave in the absence of ligand ($\tau_M{}^*$) and some other constants. Then, the full wave (i.e., the couple E_d, τ) has to be introduced to the spreadsheet.

As explained in Section 2.3.3, the free cadmium concentration (c^*_{Cd}) is obtained by SSCP Analyzer via two different ways. One estimated value of c^*_{Cd} comes from the value of $c_M(0,t_d)$ at potentials in the foot of wave (i.e., deposition potentials slightly less positive than its half-wave potential), using Eq. (15), as with these deposition potential, equilibrium conditions can be practically reached, as extensively exploited by the technique AGNES [19,22]. The second value of c^*_{Cd} results from the simultaneous solution of Eqs. (6) and (7), based on the deposition step being all the time under diffusion limited conditions. We have fitted the ε-value so that these two c^*_{Cd}-values, in all the experiments, are optimally close to each other. In the particular case of Cd-Phthalate system the fitted ε-value for the complexes is 0.923.

The values of free phthalate concentration ($[Ph^{2-}]$) all along this work have been calculated with the total ligand concentration added, ignoring any Cd^{2+} concentration (because we are in ligand excess conditions) and taking into account the protonation of phthalate at pH 5.5 and ionic strength 0.01 mol L^{-1} using MINTEQ [26].

Table 1 shows a reasonable agreement between the values of c^*_{Cd} obtained from the two different computations by SSCP Analyzer and from literature data [27,28]. Measurements with Cd-ISE carried out for the two first additions of phthalate, corresponding to a free cadmium concentration higher than 1×10^{-7} mol L^{-1}, have been included and they are also consistent. The agreement with published data is especially remarkable if we take into account the inherent complexity of this determination, corroborated by the discrepancies reported by different sources.

As two successive Cd-Phthalate complexes have been described [29], under excess ligand conditions, K_c given in Eq. (1) can be written as:

$$K_c = \frac{c_{ML}}{c_M c^*_L} = \beta_1 + \beta_2[Ph^{2-}] \quad (21)$$

where β_1 and β_2 are the overall stability constants of CdPh and $CdPh_2^{2-}$ complexes, respectively. Table 2 contains different values found in the literature [27,28] once corrected to ionic strength 0.01 mol L^{-1}. $[Ph^{2-}]$ indicates the bulk concentration of free phthalate (which is constant for any point in solution, at any time and along the SSCP wave for each addition of the titration under the studied conditions).

Table 3 compares the expected values of K_c with those obtained via computation with SSCP Analyzer for the experiments at different phthalate concentrations, showing a reasonable agreement with each other.

Alternatively, we can estimate the cumulative complexation constants from the K_c retrieved by SSCP-Analyzer using Eq. (21) with β_1 and β_2 as unknowns and K_c values

Table 1
Experimental and theoretically expected values of c^*_{Cd} for the Cd(II)-phthalate system ($[Cd^{2+}] = 1\times10^{-6}$ mol L^{-1} and 0.01 mol L^{-1} KNO_3) at different phthalate concentrations

[Phthalate] (mol L^{-1})	c^*_{Cd} ($\times10^{-7}$ mol L^{-1})				
	ISE	SSCP Analyzer foot of wave	SSCP Analyzer τ^* fixed $\varepsilon = 0.923$	Literature data[a]	Literature data[b]
1.22×10^{-3}	6.74	6.91	8.84	5.31	3.78
5.89×10^{-3}	3.20	3.46	4.04	1.92	0.81
2.15×10^{-2}	–	0.40	0.48	0.61	0.12

[a] NIST Standard Reference Database 46 Version 7.0 [27] NIST Critically selected stability constants of metal complexes.
[b] Ref. [28], data corrected to ionic strength 0.01 mol L^{-1}.

Table 2
Stability constants determined for the Cd(II)-phthalate system at pH 5.5 and 0.01 mol L^{-1} KNO_3 in a HMDE at $I_s = 10^{-8}$ A and estimated from the K_c-values reported in Table 3

Method	log β_1	log β_2
SSCP Analyzer	2.816 (0.002)	4.830 (0.002)
Literature data[a]	3.00	3.57
Literature data[b]	3.28	5.26

The standard deviations obtained in the fitting and literature data are also shown.
[a] NIST Standard Reference Database 46 Version 7.0 [27] NIST Critically selected stability constants of metal complexes.
[b] Ref. [28], data corrected to ionic strength 0.01 mol L^{-1} with Davies equation.

Table 3
Experimental and theoretically expected values of K_c for the Cd(II)-phthalate system ($[Cd^{2+}] = 1\times10^{-6}$ mol L^{-1} and 0.01 mol L^{-1} KNO_3) at different free phthalate concentrations

[Phthalate] (mol L^{-1})	K_c ($\times10^3$ mol^{-1} L)		
	K_c SSCP Analyzer fixed $\varepsilon = 0.923$	$K_{c\,\text{Literature data}}$[a]	$K_{c\,\text{Literature data}}$[b]
1.22×10^{-3}	0.74 (0.17)	1.00	2.15
5.89×10^{-3}	1.05 (0.18)	1.01	3.09
2.15×10^{-2}	2.11 (0.16)	1.05	6.23

[a] NIST Standard Reference Database 46 Version 7.0 [27] NIST Critically selected stability constants of metal complexes.
[b] Ref. [28], data corrected to ionic strength 0.01 mol L^{-1}.

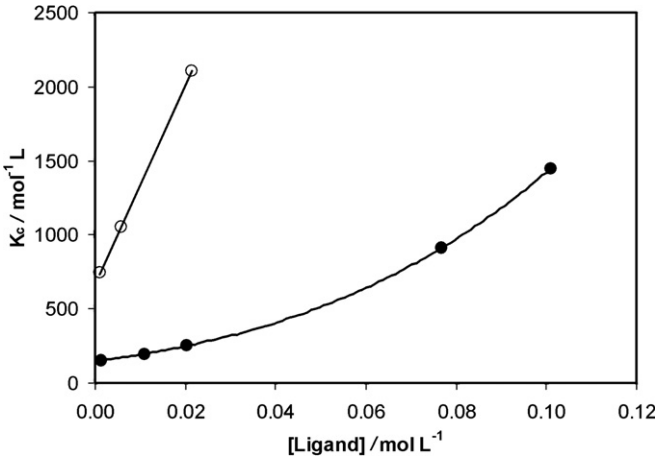

Fig. 4. Fitted curves (solid lines) to the experimental set of K_c values (Tables 3 and 5) for phthalate (–○–) and iodide (–●–) complexation with Cd^{2+} according to Eqs. (21) and (22), respectively. From the fitting, the cumulative stability constants in Tables 2 and 6 for the phthalate and iodide complexed are obtained.

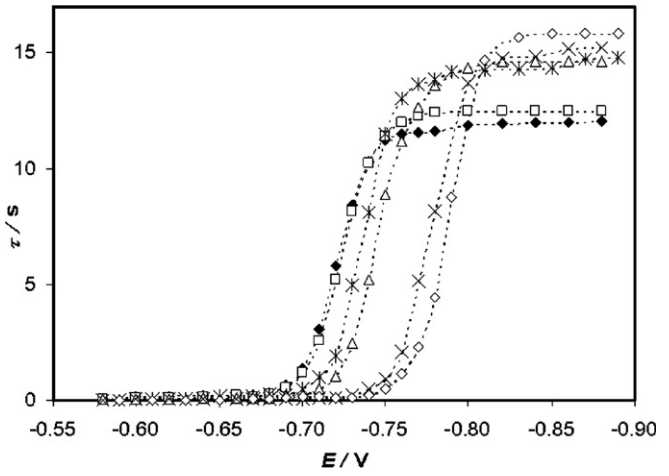

Fig. 5. Experimental SSCP curves for the Cd(II)-I^- system at different iodide concentrations. Curves were measured with a HMDE imposing $I_s = 10^{-8}$ A for 1×10^{-6} mol L^{-1} Cd (II) in 0.1 mol L^{-1} KNO_3 (–◆–), and free iodide concentration 1.48×10^{-3} (–□–), 1.09×10^{-2} (–∗–), 2.05×10^{-2} (–△–), 7.68×10^{-2} (– × –) and 1.01×10^{-1} (–◇–), mol L^{-1} at pH 5.5. Conditions: deposition time of 90 s, a rest time of 5 s and imposing $I_s = 10^{-8}$ A.

taken from first column in Table 3. The cumulative stability constants β_1 and β_2 obtained in this way are gathered in the first row of Table 2 and the fitted curve is shown in Fig. 4. As it can be seen, despite the large uncertainty of the calculations (3 points to fit a line), the stability constants obtained are relatively close to the literature values and the standard deviations of the fitting are quite small.

4.2. Study of the Cd^{2+}-iodide system as a model of small labile complexes with electrodic adsorption

The Cd(II)-iodide system has been previously studied by different techniques and complexes of stoichiometries ranging from 1:1 to 1:4 have been found depending on the experimental conditions [30]. The iodide has the advantage of not having reactions with protons, but the difficulty of the well-known presence of adsorption phenomena of iodide ions and induced adsorption of Cd on the mercury electrodes [31–34]. So, this system has been selected in order to check whether the impact of adsorption can be a hindrance for the current methodology. Depletive SSCP measurements have been carried out in this work during the titration of solutions containing 10^{-6} mol L^{-1} of Cd(II) with iodide at pH 5.5.

Fig. 5 shows the SSCP curves obtained using a HMDE. The addition of the ligand produces a shift of the sigmoidal curve to more negative potentials and a slight increase in the curve height, that confirms some previous results [35–37] showing higher diffusion coefficients for the Cd-I complexes as compared to Cd^{2+} alone. The waves are also consistent with the expected electrochemically labile behaviour of the Cd^{2+}-iodide complexes. On the other hand, as discussed in the classical literature [38,39], reactant adsorption can produce distortion of polarographic waves, with the appearance of pre- and post-waves and peaks. Thus, by analogy, adsorption could produce also some kind of distortion (e.g., deformed shape or splitting) in the individual dt/dE SCP peaks whose areas provide the points in SSCP plots, especially at the less negative deposition potentials. However, all individual SCP signals obtained in the presence of iodide (not shown) presented the same regular peak shape as for Cd^{2+} alone and only a slight broadening was detected at increasing concentrations of iodide. Such broadening suggests that adsorption could be present in SCP measurements, but also that its influence on the results should be small (especially considering that the transition times are measured as peak areas and not peak heights).

In such SSCP experiments (carried out at free iodide concentration 0, 1.48×10^{-3}, 1.09×10^{-2}, 2.05×10^{-2}, 7.68×10^{-2} and 1.01×10^{-1} mol L^{-1}), the transition time of each individual SCP measurement and the half wave potential of the only metal SSCP wave (iodide concentration 0 mol L^{-1}) were measured.

General parameters of the Cd^{2+}-iodide system, constants and values of transition time obtained for each deposition potential applied were introduced into the SSCP Analyzer, which computed $c_M(0, t_d)$ via Eq. (12), $c_{ML}(0, t_d)$ via (22) and K_c via (1).

As done in the case of Cd+Phthalate, we have fitted ε so that the two values of the free cadmium concentration (c^*_{Cd}) provided by SSCP Analyzer converge for each of iodide concentration. The value found was $\varepsilon = 1.36$, which indicates that the mobility of the complexes Cd+I is larger than the mobility of the hydrated Cd-ion, as already described in the literature [35–37]. Table 4 summarizes these c^*_{Cd} values obtained by the analysis of the foot of the wave and from the limiting transition time, which are reasonably close to each other and to those obtained by measurements with Cd-ISE and literature data [27].

Table 4
Experimental and theoretically expected values of c^*_{Cd} for the Cd(II)-I^- system ($[Cd^{2+}] = 1 \times 10^{-6}$ mol L^{-1} and 0.1 mol L^{-1} KNO_3) at different iodide concentrations

$[I^-]$ (mol L^{-1})	c^*_{Cd} ($\times 10^{-7}$ mol L^{-1})			
	ISE	SSCP Analyzer foot of wave	SSCP Analyzer τ^* fixed $\varepsilon = 1.36$	Literature data[a]
1.48×10^{-3}	7.51	8.25 (0.35)	6.92	8.17
1.09×10^{-2}	2.78	3.27 (0.20)	2.65	4.73
2.05×10^{-2}	1.85	1.59 (0.07)	1.74	2.85
7.68×10^{-2}	–	0.15 (0.01)	0.19	0.26
1.01×10^{-1}	–	0.10 (0.06)	0.10	0.12

[a] NIST Standard Reference Database 46 Version 7.0 [27] NIST Critically selected stability constants of metal complexes.

Table 5 compares the values of K_c, at different iodide concentrations, obtained experimentally by SSCP Analyzer computation and the theoretically expected values of K_c calculated according to this equation:

$$K_c = \beta_1 + \beta_2[I^-] + \beta_3[I^-]^2 + \beta_4[I^-]^3 \quad (22)$$

where β_1, β_2, β_3 and β_4 are the overall stability constants of CdI^+, CdI_2, CdI_3^- and CdI_4^{2-} complexes, respectively and their values have been taken from the literature [27,38] and adapted to ionic strength 0.1 mol L^{-1}.

Table 5 shows that the values of K_c found by SSCP Analyzer for the five iodide concentrations are quite similar to the values expected. This fact suggests that the influence of adsorption on the mercury electrode is really minimized by depletive SCP measurements.

Table 6 reports the values of the cumulative stability constants obtained by a least squares fitting of Eq. (22) to the experimental set of $[I^-]$ and K_c values. The corresponding fitted curve is shown in Fig. 4.

In the analysis of Table 6, the same uncertainties discussed for the case of phthalate have to be admitted (now, 5 points are used to fit 4 constants). Anyway, these results also exhibit a reasonable agreement of the $\log \beta_n$ estimated from experimental data and values reported in the literature [27,40].

Table 5
Experimental and theoretically expected values of K_c for the Cd(II)-I^- system ($[Cd^{2+}] = 1 \times 10^{-6}$ mol L^{-1} and 0.1 mol L^{-1} KNO_3) at different iodide concentrations

$[I^-]$ (mol L^{-1})	K_c ($\times 10^2$ mol^{-1} L)		
	K_c SSCP Analyzer fixed $\varepsilon = 1.36$	K_c Literature data[a]	K_c Literature data[b]
1.48×10^{-3}	1.52 (0.09)	0.74	1.70
1.09×10^{-2}	1.94 (0.25)	0.94	2.20
2.05×10^{-2}	2.54 (0.26)	1.20	2.90
7.68×10^{-2}	9.12 (1.27)	4.95	10.61
1.01×10^{-1}	14.49 (1.29)	8.37	16.29

[a] NIST Standard Reference Database 46 Version 7.0 [27] NIST Critically selected stability constants of metal complexes.
[b] Ref. [38], $NaClO_4$ 0.1 mol L^{-1} 25 °C.

Table 6
Stability constants determined for the Cd(II)-I^- system at pH 5.5 and 0.1 mol L^{-1} KNO_3 in a HMDE at $I_s = 10^{-8}$ A, estimated from the K_c-values reported in Table 5

Method	$\log \beta_1$	$\log \beta_2$	$\log \beta_3$	$\log \beta_4$
SSCP Analyzer	2.16 (0.01)	3.63 (0.04)	4.60 (0.09)	5.66 (0.05)
Literature data[a]	1.85	3.28	4.36	5.57
Literature data[b]	2.20	3.72	4.80	5.45

The standard deviations obtained in the fitting and literature data are also shown.
[a] NIST Standard Reference Database 46 Version 7.0 [27] NIST Critically selected stability constants of metal complexes.
[b] Ref. [38], $NaClO_4$ 0.1 mol L^{-1} 25 °C.

5. Conclusions

A new numerical data treatment has been derived to fully analyze the deposition potential scanned stripping chronopotentiometry (SSCP) waves, for depletive stripping, at conventional HMDE.

For fully labile systems, it has been shown that the time and potential dependence of the metal concentration at the electrode surface in an SSCP experiment of an electrochemical reversible system reduces to just a combined dependence in terms of a dimensionless variable ξ, (given by Eq. (19)). This combined dependence enables the use of a change of variables expression (see Eq. (20)) which leads to the direct determination of K_c with a great save of computational work. A simple Excel spreadsheet, the SSCP-Analyzer, includes all the calculations.

The full-wave SSCP analysis has been applied to two relatively simple systems, Cd(II)-phthalate and Cd(II)-iodide, as models of small labile complexes in the presence and in the absence of electrodic adsorption, respectively.

SSCP curves, τ versus E_d, obtained during the depletive chronopotentiometric titration of 10^{-6} mol L^{-1} Cd(II) solution with phthalate at pH 5.5 and ionic strength of 0.01 mol L^{-1}, lead to the determination of K_c and the overall stability constants of CdPh and $CdPh_2^{2-}$, β_1 and β_2, in accordance with literature values.

Also a good agreement results in the determination of K_c and the different successive stability constants, β_1, β_2, β_3 and β_4, for the Cd-iodide SSCP curves at the same conditions, but with 0.1 M ionic strength, suggesting that SSCP minimizes electrodic adsorption effects, as already shown in the literature [7–9,17].

The free metal concentration computed from the full-wave strategy in both systems also coincides with potentiometric measurements carried out with a cadmium ISE.

Further work considering heterogeneous complexants and non-excess ligand conditions could be tackled developing the theoretical framework here expound.

Acknowledgements

The authors are grateful to R.M. Town for her inspiration to analyse the full wave. The authors also acknowledge

support of this research by the Spanish Ministry of Education and Science (DGICYT: Projects BQU2003-9698 and BQU2003-07587) and from the ''Comissionat d'Universitats i Recerca de la Generalitat de Catalunya'' (Projects 2005SGR00186 and 2005SGR00616).

References

[1] F. Vydra, K. Stulik, E. Julakova, Electrochemical Stripping Analysis, Ellis Horwood, Chichester, 1976.
[2] J. Wang, Stripping Analysis: Principles, Instrumentation and Applications, VCH, Deerfield Beach, 1985.
[3] M. Esteban, E. Casassas, Trac-Trends Anal. Chem. 13 (1994) 110.
[4] J. Buffle, M.L. Tercier-Waeber, Trac-Trends Anal. Chem. 24 (2005) 172.
[5] D. Jagner, A. Graneli, Anal. Chim. Acta 83 (1976) 19.
[6] D. Jagner, Analyst 107 (1982) 593.
[7] R.M. Town, H.P. van Leeuwen, J. Electroanal. Chem. 523 (2002) 1.
[8] H.P. van Leeuwen, R.M. Town, J. Electroanal. Chem. 523 (2002) 16.
[9] D. Omanovic, M. Lovric, Electroanalysis 16 (2004) 563.
[10] R.M. Town, H.P. van Leeuwen, J. Electroanal. Chem. 509 (2001) 58.
[11] N. Serrano, J.M. Díaz-Cruz, C. Arino, M. Esteban, J. Electroanal. Chem. 560 (2003) 105.
[12] H.P. van Leeuwen, R.M. Town, J. Electroanal. Chem. 536 (2002) 129.
[13] H.P. van Leeuwen, R.M. Town, Environ. Sci. Technol. 37 (2003) 3945.
[14] S.D. Brown, B.R. Kowalski, Anal. Chem. 51 (1979) 2133.
[15] R.M. Town, M. Filella, J. Electroanal. Chem. 488 (2000) 1.
[16] R.M. Town, H.P. van Leeuwen, J. Electroanal. Chem. 541 (2003) 51.
[17] R.M. Town, H.P. van Leeuwen, Croat. Chem. Acta 79 (2006) 15.
[18] W.T. de Vries, E. van Dalen, J. Electroanal. Chem. 8 (1964) 366.
[19] J. Galceran, E. Companys, J. Puy, J. Cecília, J.L. Garcés, J. Electroanal. Chem. 566 (2004) 95.
[20] J.L. Garcés, F. Mas, J. Cecília, J. Galceran, J. Salvador, J. Puy, Analyst 121 (1996) 1855.
[21] J.L. Garcés, F. Mas, J. Puy, J. Galceran, J. Salvador, J. Chem. Soc. Faraday Trans. 94 (1998) 2783.
[22] E. Companys, J. Cecília, G. Codina, J. Puy, J. Galceran, J. Electroanal. Chem. 576 (2005) 21.
[23] A.I. Vogel, Textbook of Quantitative Chemical Analysis, fifth ed., Longman, London, 1989.
[24] D.R. Crow, Polarography of Metal Complexes, Academic Press, London, 1969.
[25] C.J. Milne, D.G. Kinniburgh, J.C.M. de Wit, W.H. van Riemsdijk, L.K. Koopal, J. Colloid. Interf. Sci. 175 (1995) 448.
[26] J.D. Allison, D.S. Brown, K.J. Novo-Gradac, MINTEQA2/PRODEFA2, A geochemical assessment model for environmental systems: Version 3.0 user's manual. Washington, DC.7. US Environmental Protection Agency, Office of Research and Development. 1991; EPA 600/3-91/021; US.
[27] R.M. Smith, A.E. Martell, R.J. Motekaitis, NIST crititically selected stability constants of metal complexes database. NIST Standard Reference Database 46, Version 7.0., NIST, Gaithersburg, MD, 2003.
[28] P. Amico, R.P. Bonomo, R. Cali, V. Cucinotta, P.G. Daniele, G. Ostacoli, E. Rizzarelli, Inorg. Chem. 28 (1989) 3555.
[29] N. Serrano, J.M. Díaz-Cruz, C. Ariño, M. Esteban, Electroanalysis 18 (2006) 955.
[30] R.M. Smith, A.E. Martell, Critical Stability Constants, Inorganic Complexes, vol. 4, Plenum Press, New York, 1976.
[31] R. Kalvoda, W. Anstine, M. Heyrovsky, Anal. Chim. Acta 50 (1970) 93.
[32] E. Casassas, C. Ariño, J. Electroanal. Chem. 213 (1986) 235.
[33] M. Sluyters, J.H. Sluyters, J. Electroanal. Chem. 39 (1972) 339.
[34] F. Berbel, J.M. Díaz-Cruz, C. Ariño, M. Esteban, J. Electroanal. Chem. 432 (1997) 243.
[35] R. Paterson, C. Devine, J. Chem. Soc. Faraday Trans. I 76 (1980) 1052.
[36] R. Paterson, Lutfullah, J. Chem. Soc. Faraday Trans. I 74 (1978) 93.
[37] R. Paterson, Lutfullah, J. Chem. Soc. Faraday Trans. I 74 (1978) 103.
[38] G.C. Barker, J.A. Bolzan, Fres. Z. Anal. Chem. 216 (1966) 215.
[39] J.B. Flanagan, K. Takahashi, F.C. Anson, J. Electroanal. Chem. 85 (1977) 257.
[40] J. Ambrose, A.K. Covington, H.R. Thirsk, Trans. Faraday Soc. 65 (1969) 1897.

DISCUSSIÓ DELS RESULTATS

Cas de la formació de complexos làbils senzills sense adsorció electròdica: sistema Cd(II)-ftalat

Les corbes SSCP obtingudes pel sistema Cd(II)-ftalat (figura 3 del treball 9.1) mostren una disminució en l'alçada de l'ona i un desplaçament cap a valors de potencial de deposició més negatius, a mesura que augmenta la concentració de ftalat. Aquest comportament és consistent amb la formació esperada de complexos electroquímicament làbils d'estequiometria 1:1 i 1:2 amb coeficients de difusió més petits, però relativament semblants al de l'ió metàl·lic lliure.

A partir dels paràmetres i constants introduïdes al full de càlcul SSCP-Analyzer, s'obtenen els valors de la concentració de cadmi lliure (c^*_{Cd}) per dues vies d'anàlisi de la corba SSCP diferents (taula 9.1). Per una banda s'estima el valor de la (c^*_{Cd}) al peu de la corba o, el que és el mateix, en el límit dels potencials de deposició menys negatius i, per altra banda, la (c^*_{Cd}) s'obté a partir dels valors del temps de transició límit de les mesures SCP. Al mateix temps, el SSCP-Analyzer ens proporciona els valors de les constants de complexació (K_c). A partir d'aquests valors de K_c i de les diferents concentracions de ftalat, es calculen les constants d'estabilitat dels complexos Cd-ft i Cd-ft_2 (taula 9.1).

Cas de la formació de complexos làbils senzills amb adsorció electròdica: sistema Cd(II)-iodur

Estudis previs del sistema Cd(II)-iodur per diferents tècniques descriuen l'existència de fins a quatre complexos d'estequiometria compresa entre 1:1 i 1:4 en funció de les condicions experimentals. La presència d'adsorció electròdica en la superfície del mercuri converteix al sistema Cd(II)-iodur en un candidat perfecte per comprovar si l'adsorció és un impediment o no per a la metodologia SSCP-Analyzer.

Les corbes SSCP obtingudes pel sistema Cd(II)-iodur (figura 5 del treball 9.1) són consistents amb un comportament electroquímicament làbil de complexos Cd(II)-iodur amb coeficients de difusió més grans que el de l'ió metàl·lic lliure, ja que l'addició de

lligand produeix un lleuger increment en l'alçada de les corbes sigmoïdals i un desplaçament d'aquestes cap a potencials de deposició més negatius.

La introducció en el SSCP-Analyzer dels paràmetres generals del sistema Cd(II)-iodur, les constants i els valors dels temps de transició (τ) per a cada potencial de deposició aplicat, permet calcular, entre d'altres, els valors de la (c^*_{Cd}) (taula 9.1) i K_c. A partir d'aquests valors de K_c i de les diferents concentracions de iodur, es calculen les constants d'estabilitat dels complexos Cd-I, Cd-I_2, Cd-I_3 i Cd-I_4 (taula 9.1).

La concordança d'aquests valors amb els recollits de la literatura, suggereix que la SSCP minimitza els efectes de l'adsorció electròdica i que la metodologia SSCP-Analyzer és adequada tan per a l'estudi de sistemes amb lligands senzills sense adsorció electròdica com per a sistemes amb lligands senzills amb adsorció electròdica.

Taula 9.1. Resum dels sistemes M-lligand estudiats en el capítol 9.

<table>
<tr><td rowspan="4">Cd(II)-ftalat

pH 5.5
Força iònica 0.01 M</td><td rowspan="4">SSCP, I_{ox}: 10^{-8}A

HMDE</td><td>[ftalat] (M)</td><td colspan="2">c^*_{Cd} (x 10^{-7} M)
SSCP-Analyzer
al peu de l'ona</td><td colspan="2">c^*_{Cd} (x 10^{-7} M)
SSCP-Analyzer
τ_{lim} , ε = 0.923</td><td>c^*_{Cd} (x 10^{-7} M)
ISE</td></tr>
<tr><td>1.22 x 10^{-3}
5.89 x 10^{-3}
2.15 x 10^{-2}</td><td colspan="2">6.91
3.46
0.40</td><td colspan="2">8.84
4.04
0.48</td><td>6.74
3.20
---</td></tr>
<tr><td rowspan="2">SSCP-Analyzer</td><td colspan="3">log β_1</td><td colspan="3">log β_2</td></tr>
<tr><td colspan="3">2.816 (0.002)</td><td colspan="3">4.830 (0.002)</td></tr>
<tr><td rowspan="4">Cd(II)-iodur

pH 5.5
Força iònica 0.1 M</td><td rowspan="4">SSCP, I_{ox}: 10^{-8}A

HMDE</td><td>[iodur] (M)</td><td colspan="2">c^*_{Cd} (x 10^{-7} M)
SSCP-Analyzer
al peu de l'ona</td><td colspan="2">c^*_{Cd} (x 10^{-7} M)
SSCP-Analyzer
τ_{lim} , ε = 1.36</td><td>c^*_{Cd} (x 10^{-7} M)
ISE</td></tr>
<tr><td>1.48 x 10^{-3}
1.09 x 10^{-2}
2.05 x 10^{-2}
7.68 x 10^{-2}
1.01 x 10^{-1}</td><td colspan="2">8.25 (0.35)
3.27 (0.20)
1.59 (0.07)
0.15 (0.01)
0.10 (0.06)</td><td colspan="2">6.92
2.65
1.74
0.19
0.10</td><td>7.51
2.78
1.85

---</td></tr>
<tr><td rowspan="2">SSCP-Analyzer</td><td>log β_1</td><td>log β_2</td><td>log β_3</td><td colspan="2">log β_4</td></tr>
<tr><td>2.16 (0.01)</td><td>3.63 (0.04)</td><td>4.60 (0.09)</td><td colspan="2">5.66 (0.05)</td></tr>
</table>

CAPÍTOL 10

Estudis cronopotenciomètrics de redissolució amb acumulació per adsorció

CAPÍTOL 10. Estudis cronopotenciomètrics de redissolució amb acumulació per adsorció dels complexos metàl·lics amb pèptids amb un contingut elevat de grups tiol

Els complexos de metalls pesants amb pèptids amb un nombre elevat de grups tiol (-SH), com les metal·lotioneïnes (MT), el glutatió (GSH) o les fitoquelatines (PC_n), han estat estudiats prèviament mitjançant tècniques polarogràfiques i voltamperomètriques. L'estudi d'aquests sistemes mostra senyals solapats corresponents a la reducció reversible de l'ió metàl·lic lliure, a la reducció irreversible dels ions metàl·lics enllaçats fortament amb el pèptid i alguns processos d'oxidació del mercuri, però el major inconvenient d'aquestes tècniques és la seva limitada sensibilitat que en dificulta l'estudi a les baixes concentracions existents en els medis naturals.

La voltamperometria de redissolució anòdica semblava inicialment una alternativa al problema, però a la pràctica no es pot aplicar degut a la forta adsorció de l'espècie tiol i

especialment pel caràcter irreversible dels senyals de reducció dels complexos metàl·lics amb els pèptids.

Aquest capítol conté dos treballs on es presenta l'estudi de l'aplicació de la cronopotenciometria de redissolució amb acumulació per adsorció a intensitat constant (AdSCP) als complexos metàl·lics amb diferents pèptids a concentracions μM.

10.1 *Constant current stripping chronopotentiometry for the study of adsorbing inert and electrochemically nonreversible metal complexes at low concentrations: application to Cd and Zn metallothioneins*

N. Serrano, I. Šestáková, J.M. Díaz-Cruz

Electroanalysis 18 **(2006)** 169-176

Full Paper

Constant Current Stripping Chronopotentiometry for the Study of Adsorbing Inert and Electrochemically Nonreversible Metal Complexes at Low Concentrations: Application to Cd and Zn Metallothioneins

Núria Serrano,[a] *Ivana Šestáková*,[b]* *José Manuel Díaz-Cruz*[a]

[a] Departament de Química Analítica, Facultat de Química, Universitat de Barcelona, Av. Diagonal 647, E-08028 Barcelona, Spain
[b] J. Heyrovský Institute of Physical Chemistry, Academy of Sciences of the Czech Republic, Dolejškova 3, CZ-18223 Prague 8, Czech Republic
*e-mail: sestakov@jh-inst.cas.cz

Received: August 30, 2005
Accepted: August 30, 2005

Abstract
Constant current chronopotentiometric stripping analysis using adsorptive accumulation and negative stripping current (AdSCP) was applied for the study of behavior of rabbit liver Cd-Zn and Zn metallothionein (Cd-Zn-MT, ZnMT) on hanging mercury drop electrode. Electrochemically inert or labile behavior of complexes can be distinguished with the application of high (1000 nA) or low (100 to 20 nA) current. Using high current, no influence of added Cd^{2+} or Zn^{2+} ions on the reduction of Cd(II) or Zn(II) complexed within MT molecule was observed, except of additions of Cd^{2+} to ZnMT, where bound Zn(II) was substituted by cadmium ions. With lowering of stripping current and increasing concentration of added Cd^{2+} or Zn^{2+} ions in solution progressive formation of reorganized complex with labile behavior is observed. Parallel measurement using DC voltammetry with different rates of polarization or differential pulse voltammetry were in agreement with AdSCP measurement. However, only chronopotentiometric method combines good sensitivity and signal separation at μM concentrations, inevitable in MT studies.

Keywords: Metallothionein, Constant current chronopotentiometry, Voltammetry

DOI: 10.1002/elan.200503390

This Paper is Dedicated to Professor Karel Štulík on the Occasion of His 65th Birthday.

1. Introduction

Metallothioneins (MTs) are a class of low molecular weight proteins (6 – 7 KDa) with a very high capability to bind metals such as Zn, Cd, Cu or Hg due to their high cysteine (Cys) content and, in particular, the spatial distribution of the Cys residues [1]. An important characteristic of metallothioneins is the formation of metal-thiolate bonds possessing specific spectroscopic features and arranged in metal-thiolate clusters. MTs are important in homeostatic control, metabolism and detoxification of several essential or toxic trace metals.

Mammalian metallothioneins were studied most extensively, and results from NMR and X-ray diffraction studies showed that in Cd_7 MT, Zn_7 MT and Cd_5Zn_2 MT the metals are tetrahedrally coordinated by sulfur atoms. Two metal binding domains (α and β) are recognized, which participate in formation of two metal-thiolate clusters with Cd(II) or Zn(II), having stoichiometries Me_4S_{11}-cluster α, and Me_3S_9-cluster β. In rabbit liver Cd_5Zn_2 MT, clusters composition $Cd_4S_{11}(\alpha)$ and $CdZn_2S_9(\beta)$ were found [2]. These structures were further confirmed using ESI-MS method or molecular modeling techniques [3, 4].

Due to their electrochemical activity, mammalian metallothioneins were also subject for application of a great variety of polarographic and voltammetric techniques using dropping, stationary or hanging mercury electrodes [5 – 18] or carbon composite electrode [19 – 21]. On mercury electrode, two types of electrochemical reactions were described for Cd and Zn containing mammalian metallothioneins: reduction of tetracoordinated Cd(II) or Zn(II) and oxidation of mercury electrode in the presence of thiol groups complexed in MT. Apart from that, additions of excessive cadmium or zinc ions into solutions with MT were studied and revealed new peaks, which were attributed to the formation of mixed metal complexes with stoichiometries different from original Me_4S_{11} and Me_3S_9. Such different complexes were confirmed by studies of complexation of separate (α) or (β) metallothionein domain with cadmium and zinc ions using differential pulse polarography [22 – 24] and also with electrospray ionization mass spectrometry [25]. New complexes are formed by reorganization of initially present structures and contain different amount of

bound metals. Nevertheless, no differences in voltammetric signals due to cadmium and zinc binding with (α) or (β) metallothionein domain were found.

It has been shown that stripping chronopotentiometry (SCP), also termed potentiometric stripping analysis (PSA), constitutes a valuable alternative to voltammetry and is less sensitive to the presence of important quantities of organic matter (mainly by comparison of SCP results with GFAAS and ICP-OES data) [26–28].

Stripping chronopotentiometry can be performed in two different manners. In the first, a deposition step identical with that of anodic stripping voltammetry is included. During stripping step the accumulated metal is reoxidized by the action of a chemical oxidant or by imposing a constant oxidizing current. The other mode of SCP is an analogy to cathodic stripping voltammetry (CSV) with adsorptive accumulation (AdSV), where negative stripping current is applied. SCP has been exploited for determination of total amount of heavy metals in foods, beverages and biological samples, but the use of SCP in the field of heavy metal speciation is scarce.

There are some theoretical considerations and experimental evidence on the use of constant-current SCP (CCSCP) with hanging mercury drop electrode (HMDE) [29, 30] and with rotating disk mercury film electrode (RDE-MFE) [31] for heavy metal speciation. In these the effect of SCP oxidative current on the stripping regime in both HMDE and MFE-RDE electrodes was studied. In the case of HMDE [29, 31], the presence of three characteristic regions was confirmed: high currents ensure semi-infinite linear diffusion, low currents produce total depletion and very low currents suffer from interference of dissolved oxygen. In MFE-RDE [31], the total depletion regime predominates in a wide range of oxidation currents.

Recently, stripping chronopotentiometry on HMDE has been applied for very sensitive determination of metallothioneins based on catalytic hydrogen evolution [32–34], but no study of behavior of Cd-Zn-MT or Zn-MT has been performed. In order to fill this gap, we used CCSCP with negative current (AdSCP) or with positive stripping current to study rabbit liver Cd-Zn-metallothionein and Zn-metallothionein II on HMDE, in absence or in presence of excessive cadmium or zinc ions. In parallel, DC and differential pulse voltammetry measurements were performed for possible comparison with literature data.

Additionally, we studied voltammetric behavior of Cd-Zn-metallothionein on mercury film prepared on glassy carbon disk electrode (MF-GC) and on newly introduced silver solid amalgam electrode (MF-AgSAE) [35]. Behavior of metallothionein on mercury film electrode after prolonged adsorption was described in recent literature [36–38].

2. Experimental

2.1. Reagents

The Cd-Zn-MT (lot 052K7012, cadmium content 3% and zinc content 1%) and the Zn-MT II (lot 51K7005, zinc content 4.1% and cadmium content 0.3%) were obtained from Sigma Chemicals. Freshly prepared stock solution in buffer of pH 8.5 was used for measurements. Doubly distilled water (quartz apparatus), suprapure chemicals $Na_2B_4O_7$, and HNO_3 65% , standard solutions of cadmium or zinc (metal concentration of 1.000 ± 0.002 g L^{-1}) (Merck), were used.

2.2. Apparatus

Chronopotentiometric and voltammetric measurements were performed using PC-ETP analyzer with Polar4 software (Polaro Sensors, Czech Republic). The reference electrode (to which all potentials are referred) and the auxiliary electrode were $Ag/AgCl/KCl_{sat}$ and Pt wire, respectively. The working electrode was a pen-type mercury electrode (Polaro Sensors, Czech Republic) working in HMDE mode.

In some cases, working electrode was a mercury film deposited on a glassy carbon disk electrode of 1.5 mm diameter (MF-GC) or a mercury film deposited on a silver solid amalgam electrode of 0.4 mm diameter (MF-AgSAE) [35]. Pure nitrogen was used for degassing solutions prior to measurements, and for passing above the solution during the measurements.

2.3. Preparation of Mercury Film on the MF-GC

First the glassy carbon disk was polished using a suspension of alumina particles of 0.05 μm diameter. Then, the electrode was attached to the stand with the reference and auxiliary electrodes and immersed into a solution containing 200 mg L^{-1} of $HgCl_2$ and 0.1 mol L^{-1} HCl. After deaeration of the solution for 10 min, a deposition potential of -0.5 V was applied for 2 min with solution stirring, followed by a rest period (without stirring) of 30 s. Then, both deposition and resting periods were repeated at -0.6, -0.7, -0.8 and -0.9 V and, finally, three further times at -0.9 V. Once the mercury film had been deposited, the three electrodes were rinsed with water and transferred into measuring cell. The described procedure has been proven [31] to produce a stable mercury film.

2.4. Preparation and Activation of Mercury Film on the MF-AgSAE

Prior to deposition of the film, a solid amalgam disk was polished using a suspension of alumina particles of 0.05 μm diameter. Then, the electrode with the reference and

auxiliary electrodes was attached to the stand and introduced into the cell with a solution containing 0.01 mol L^{-1} $HgCl_2$ and 0.1 mol L^{-1} HCl. A deposition potential of -0.8 V was applied for 10 min with solution stirring. After depositing the mercury film, the surface was electrochemically activated in 0.2 mol L^{-1} KCl by applying -2.2 V for 5 min while stirring the solution.

2.5. Voltammetric and Chronopotentiometric Measurements

Before each set of measurement, whole electrochemical cell including borate buffer was analyzed for traces of metals using anodic stripping voltammetry on HMDE. (Detection limits 1×10^{-10} mol L^{-1} for Cd and Pb, 1×10^{-9} mol L^{-1} for Cu and 1×10^{-8} mol L^{-1} for Zn). Into the clean cell a new solution of 10 mL of freshly prepared borate buffer of pH 8.5 was placed and 600 μL of freshly prepared stock solution of metallothionein was added. (Stock solution concentration was 4.00×10^{-5} M for Zn-MT (II) and 4.14×10^{-5} M for Cd-Zn-MT). Then, the sample was deaerated with pure nitrogen for 10 min and the measurement was performed. Further, aliquots of Cd^{2+} or Zn^{2+} stock solutions were added into the cell. For each composition of analyzed solution, chronopotentiometric curves with different constant values of stripping current were recorded, further differential pulse voltammetric curves with scan rate 10 mV s^{-1} and DC voltammetric curves with different scan rates were recorded. For every measurement, new mercury drop was formed. In all measurements we avoid formation of mercury compounds-therefore potentials more positive than -0.5 V were not included. The same values of potential and of accumulation time were maintained for chronopotentiometric and voltammetric measurements.

3. Results and Discussion

3.1. Voltammetry on HMDE

The voltammogram of Cd-Zn-MT recorded with hanging mercury electrode (HMDE) using DC voltammetry (Fig. 1)

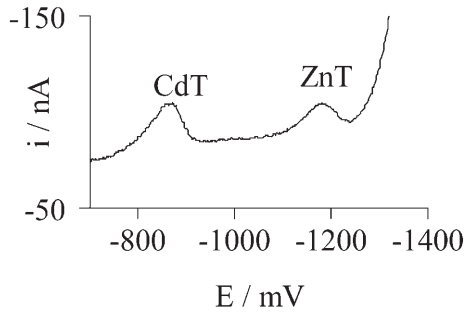

Fig. 1. DC voltammogram of 2.34×10^{-6} M Cd-Zn-MT on HMDE, borate buffer pH 8.5. Scan from -0.6 V to -1.4 V. Scan rate 25 mV s^{-1}.

shows the reduction of complexed Cd(II) at $E_p = -0.85$ V and of complexed Zn(II) at $E_p = -1.2$ V.

The electrochemical reactions involved are:

$$CdT + 2e^- \rightarrow Cd(Hg) + T \quad (1)$$

$$ZnT + 2e^- \rightarrow Zn(Hg) + T \quad (2)$$

where CdT and ZnT represent complex where Cd(II) or Zn(II) are bound to sulfur, T is a molecule from which the metal ion is missing (apoform of MT). Using the starting potential of -0.6 V, oxidation of mercury electrode in the presence of S-Cd or S-Zn groups is not taking place – therefore no substitution of bound metals by mercury ions occurs and no reduction of mercury compounds is recorded.

As the CdT or ZnT reduction peaks are diffusion controlled [10, 17], the theory of elimination voltammetry [39] was applied in the case of Cd-Zn-MT or CdMT [18]. Theory of elimination voltammetry was developed in order to separate the effect of diffusion, kinetic and charging current on the total measured current, and is able to supply more detailed information about the process on the electrode [40–44]. For diffusion controlled peaks, current function, where diffusion current is conserved and kinetic and charging current are eliminated, was calculated according to Equations 23 and 31 in [39]:

$f(I_d) = 17.4857\, I - 11.657\, I_{1/2} - 5.8284\, I_2$
Equation 23 in [39],

or

$f(I_d) = 43.213\, I - 48.041\, I_{1/2} - 11.657\, I_2 + 16.485\, I_{1/4}$
Equation 31 in [39]

In case that the transported species is adsorbed before reduction, a characteristic peak-counterpeak form for $f(I_d)$ current function is obtained [41–44]. The described shape of current function was found in EVLS measurement for Cd (II) reduction in rabbit liver CdMT and for both, Cd(II) and Zn(II) reduction in Cd-Zn-MT [18].

For ZnMT, we made analogous EVLS measurement, applying polarization rates of 100, 200, 400 and 800 mV s^{-1} in DC measurement. From the set of digital data current functions $f(I_d)$ according to Equations 23 or 31 were calculated. As is shown in Figure 2, reduction of Zn(II) in ZnMT also takes place on HMDE in adsorbed state.

Therefore for both, Cd-Zn-MT and ZnMT, a short time (15 s) of adsorptive accumulation is sufficient for application of constant current chronopotentiometry with negative current.

3.1.1. Study of the Cd-Zn-MT System by CCSCP, DCV and DPV

The application of negative stripping currents to Cd-Zn-MT adsorbed on HMDE produces a chronopotentiogram with two separate peaks in a wide range of currents (Fig. 3). In

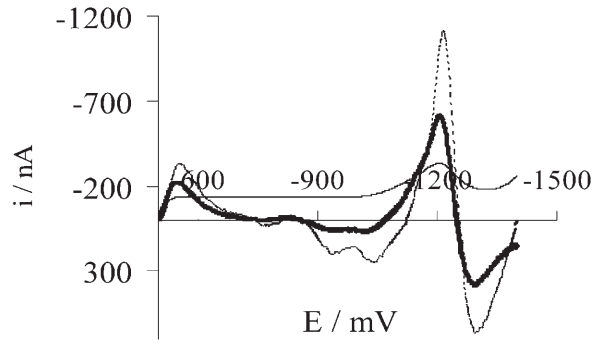

Fig. 2. Elimination voltammetry with linear scan. 2.26×10^{-6} M Zn-MT [(—) $v_{ref} = 400$ mV/s, (bold curve) $f(I_d) =$ Eq. 23 and (dotted curve) $f(I_d) =$ Eq. 31].

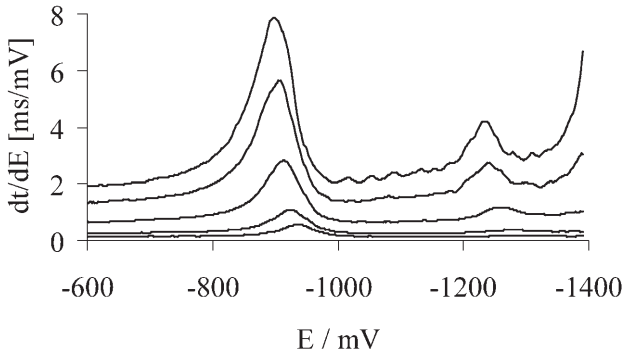

Fig. 3. Chronopotentiogram of 2.34×10^{-6} M Cd-Zn-MT, dependence on negative currents at $E_A = -0.5$ V applying rest time of 15 s. $I = -1000$, -500, -200, -100 and -70 nA.

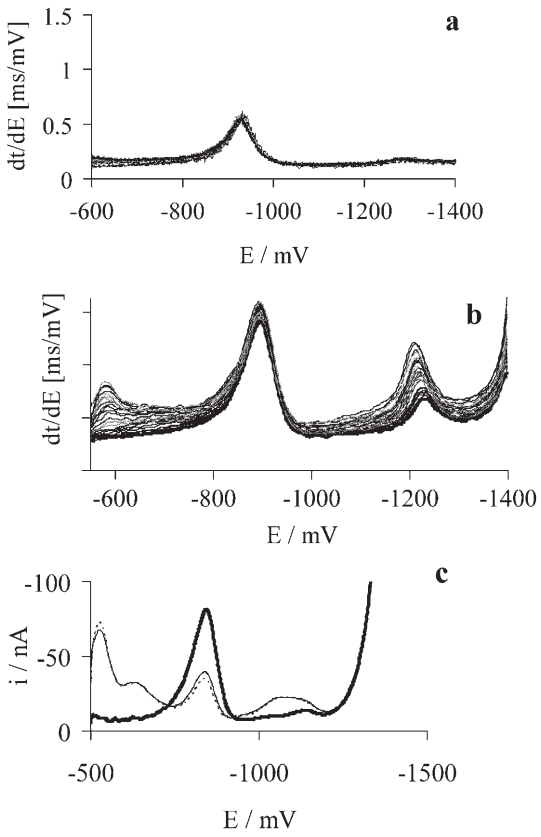

Fig. 4. Signals measured on HMDE during additions of 5×10^{-5} M Cd^{2+} solution to 2.34×10^{-6} M Cd-Zn-MT in borate buffer pH 8.5. Cd^{2+}additions from 50 μL to 2000 μL (concentration in cell from 2.5×10^{-7} to 7.9×10^{-6} M Cd^{2+}). AdSCP using rest time of 15 s at -0.5 V, a) $I = -1000$ nA, b) $I = -100$ nA. c) DPV signals measured from -0.5 V with scan rate of 10 mV s^{-1} after rest time of 15 s. Shown only 2.34×10^{-6} M Cd-Zn-MT (bold curve), 6.4 and 7.9×10^{-6} M Cd^{2+}).

agreement with voltammetric measurements, the peak at potential range between -0.90 and -0.93 V is attributed to a complexed Cd (II) within metallothionein (CdT peak) and the second peak at potentials between -1.23 and -1.27 V is due to the complexed Zn(II) – peak ZnT.

Monotonous increase of peaks was observed with decreasing value of reducing current, no other peaks were observed. This is in agreement with inert behavior of Cd(II) and Zn(II) complexes in Cd-Zn-MT as shown earlier with cyclic voltammetry [10, 17, 18].

3.1.1.1. Additions of Cd^{2+} to a Cd-Zn-MT Solution

After successive additions of Cd^{2+}, different behavior is observed with stripping chronopotentiometry in the dependence on value of stripping current: using a stripping current of -1000 nA, practically no changes in the height or position of CdT and ZnT peaks are observed (Fig. 4a). When stripping current of -100 nA is used, a shoulder appears on each original peak and increases with additions of Cd^{2+}; finally a small peak at $E_p = -0.58$ V is visible (Fig. 4b).

Voltammetric measurement performed parallel to chronopotentiometry is in agreement with already published MT behavior in the presence of cadmium ions in solution [8 – 12, 17]. In Fig. 4c a DP voltammogram is shown with two initial peaks CdT and ZnT. With the additions of Cd^{2+} the peak CdT is decreasing and two new peaks in the Cd-region are observed, the peak CdT′ attributed to the reduction of Cd(II) in the newly formed complex (E_p close to -0.63 V) and the peak at about -0.52 V related to the reduction of the free Cd^{2+}. In the Zn-region, a new peak ZnT′ increases at about -1.05 V.

DC voltammetric measurement of solution where ratio of added Cd^{2+} to [Cd-Zn-MT] was equal 3.4 : 1 shows the dependence of peaks on applied polarization rate. Using 160 mV s^{-1}, only CdT and ZnT peaks are visible. With decreasing scan rate, shoulder at about -1.1 V (peak ZnT′) grows on original ZnT signal. Using scan rate of 40 mV s^{-1}, signal of Zn^{2+} at about -0.98 V is observed. (Fig. 5)

Rather complex records of the system Cd-Zn-MT with added Cd^{2+}, as observed with different methods, can be explained by electrochemically inert and labile behavior of the involved complexes, considered in the time-scale of electrochemical measurement. In our case, inert behavior is exhibited when the complex practically does not dissociate within the time scale of the measurement, whereas labile behavior appears when dissociation is much faster than measurement [45, 46].

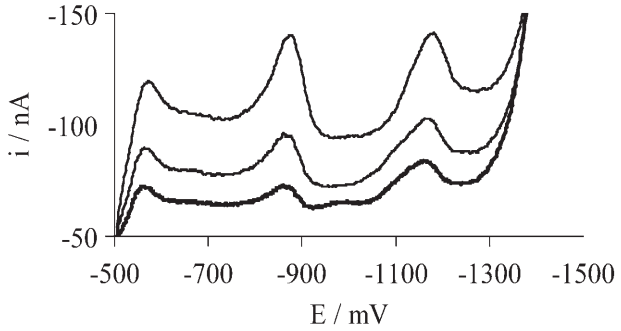

Fig. 5. Labile behavior of Zn complex in 2.34×10^{-6} M Cd-Zn-MT and 7.9×10^{-6} M Cd^{2+} in borate buffer pH 8.5, DCV on HMDE from -0.5 V, scan rate [mV s^{-1}]: (bold curve) 40, (—) 80, (dotted curve) 160.

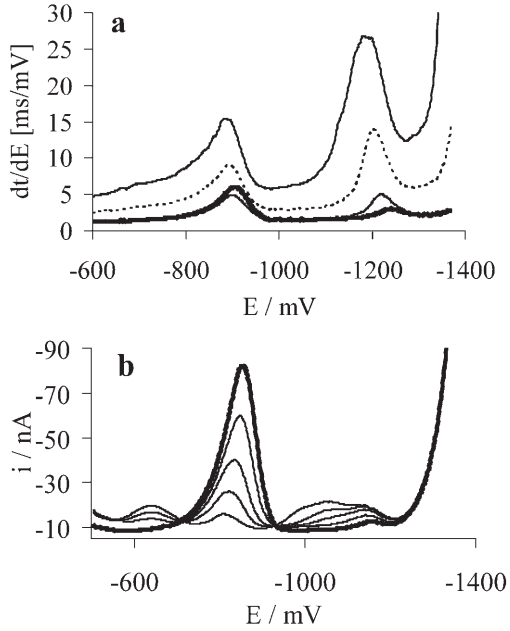

Fig. 6. Additions of Zn^{2+} to 2.34×10^{-6} M Cd-Zn-MT in borate buffer pH 8.5. a) AdSCP, rest time of 15 s at -0.5 V, only 2.34×10^{-6} M Cd-Zn-MT, $I = -100$ nA (bold curve); added 2.3×10^{-6} M Zn^{2+}, $I = -100$, -50, and -30 nA. b) DPV from -0.5 V with rest time of 15 s. Concentrations of added Zn^{2+}: 0 (bold curve), 0.93, 1.4, 1.85 and 2.3×10^{-6} M.

With the addition of Cd^{2+} into solution containing Cd-Zn-MT, reorganization of metals bound in original clusters takes place. This has been shown not only by differential pulse polarography [22–24] but also using electrospray ionization mass spectrometry [25]. In chronopotentiometry, application of high currents is connected with short stripping times, and therefore there is no time for such reorganization of the original structure. Similar case is DC voltammetry with sufficiently high polarization rate. In both cases, only inert complex is observed, and no changes appear on recorded chronopotentiometric or voltammetric curves.

When long-time measurement is applied (chronopotentiometry with small current, DC voltammetry with slow scan rate or differential pulse voltammetry), there is enough time for reorganization of the original complex, and further for noticeable dissociation of some of the Zn(II) or Cd(II) ions bound within this reorganized complex. In such measurements, increase of new peaks due to the reduction of metals bound in the reorganized complex (CdT′, ZnT′) or even reduction peak of unbound metal could be observed. The question arises concerning the role of mercury electrode in connection with the observed labile behavior. Unfortunately, measurements on various types of carbon electrodes [19–21] are not sensitive enough to provide the answer.

3.1.1.2. Additions of $Zn^{2+}$to a Cd-Zn-MT Solution

The chronopotentiograms corresponding to additions of Zn^{2+} to Cd-Zn-MT solution applying negative currents are again different according to the value of the current applied. With current -1000 nA, practically no changes with the additions of Zn^{2+} are observed. When currents -100 nA or lower are applied, the initial peak of complexed Cd(II) at $E_p = -0.90$ V is decreasing and shoulder appears at about -0.65 V (peak CdT′). The original Zn(II) peak at $E_p = -1.23$ V is increasing and shifting towards less negative potentials. (Fig. 6a). The described behavior is observed also with DC voltammetry using scan rates 40–320 mV s^{-1}(not shown), and even more pronounced, when DPV is applied (Fig. 6b). Here we can clearly observe three peaks in Zn-region: original ZnT signal at E_p ca. -1.15 V, second signal of complexed Zn(II) at about -1.05 V and signal of free Zn^{2+} at about -0.98 V. The behavior observed in DC and DP voltammetry is again similar as described earlier in literature, with new peaks CdT′ and ZnT′ belonging to the reorganized complex.

3.1.2. Study of the Zn-MT II System by CCSCP, DCV and DPV

The behavior of Zn-MT studied by voltammetric methods was found more complex, and two peaks of complexed Zn(II) -ZnT and ZnT′, together with peak corresponding to uncomplexed zinc, were described in studies using differential pulse polarography or square wave voltammetry [13, 16, 17]. Also, in studies of complexation of the synthetically prepared α-MT or β-MT domain with zinc ions, two peaks ZnT and ZnT′ are present in the exces of each domain, whereas at excess of metal, only peak ZnT′ is observed [22–24].

In our study of the Zn-MT II system by CCSCP using adsorptive accumulation on HMDE, the dependence on value of applied stripping current again appears (Fig. 7a). For currents between -1000 and -300 nA we can clearly see only one peak at about -1.22 V (ZnT). When stripping currents lower than -200 nA are used, a second peak appears (ZnT′) and peak potentials for both, ZnT and ZnT′ are shifting towards less negative values – thus, in the potential range between -1.03 and -1.30 V, two overlapping peaks are observed. Those peaks at E_p close to -1.13 and -1.18 V are attributed, in agreement with

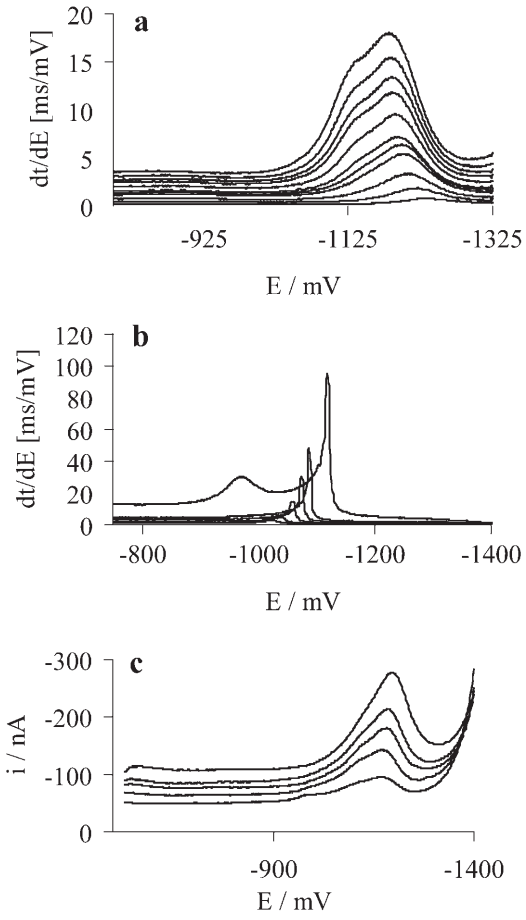

Fig. 7. 2.26×10^{-6} M Zn-MT II in borate buffer pH 8.5 on HMDE. a) chronopotentiogram, dependence on negative currents at $E_A = -0.5$ V applying rest time of 15 s. – $I = 1000$, 400, 300, 200, 170, 150, 120, 100, 90, 80, 70 nA. b) Chronopotentiogram, dependence on positive currents at $E_A = -1.4$ V using deposition time of 10 s (stirring) and rest time of 15 s. $I = 200$, 150, 100, 70, 50 and 20 nA. c) DC voltammogram, scan from -0.5 V to -1.4 V. Scan rate 320, 200, 160, 100 and 40 mV s^{-1}.

previous studies, to two differently complexed Zn(II). Chronopotentiometric measurement suggest, that reorganization connected with the appearance of peak ZnT′ is slow (therefore only one peak is observed with high current applied) and during long time measurement, some Zn(II) bound in slowly formed complex dissociates and a peak of free Zn appears.

In agreement with this is also the dependence on current value, when positive current is used after accumulation of ZnMT at -1.4 V (Fig. 7b).

In DC voltammetry using a wide range of polarization rates (Fig.7c), a differentiation between labile and inert behavior also appears – even when peak separation is much worse than in chronopotentiometry. Applying scan rates higher than 320 mV s^{-1} just one peak close to -1.20 V is shown, with scan rates between 300 and 150 mV s^{-1} a second peak at ca. -1.10 V appears, and finally using scan rates lower than 150 mV s^{-1}, three peaks are observed. The peaks at ca. -1.20 V (ZnT) and -1.10 V (ZnT′), and a new peak at ca. -0.99 V which is attributed to the reduction of free Zn^{2+}.

3.1.2.1. *Additions of Cd^{2+} to a Zn-MT II Solution*

The chronopotentiograms corresponding to the addition of Cd^{2+} to Zn-MT II solution are shown in Figure 8. Applying a stripping current of -1000 nA (Fig. 8a) the chronopotentiogram before the addition of Cd^{2+} shows only one peak in the Zn-region at ca. -1.24 V (peak ZnT) and a very small peak CdT close to -0.9 V. After the progressive addition of Cd^{2+}, the initial peak at -0.9 V increases steadily and simultaneously the peak due to a Zn-T complex decreases. This is consistent with substitution of Zn(II) by Cd(II) inside the original MT molecule.

When lower stripping current is used, there is time for reorganization, and two peaks of complexed Zn(II) are observed (Fig. 8b, ZnT′ peak with E_p close to -1.13 and ZnT peak at -1.20 V). With Cd^{2+} additions, two peaks at Cd-region are increasing (CdT′ – 0.69 V and CdT – 0.85 V), together with increasing shoulder at Zn-region (ZnT′at -1.13 V).

In simultaneously performed DP measurement (Fig. 8c) there is no peak corresponding to original ZnT peak (only shoulder is present), and the increase of peaks ZnT′ (at about -1.1 V), CdT′ (-0.65 V) and of free Zn (-0.96 V) is observed.

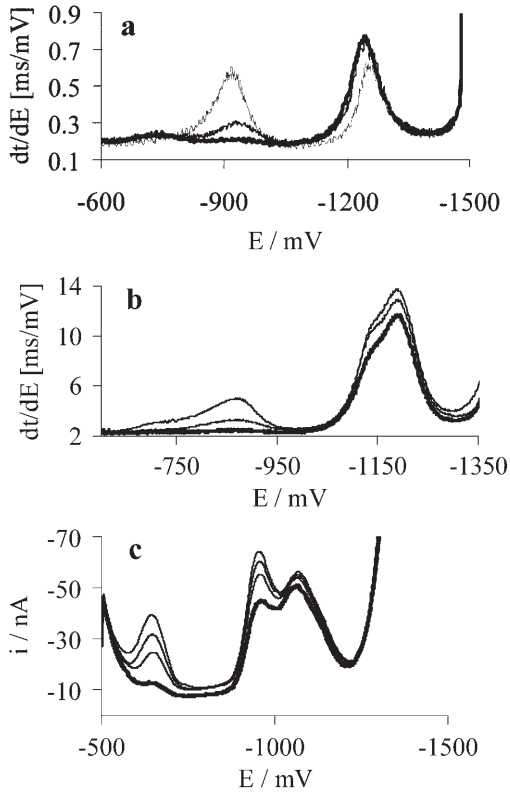

Fig. 8. Signals measured on HMDE during the addition of 4×10^{-5} M Cd^{2+} solution to 2.26×10^{-6} M Zn-MT in borate buffer pH 8.5. a) AdSCP using rest time of 15 s at -0.5 V and $I = -1000$ and b) -100 nA. c) DPV from -0.5 V after rest time of 15 s. Added Cd^{2+} concentrations from 0 (bold curve) to 4.28×10^{-6} M.

3.1.2.2. Additions of Zn^{2+} to a Zn-MT II Solution

Using a stripping current of -1000 nA only one signal at ca. -1.25 V (peak ZnT) is shown, and no apparent changes with the successive additions of Zn^{2+} are observed.

Apparent changes are not observed for additions of Zn^{2+} to a Zn-MT II solution even with current of -100 nA, as is shown in Figure 9. But when even lower current is used, there is time enough for formation of reorganized complex, exhibiting labile behavior. As is demonstrated by chronopotentiogram in Figure 9, with application of current -20 nA, an apparent increase of the shoulder at ca. -1.10 V corresponding to newly formed complex is observed, and also another new peak at about -1.0 V, corresponding to the reduction of free Zn^{2+}, could be seen.

On DP voltammogram of 2.26×10^{-6} M Zn-MT (Fig. 9b), mainly ZnT′ peak is observed (at about -1.07 V) with only a shoulder corresponding to the ZnT peak at about -1.15 V and peak of free Zn reduction (-0.96 V). When successive additions of Zn^{2+} to a solution of Zn-MT II were carried out, a great increase of the free Zn^{2+} signal could be seen, together with a smaller increase of peak at -1.15 V.

Our measurements are again consistent with earlier differential pulse polarographic studies, where Zn^{2+} ions were added to Zn-MT [47–48] or to separate (α) or (β) metallothionein domain [22–24]. There ZnT′ peak is ascribed to Zn(II) bound in a less stable position and increases with increasing concentration of metal in solution. Our chronopotentiometric measurements are showing that reorganization of the original molecule (connected with the appearance of peak ZnT′) is slow and therefore is not observed when fast method is applied. On the other hand, the exchange of Zn (II) for Cd(II) within the original molecule is fast and therefore the application of high stripping current can follow such reaction without disturbances.

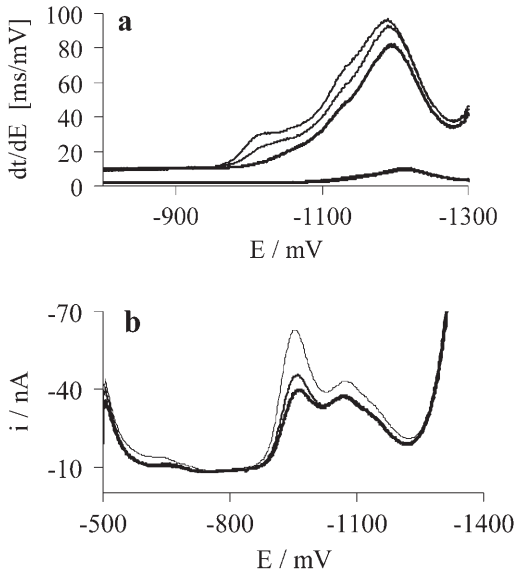

Fig. 9. Signals measured on HMDE during the addition of 10^{-4} M Zn^{2+} solution to 2.26×10^{-6} M Zn-MT in borate buffer pH 8.5. a) AdSCP using rest time of 15 s at -0.5 V and $I = -100$ and -20 nA. b) DPV from -0.5 V after rest time of 15 s. Added Zn^{2+} concentrations: 0 (bold curve), 1.4 and 2.3×10^{-6} M.

3.2. Mercury Film Electrodes

DC and DP voltammetric measurements recorded with 2.34×10^{-6} M Cd-Zn-MT on MF-GC electrode, prepared according the procedure in Experimental part exhibited poor sensitivity and were not reproducible.

The measurement on silver solid amalgam electrode with mercury film (MF-AgSAE) was sensitive enough, but the problem arises with the reproducibility. The usual procedure, when the MF-AgSAE is electrochemically cleaned by application of negative or positive potential (or by cycling between two selected values) [49] is not possible in case of metallothioneins. During this procedure, the bound metals are released, and under nitrogen atmosphere applied in our measurement, no oxidation takes place, and only reduction of mercury compound corresponding to apometallothionein (E_p at about -0.75 V) is seen. Therefore, the only possibility is to use MF-AgSAE for single measurement, after activation in 0.2 KCl in a separate solution. As is shown in Figure 10, DPV record corresponds to that on HMDE (Fig. 1). To perform the study with addition of metal ions would be nevertheless much more difficult than on HMDE, and was not attempted.

4. Conclusions

The adsorptive accumulation constant current chronopotentiometric stripping analysis (AdSCP) appears to be a valuable alternative to the polarographic techniques (mainly DPP and SWP) for the study of metallothioneins, phytochelatins and related compounds and, in general, for the study of adsorbing inert electrochemically non reversible metal complexes.

The application of AdSCP on HMDE presents a great experimental simplicity and reproducibility and a wide range of stripping currents with a total depletion regime can be used. This wide range permits to change the measurement time to study behavior of electrochemically inert or labile complexes. Moreover, the interferences of free ions

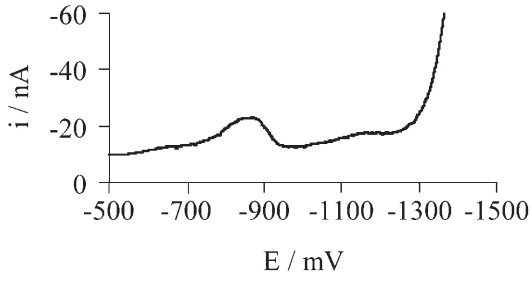

Fig. 10. 1.9×10^{-6} M Cd-Zn-MT in borate buffer pH 8.5, DP voltammetry after activation of mercury film in 0.2 M KCl.

(which do not adsorb onto the electrode) are in this mode suppressed, especially when high currents are used.

The AdSCP measurement of Cd-Zn-MT or ZnMT solutions with the additions of cadmium or zinc ions are in agreement with earlier results obtained by polarographic or voltammetric methods. However, the chronopotentiometric method combines the possibility to study both, long-time and short time processes with very good sensitivity and signals separation, which is not possible using voltammetric method (DPV is slow, DC or CV have poor sensitivity using slow scan rates at low concentrations).

Newly introduced MF-AgSAE appeared sensitive enough for μM concentrations of metallothioneins, but suitable only for single measurement. Activation or electrochemical pretreatment of the electrode is necessary in a separate solution.

5. Acknowledgements

The authors gratefully acknowledge financial support from the project COST OC-D21.002 from The Ministry of Education, Youth and Sports of the Czech Republic, project BQU2003-07587-C02-01 from the Spanish Ministry of Science and Technology and project 2001SGR-00056 from the Generalitat de Catalunya. Núria Serrano acknowledges the University of Barcelona for a Ph.D. grant and for the financial support for the stay in the J. Heyrovský Institute of Physical Chemistry, Academy of Sciences of the Czech Republic.

6. References

[1] M. J. Stillman, *Metallothioneins, Synthesis, Structure and Properties of Metallothioneins, Phytochelatins and Metal-Thiolate Complexes* (Eds: M. J. Stillman, C. F. Shaw III, K. T. Suzuki), VCH, New York **1992.**
[2] M. J. Stillman, *Coord. Chem. Rev.* **1995**, *144*, 461.
[3] J. Chan, Z. Huang, M. E. Merrifield, M. T. Salgado, M. J. Stillman, *Coord. Chem. Rev.* **2002**, *233–234*, 319.
[4] N. Romero-Isard, M. Vašák, *J. Inorg. Biochem.* **2002**, *88*, 388.
[5] A. Muñoz, A. R. Rodríguez, *Electroanalysis* **1995**, *7*, 674.
[6] M. Fedurco, I. Šestáková, *Bioelectrochem. Bioenerg.* **1996**, *40*, 223.
[7] B. Raspor, J. Pavičić, *Fresenius J. Anal. Chem*. **1996**, *354*, 529.
[8] C. Ruiz, A. R. Rodríguez, *Anal. Chim. Acta* **1997**, *350*, 305.
[9] O. Nieto, G. Hellemans, G. Bordin, M. De Ley, A. R. Rodríguez, *Bioelectrochem. Bioenerg.* **1998**, *46*, 45.
[10] C. Harlyk, O. Nieto, G. Bordin, A. R. Rodríguez, *J. Electroanal. Chem*. **1998**, *458*, 199.
[11] C. Harlyk, O. Nieto, G. Bordin, A. R. Rodríguez, *J .Electroanal. Chem*. **1998**, *451*, 267.
[12] M. Erk, B. Raspor, *J .Electroanal. Chem*. **1999**, *466*, 71.
[13] M. Dabrio, A. R. Rodríguez, *Anal. Chim. Acta* **1999**, *385*, 295.
[14] O. Nieto, A. R. Rodríguez, *Electroanalysis* **1999**, *11*, 175.
[15] M. Esteban, C. Harlyk, A. R. Rodríguez, *J. Electroanal. Chem*. **1999**, *468*, 202.
[16] M. Dabrio, A. R. Rodríguez, *Electroanalysis* **2000**, *12*, 1026.
[17] A. R. Rodríguez, M. Esteban, *Cell. Mol. Biol.* **2000**, *46*, 237.
[18] I. Šestáková, T. Navrátil, *Bioinorg. Chem. Appl.* **2005**, *3*, 43.
[19] I. Šestáková, D. Miholová, H. Vodičková, P. Mader, *Electroanalysis* **1995**, *7*, 237.
[20] I. Šestáková, P. Mader, *Cell. Mol. Biol.* **2000**, *46*, 257.
[21] I. Šestáková, M. Kopanica, L. Havran, E. Paleček, *Electroanalysis* **2000**, *12*, 237.
[22] M. Dabrio, A. R. Rodríguez, *Analusis* **2000**, *28*, 370.
[23] M. Dabrio, A. R. Rodríguez, *Anal. Chim. Acta* **2000**, *424*, 77.
[24] M. J. Lopez, C. Ariño, S. Díaz-Cruz, J. M. Díaz-Cruz, R. Tauler, M. Esteban, *Environ. Sci. Technol.* **2003**, *37*, 5609.
[25] M. Dabrio, G. V. Vyncht, G. Bordin, A. R. Rodríguez, *Anal. Chim. Acta* **2001**, *435*, 319.
[26] J. M. Estela, C. Tomás, A. Cladera, V. Cerdà, *Crit. Rev. Anal. Chem.* **1995**, *25*, 91.
[27] D. Jagner, *Analyst* **1982**, *107*, 593.
[28] M. L. Gozzo, L. Colacicco, C. Callà, G. Barbaresi, R. Parroni, B. Giardina, S. Lippa, *Clin. Chim. Acta* **1999**, *285*, 53.
[29] R. M. Town, H. P. van Leeuwen, *J. Electroanal. Chem*. **2001**, *509*, 58.
[30] R. M. Town, H. P. van Leeuwen, *J. Electroanal. Chem*. **2002**, *523*, 1.
[31] N. Serrano, J. M. Díaz-Cruz, C. Ariño, M.Esteban, *J. Electroanal. Chem*. **2003**, *560*, 105.
[32] M. Tomschik, L. Havran, E. Paleček, M. Heyrovský, *Electroanalysis* **2000**, *12*, 274.
[33] R. Kizek, L. Trnková, E. Paleček, *Anal. Chem.* **2001**, *73*, 4801.
[34] L. Trnková, R. Kizek, J. Vacek, *Bioelectrochemistry* **2002**, *56*, 57.
[35] B. Yosypchuk, L. Novotný, *Electroanalysis* **2002**, *14*, 1733.
[36] F. Song, A. L. Briseno, F. Zhou, *Langmuir* **2001**, *17*, 4081.
[37] A. J. Briseno, F. Song, A. J. Baca, F. Zhou, *J. Electroanal. Chem*. **2001**, *513*, 16.
[38] A. J. Baca, Y. Garcia, A. L. Briseno, F. Zhou, *J. Electroanal. Chem*. **2001**, *513*, 23.
[39] O. Dračka, *J. Electroanal. Chem.* **1996**, *402*, 19.
[40] L. Trnková, O. Dračka, *J. Electroanal. Chem.* **1996**, *413*, 123.
[41] L. Trnková, R. Kizek, O. Dračka, *Electroanalysis* **2000**, *12*, 905.
[42] L. Trnková, R. Kizek, O. Dračka, *Bioelectrochemistry* **2002**, *55*, 131.
[43] L. Trnková, *Talanta* **2002**, *56*, 887.
[44] L. Trnková, *J. Electroanal. Chem.* **2005**, *582*, 258.
[45] M. Fernández, Ch. Ariño, J. M. Díaz-Cruz, R. Tauler, M. Esteban, *Electroanalysis* **2001**, *13*, 1405.
[46] J. Pinheiro, A. M. Mota, M. L.S. Simões Gonçalves, *J. Electroanal. Chem.* **1996**, *402*, 47.
[47] O. Nieto, G. Hellemans, G. Bordin, M. De Ley, A. R. Rodríguez, *Talanta* **1998**, *46*, 315.
[48] M. S. Díaz-Cruz, M. J. López, J. M. Díaz-Cruz, M. Esteban, *J. Electroanal. Chem*. **2002**, *523*, 114.
[49] R. Fadrná, K. Cahová-Kuchaříková, L. Havran, B. Yosypchuk, M. Fojta, *Electroanalysis* **2005**, *17*, 459.

10.2 *Adsorptive accumulation in constant current stripping chronopotentiometry as an alternative for the electrochemical study of metal complexation by thiol-containing peptides*

N. Serrano, I. Šestáková, J.M. Díaz-Cruz, C. Ariño

Journal of Electroanalytical Chemistry 591 **(2006)** 105-117

Available online at www.sciencedirect.com
SCIENCE DIRECT
Journal of Electroanalytical Chemistry 591 (2006) 105–117
Journal of Electroanalytical Chemistry
www.elsevier.com/locate/jelechem

Adsorptive accumulation in constant current stripping chronopotentiometry as an alternative for the electrochemical study of metal complexation by thiol-containing peptides

Núria Serrano [a], Ivana Šestáková [b], José Manuel Díaz-Cruz [a,*], Cristina Ariño [a]

[a] Departament de Química Analítica, Facultat de Química, Universitat de Barcelona, Martí i Franquès, 1-11, E-08028 Barcelona, Spain
[b] J. Heyrovský Institute of Physical Chemistry, Academy of Sciences of the Czech Republic, CZ-182 23 Prague 8, Czech Republic

Received 5 October 2005; received in revised form 9 February 2006; accepted 24 March 2006
Available online 11 May 2006

Abstract

Constant current chronopotentiometric stripping analysis using adsorptive accumulation and negative current (AdSCP) was applied as an alternative for the study of metal complexation of glutathione (GSH) or (γ-Glu-Cys)$_2$-Gly (PC_2) with zinc ions on hanging mercury drop electrode. The behavior of the formed Zn-complexes was studied using voltammetric and chronopotentiometric methods. A multivariate curve resolution method by alternating least-squares (MCR-ALS) applied to DP voltammetric and chronopotentiometric measurements of Zn–PC_2 system made possible the formulation of a complexation model. Moreover, the use of small currents in AdSCP allows one to obtain acceptable sensitivities and signal separation at very low concentrations, which is important in peptide studies under conditions similar to these of natural media.

Keywords: Stripping chronopotentiometry; Adsorptive accumulation; Phytochelatins; Glutathione; Zinc complexes; Multivariate curve resolution by alternating least squares

1. Introduction

Glutathione (GSH) is widely present in living systems and it is usually the most abundant intracellular nonprotein thiol [1]. GSH (γ-Glu-Cys-Gly) has two peptide bonds, two carboxylic acid groups, one amino group and one thiol group. The addition of a γ-Glu-Cys fragment from glutathione to another glutathione allows to synthesize a phytochelatin (γ-Glu-Cys)$_n$-Gly with $n = 2$. To increase the repeating unit from n to $n + 1$, where n ranges from 2 to 11 [2], another γ-Glu-Cys fragment is added to the phytochelatin chain. Phytochelatins (PC), as their structure shows, are thiol-rich peptides and they are synthesized enzymatically by plants in response to an excessive uptake of certain heavy metal ions, especially Cd^{2+}. Other metal ions were found to be active in provoking PC synthesis, e.g. Pb^{2+}, Zn^{2+}, Ag^{+}, Hg^{2+}, Cu^{+} [2–7]. Because of the affinity of the thiol group for heavy metals, complexation by these thiol-containing peptides is important in toxicology and in environmental sciences.

Polarographic and voltammetric techniques, especially in differential pulse mode (DPP or DPV), have been widely used for the study of heavy metal complexes of thiol-containing peptides as GSH [8–12] or PCs [13–15]. In general terms, they produce intrincate sets of overlapping signals corresponding to the reversible reduction of the free metal ion, the irreversible reduction of strongly bound metal ions and some oxidation processes of mercury. A major drawback of these techniques is the limited sensitivity, which hinders the study at the low concentrations existing in natural media. Despite anodic stripping voltammetry (ASV) seems a priori a solution for this problem, it cannot be applied in practise due to the strong adsorption of thiol

* Corresponding author. Tel.: +34 93 403 91 16; fax: +34 93 402 12 33.
E-mail address: josemanuel.diaz@ub.edu (J.M. Díaz-Cruz).

0022-0728/$ - see front matter © 2006 Elsevier B.V. All rights reserved.
doi:10.1016/j.jelechem.2006.03.038

species but especially because of the irreversible character of the reduction of metal complexes, which does not produce the corresponding oxidation signals during the stripping step.

Stripping chronopotentiometry techniques (SCP) appear as an alternative to voltammetry because it has been empirically proved to be less sensitive to the presence of important quantities of organic matter (mainly by comparison of SCP results with GFAAS and ICP-OES data) [16–19].

Stripping chronopotentiometry can be performed in two different manners. The first includes a deposition step of metal reduction identical to that of anodic stripping voltammetry and a stripping step where the accumulated metal is reoxidised by the action of a chemical oxidant or by imposing a constant oxidising current. The other mode of SCP is a chronopotentiometric stripping analysis with adsorptive accumulation (AdSCP), where negative stripping currents are applied to reduce the species adsorbed on the electrode during the deposition step. The later modality presents the advantage of revealing irreversible reduction processes that would not produce the corresponding oxidation signals during an oxidative stripping.

Also the use of elimination voltammetry with linear scan (EVLS) permits to supply more detailed information about the process on the electrode, mainly to distinguish between reaction of the electroactive substance transported to the electrode by diffusion only and reaction where transported substance is adsorbed [20–24]. This has been reported for calf thymus DNA on HMDE [20] or on silver electrode [22], azidothymidine on HMDE [23,24] and rabbit liver metallothioneins on HMDE [25]. In case of metallothioneins, it has been shown that the adsorptive accumulation constant current chronopotentiometric stripping analysis (AdSCP) constitutes a valuable alternative to the polarographic techniques (mainly DPP and SWP) for the study of metallothioneins (MT) [26,27].

In the present study, AdSCP on a hanging mercury drop electrode (HMDE) is applied to the analysis of complexes of Zn(II) with GSH or with (γ-Glu-Cys)$_2$Gly. In particular, the wide range of reduction currents available has been applied to investigate the changes in the electron transfer kinetics of some of the complexes involved. For comparative purposes, additional measurements have been carried out by SCP (to notice which irreversible processes appear in AdSCP but not in SCP) and by two diffusion-controlled techniques of different time scale like direct current voltammetry (DCV) and differential pulse voltammetry (DPV) (to notice which diffusion-controlled signals are not present in AdSCP). Using chronopotentiometric and voltammetric techniques, different type of reduction or oxidation signals of Zn–GSH and Zn-phytochelatin complexes were obtained at pH 8.5. The possibility of overlapping signals for some concentrations ratio was apparent from DPV, SCP and AdSCP. Such a problem can be solved satisfactorily by applying a multivariate curve resolution method based on an alternating least-square optimization (MCR-ALS) [30,31].

2. Experimental

2.1. Reagents

The glutathione (L-glutathione reduced, $\geqslant$98%, Sigma–Aldrich)-freshly prepared solution in buffer pH 8.5 was used for measurements. Double distilled water (quartz apparatus), suprapure grade chemicals $Na_2B_4O_7$, standard solution of zinc, with a metal concentration of $1.000 \pm 0.002\ g\ l^{-1}$ and HNO_3 65% (Merck) were used. (γ-Glu-Cys)$_2$Gly was synthesized in the Institute of Organic Chemistry and Biochemistry, AS CR, Prague. The Merrifield method [28] with procedure modification described in [15] was applied. For measurements, freshly prepared solutions of peptide in borate buffer pH 8.5 were used.

2.2. Apparatus and measurements

Chronopotentiometric and voltammetric measurements were performed using PC-ETP analyzer with Polar4 software (Polaro Sensors, Czech Republic). The reference electrode (to which all potentials are referred) and the auxiliary electrode were $Ag/AgCl/KCl_{sat}$ and Pt wire, respectively. The working electrode used was a pen-type mercury electrode, drop surface area of $0.013\ mm^2$ (HMDE). Pure nitrogen was used for degassing of solution prior to the measurements and passing above the solution during the measurements.

When not otherwise indicated, DCV and DPV measurements were done in a single mercury drop (HMDE) at scan rates of 100 and $10\ mV\ s^{-1}$, respectively, using a pulse amplitude of 50 mV in the case of DPV. Stripping chronopotentiograms were carried out using a deposition time of 15 s without solution stirring followed by the application of a constant stripping current. The deposition potential was -1.4 V for the SCP modality which applies anodic stripping currents and -0.3, -0.6 or -0.7 V for the modality which uses cathodic stripping currents (AdSCP).

2.3. Data treatment

Elimination voltammetry with linear scan (EVLS) was developed [29] as method comprising the elimination of some particular currents from the measurement of linear scan voltammetry. The total current, measured at different scan rates is expressed as sum of particular currents

$$I = \sum I_j, \quad I = I_d + I_c + I_k + \cdots \tag{1}$$

and each particular current is expressed in the form of two independent functions:

$$I_j = W_j(v) Y_j(E) \tag{2}$$

where $W_j(v)$ is the scan rate function and $Y_j(E)$ is a function specific for every current, independent on scan rate v (e.g., $I_d = v^{1/2} Y_d(E)$ diffusion current, $I_k = v^0 Y_k(E)$ kinetic current, $I_c = v^1 Y_c(E)$ charging current). The elimination

function is constructed as linear combination of total currents, measured at v (reference scan rate), and at multiples or fractions of reference scan rate

$$f(I) = \sum_k a_k I(v_k) \quad (3)$$

By solving a set of equations with $m + 1$ v_k values, one particular current could be conserved, m particular currents eliminated ($f(I_j) = 0$) and coefficients a_k calculated. Detailed procedure is described in original papers [29,22]. The current function eliminating the kinetic and charging current and conserving the diffusion current calculated in the original paper [29] for scan rates v, $2v$, $1/2v$:

$$f(I_d) = 17.4857I - 11.657I_{1/2} - 5.8284I_2 \quad \text{Eq. (23) in [29]} \quad (4a)$$

and for scan rates v, $2v$, $1/2v$ and $1/4v$:

$$f(I_d) = 43.213I - 48.041I_{1/2} - 11.657I_2 + 16.485I_{1/4} \quad \text{Eq. (31) in [29]} \quad (4b)$$

revealed in further studies characteristic peak-counterpeak form in case that transported species is adsorbed on the electrode [20,22,24].

For solutions of GSH or $(\gamma\text{-Glu-Cys})_2$Gly with zinc ions, a set of DC-voltammograms with different rates of polarisation (v_{ref}, $v_{1/2}$, $v_{1/4}$, $2v$) was recorded on HMDE, within the same potential range and the same resolution. Digital set of current values was then used for calculation according to Eqs. (4a) and (4b) in Excel.

The application of MCR-ALS to experimental data requires a linear contribution of all components to the overall signal, which is not necessarily true in electrochemical measurements. However, previous studies show that voltammetric signals of inert electroactive complexes are reasonably close to linearity [30]. Then, signals measured under different conditions are arranged in a data matrix $\boldsymbol{S}$ with as many rows as the number of recorded signals and as many columns as the number of registered potentials. Then, singular value decomposition (SVD) is applied to estimate the number of mathematical components or factors contributing linearly to the signal. In some cases, as for instance in spectroscopic measurements, such components are the chemical species [31]. In some others, as for instance in electrochemical ones, the component or the factor must be interpreted as the electrochemical process which generates the measured signal [9,30,32]. Finally, the matrix $\boldsymbol{S}$ is decomposed as a product of a matrix $\boldsymbol{C}$ (containing the concentration of every component) and a matrix $\boldsymbol{V}^T$ (containing the corresponding pure signals) plus an error matrix $\boldsymbol{X}$ [30,31]:

$$\boldsymbol{S} = \boldsymbol{C}\boldsymbol{V}^T + \boldsymbol{X}, \quad (5)$$

where 'T' denotes transposed matrix. This procedure is carried out in an iterative way from an initial estimation of concentration profiles or pure signals for the postulated number of components [30,31]. Along the iterations, several restrictions (constraints) can be imposed, such as *selectivity* (only one component is present in some parts of the matrix), *non-negativity* (of concentrations and/or signals) or *signal shape* (fitting of the signals to an empirical equation) [31]. The relative error of the matrix decomposition is expressed as a percentage of lack of fit (lof) [30,31]. All these MCR-ALS procedures are carried out through several programs implemented in MATLAB [33], which are freely available (http://www.ub.es/gesq/mcr/mcr.htm).

In the present work, the applicability of the described MCR-ALS methodology is discussed for the case of dt/dE signals obtained in SCP and AdSCP measurements.

3. Results and discussion

3.1. General considerations on the nature of the processes involved in SCP and AdSCP

It is out of the scope of the present work to provide a rigorous theoretical basis for SCP and, especially, AdSCP in the simultaneous presence of reversible and irreversible processes. Indeed, we believe that a first theoretical approach should consider simpler situations such as an adsorbing metal complex that can be reversibly reduced onto the electrode. Nevertheless, we would like to introduce some qualitative considerations for a better understanding of the nature and evolution of SCP and AdSCP signals in the systems considered in this work.

According to previous voltammetric investigations, in this kind of systems three major types of electrochemical processes take place:

(i) The reduction of the free metal ion and, eventually, of some weak, labile complexes, which usually produces a single, reversible signal (although in certain media, Zn(II) can suffer losses of reversibility).
(ii) The reduction of strong, inert metal complexes, which usually produces an irreversible signal for each different type of metal strongly bound to the ligand. The electrochemical irreversibility is reflected in the wider shape of the voltammetric signals and, especially, in the absence of anodic signal in CV.
(iii) The anodic oxidation of the mercury of the electrode in the presence of the free ligand and their metal complexes, which usually involves Hg(I) and Hg(II) species.

Thus, signals related to all these processes are expected in stripping chronopotentiometric measurements on heavy metal–thiol peptide systems.

In conventional SCP measurements at a mercury drop electrode (HMDE), the application of a deposition potential sufficiently negative allows the reduction of both free metal and inert electroactive complexes to the mercury amalgam. Then, the application of a constant positive current during the stripping step produces the oxidation of the deposited cadmium to free metal ion and some complexes

whose electrochemical reduction/oxidation process is not too irreversible. However, the oxidation to complexes with a high electrochemical irreversibility is not possible and their presence could be not detected in SCP. If the stripping current is relatively low, a *total depletion* regime can be assumed and a linear behaviour is expected between the transition time τ and the bulk concentration of the metal c^*_M [19]:

$$\tau = \text{ct.} \cdot c^*_M / I, \tag{6}$$

where ct. is a constant depending of several parameters like the electrode surface or the deposition time and I is the stripping current. In principle, the signals of inert complexes should follow an analogous equation with c^*_{ML} instead of c^*_M.

In the case of AdSCP measurements, the electrochemical processes involved are quite different. During the deposition step, carried out in the absence of stirring, metal complexes are being adsorbed onto the electrode surface at a potential which does not allow reduction of the free metal ion. In the case of strong adsorption (typical of thiol compounds) and for short deposition times that prevent saturation of the adsorbed layer, adsorptive accumulation can be assumed to be diffusion-controlled and, hence, proportional to the concentration of the complex in the bulk solution c^*_{ML}:

$$\Gamma_{ML} = \text{ct.} \cdot c^*_{ML}, \tag{7}$$

where Γ_{ML} is the surface excess of the complex and ct. is a constant. When the stripping step starts in the unstirred sample, the application of the negative current I causes first the reduction of the free metal ion from the solution. If all complexes are electrochemically inert in both dissolved and adsorbed phases for the time window of the technique (which is determined by the magnitude of the stripping current), there will be no additional contribution of metal ion coming from the dissociation of the complex in both the solution and the adsorbed layer. Then, the transition time τ can be described according to a *semi-infinite linear diffusion regime* for which the Sand's equation holds [35,36]:

$$\tau^{1/2} = (nFAD_M^{1/2}\pi^{1/2}c^*_M)/(2I) \tag{8}$$

where I is the constant cathodic current and D_M, c^*_M are, respectively, the diffusion coefficient and the bulk concentration of the free metal ion *in the solution* (not in the mercury amalgam like in the case of conventional SCP, where the metal is oxidised *from the electrode*). On the contrary, if the time window of AdSCP allows a significant dissociation of some complexes (in solution and/or in adsorbed phase), the diffusive flux of the metal ion would be enhanced in a way quite difficult to quantify. The analogy with previous experiences in voltammetry suggests that complex dissociation should produce a decrease of the reduction signals of the complexes and also an increase and a negative potential shift of the signal of free metal ion [37].

Afterwards, when the concentration of free metal ion on the electrode surface approaches zero, the potential becomes more negative and the reduction of the adsorbed complexes starts. For the case of electrochemically inert complexes which do not dissociate appreciably in adsorbed phase during the stripping step, it is reasonable to assume a *total depletion regime* (molecules are restricted to a very thin film around the electrode, so that they can be fast and easily reduced to atomic metal and free ligand, which later diffuse inside the mercury and the solution, respectively). If the prefixed deposition time produces a surface excess Γ_{ML}, then, the application of electrolysis laws leads to the equation:

$$\tau = (nFA\Gamma_{ML})/I, \tag{9}$$

where I is again the cathodic stripping current. Thus, taking into account Eq. (7), a linear dependence is expected between the transition time and the bulk concentration of each complex:

$$\tau = nFA\text{ct.} \cdot c^*_{ML}/I. \tag{10}$$

Concerning to the shape of the adsorptive signals of complexes, it should be not very different from that of conventional SCP measurements under depletive conditions, provided that the electrochemical irreversibility does not produce a significant broadening of the signal. From a qualitative point of view, it is clear that the transition time τ (i.e., the area of dt/dE peaks) should be proportional to the concentration of the complex in the bulk solution (Eq. (10)) and also that the characteristic potential is related to the formal reduction potential of the complex including contributions of adsorption energy and irreversibility. Nevertheless, a rigorous quantitative relationship between the shape and relevant parameters of the electrochemical system is not yet available.

It must be pointed out that, besides the reduction of the adsorbed phase, the transition time associated to metal complexes has also a contribution from the complex molecules in solution which diffuse towards the electrode. The diffusive component of the signal should follow a semi-infinite linear regime (Eq. (8)) that could affect the linearity between τ and c^*_{ML}. However, such component is expected to be much lower than the contribution of the accumulated material, especially considering that the accumulation has previously depleted the amount of complex in the electrode vicinity.

At this point, it is valuable to remark that in AdSCP measurements on electrochemically inert systems, apart from the quite unpredictable presence of anodic signals of mercury, the diffusional signal of the free metal (and eventually, of the complexes) and the adsorptive signals of the complexes will coexist. Increasing the accumulation time would surely augment the relative importance of adsorption signals (provided the adsorbed layer is not saturated). On other hand, the inspection of Eqs. (8) and (9) shows that high reduction currents favour the predominance of adsorptive signals (τ is proportional to $1/I$, whereas in the diffusive case τ is proportional to $1/I^2$) and, obviously, low reduction currents increase the contribution of diffusional signals.

In the case of non-inert systems, a significant fraction of the deposited complexes could dissociate in adsorbed phase during the reduction of the free metal ion in the beginning of the stripping step (i.e., at more positive potentials), thus increasing the transition time of the free metal ion and decreasing the transition time of the complexes in their further reduction at more negative potentials. Additionally, complex dissociation can produce an unpredictable potential shift in the signal of the free metal (coming from diffusion, dissociation in solution and dissociation in adsorbed phase). All these considerations suggest that AdSCP signals obtained under conditions favouring a non-inert behaviour of the complexes (fast measurements) can be quite far from linearity, i.e., from a direct proportionality between τ_i and c_i^*. Fortunately, previous studies by cyclic, square wave and pulse voltammetry have shown that complexes in thiol-metal systems are quite strong and electrochemically inert in a wide range of time windows.

Indeed, an interesting feature of constant-current SCP and AdSCP is the possibility of changing the time window of the measurement by modifying the striping current. In SCP at a mercury drop electrode (HMDE), such possibility is restricted by the need of ensuring a total depletion regime, which demands small currents. In contrast, the adsorptive nature of most of the AdSCP signals should preserve such regime even when high currents are used, thus increasing the range of available time windows. This can be used to explore some kinetic characteristics of the electrochemical systems here considered: fast stripping steps (i.e., high currents) would reveal mostly the irreversible reduction of undissociated metal complexes in adsorbed state and could hinder the reduction of some complexes especially irreversible; in contrast, slow stripping steps (i.e., low currents) would render such reduction processes less irreversible, decreasing in some cases the overpotential (and/or the width of the signal) and allowing some reductions that were not possible at shorter time scales. Nevertheless, it is important to remember that increasing the time scale of the measurement can also lead to a non-negligible dissociation of the adsorbed complexes or to a significant interconversion between the metal ions bound to the adsorbed ligand in different manners, thus modifying the position and height of $d\tau/dE$ signals.

As for the applicability of MCR-ALS to chronopotentiometric signals, the previous discussion suggests that the requirement of linearity can be reasonably fulfilled under the following circumstances:

(i) The stripping regime is total depletion, so that Eqs. (6) or (10) holds (this appears to be true for adsorptive AdSCP signals and also for SCP signals measured at low oxidative currents).
(ii) $d\tau/dE$ peaks are enough symmetrical to assume that the area (τ) is directly proportional to the height (which means that $d\tau/dE$ data can be treated in the same way as current data in previous MCR-ALS studies).
(iii) Inside the time window of the stripping step, complexes do not dissociate and do not interconvert appreciably in adsorbed or dissolved state (which can be confirmed by a constant characteristic potential of the signals involved along the titration of metal with ligand and vice versa).
(iv) There are no changes in the electrochemical (ir)reversibility of the reduction processes along the titration.

This means that SCP and AdSCP signals measured in Zn(II)-GSH and Zn(II)–PC_2 systems are expected to be essentially linear with respect to the concentration of the species with some possible sources of non-linearity (complex dissociation, changes in the electrochemical reversibility, diffusive signals in AdSCP, etc.) whose presence usually produces a progressive potential shift of the signals along the chronopotentiometric titration. Then, MCR-ALS seems a priori fully applicable to depletive SCP and AdSCP $d\tau/dE$ data provided that the predominant signals increase or decrease maintaining a constant characteristic potential. Moreover, the strong character of Zn(II)-thiol complexes does not require an accurate determination of the contributions to the signal intensity of individual species. Indeed, a MCR-ALS semiquantitative analysis of the ligand-to-metal ratios at which the signals appear, disappear or stabilize can be enough to provide valuable information about stoichiometries.

3.2. Study of the Zn–GSH system by CCSCP, DCV and DPV

A great number of studies have been related to the binding of Zn^{2+} by GSH due to the multiple binding sites in GSH, but in a recent work [10] it has been proposed that the predominant GSH-Zn complex has a 2:2 GSH:Zn^{2+} stoichiometry and contains a binuclear cluster of high stability, where two cysteines and two deprotonable groups, most probably the two amino terminals, are entailed. The mechanism proposed by Díaz-Cruz et al. [10] involves two reductions steps. The first step is associated to the reduction of the Zn^{2+} coordinated to the two binding sulfhydryl groups and the two amino groups of the glutamyl residues and the second step, at more negative potentials, is associated to the reduction of the Zn bound to the two sulfhydryl groups and the two glycine carboxylic acids. This electrode reaction mechanism for the reduction process of the 2:2 GSH:Zn^{2+} complex is shown in Fig. 1.

A recent work [27] proves that the adsorptive accumulation constant current chronopotentiometric stripping analysis (AdSCP) is a good alternative to the polarographic techniques and a very sensitive tool for the study of adsorbing inert electrochemically non reversible metal complexes. Then, different comparative experiments using voltammetric and chronopotentiometric techniques were carried out in order to evaluate the possibilities of this SCP modality in the study of the Zn–GSH system.

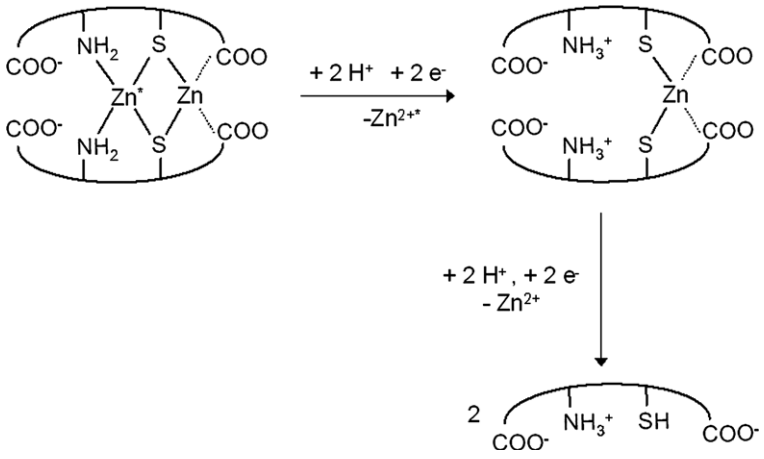

Fig. 1. Proposed electrode reaction mechanism for the reduction process of the 2:2 GSH:Zn^{2+} complex.

The EVLS measurements in case when GSH is added to the excess of zinc (Fig. 2a) or zinc is added to the excess of GSH (Fig. 2b) show a similar character of observed peak-counterpeak shape, so that the application of chronopotentiometry with negative stripping currents can be used because the reduction of Zn–GSH takes place on HMDE in adsorbed state.

The Zn–GSH system, when Zn^{2+} is added to a GSH solution, was studied by AdSCP with a wide range of negative stripping currents. At a Zn^{2+}-to-GSH ratio of 1 (Fig. 3a) the chronopotentiograms, applying stripping currents between −700 and −100 nA, show only a peak which increases and shifts to positive potentials with lower stripping currents. Finally with a stripping current of −50 nA two peaks could be detected: a peak at ca. −1.04 V due to the reduction of the Zn^{2+} bound to the two binding sulfhydryl group and the two amino groups and the peak at ca. −1.17 V attributed to the reduction of the second Zn^{2+} bound to the two sulfhydryl groups and the two glycine carboxylic acids. This is consistent with the fact that the

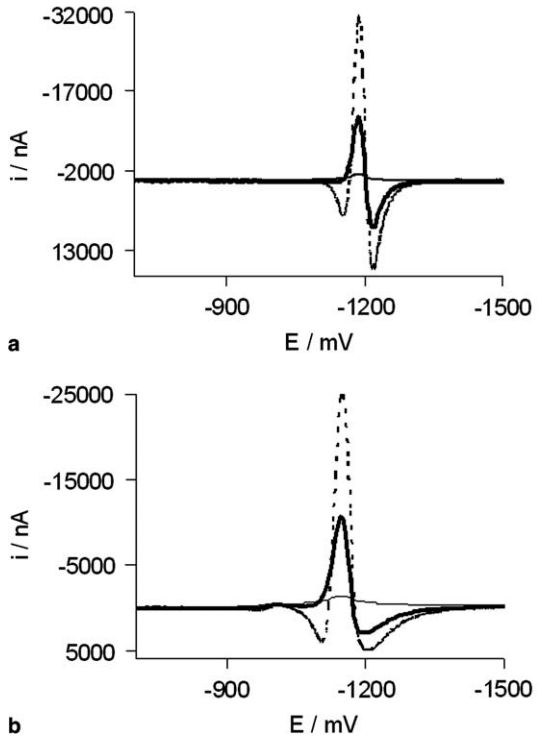

Fig. 2. Elimination voltammetry with linear scan when: (a) GSH is added to an excess of Zn^{2+} and (b) Zn^{2+} is added to an excess of GSH. — v_{ref} 160 mV s^{-1}, — $f(I_d)$ = Eq. (23) and --- $f(I_d)$ = Eq. (31).

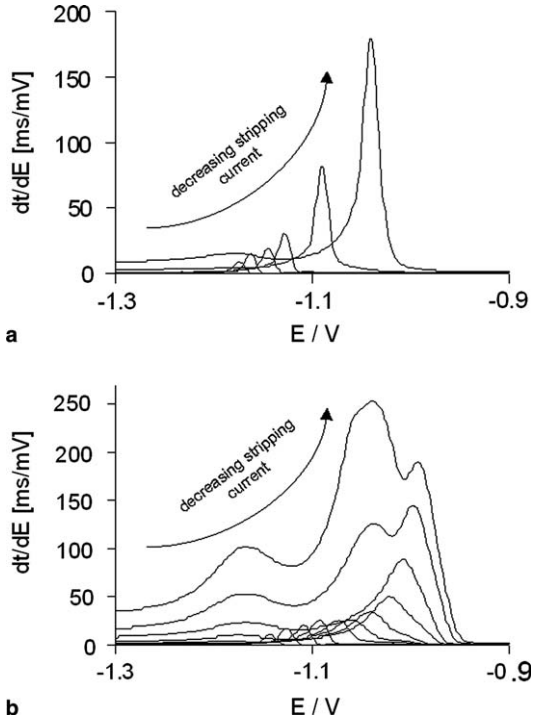

Fig. 3. Chronopotentiograms of Zn^{2+}-GSH system in borate buffer pH 8.5 on HMDE, dependence on negative currents at $E_A = -0.7$ V applying a deposition time of 15 s. (a) Zn^{2+}-to-GSH ratio of 1, $-i$ = 700, 500, 300, 200, 100 and 50 nA. (b) Zn^{2+}-to-GSH ratio of 4, $-i$ = 1000, 700, 500, 400, 300, 250, 200, 150, 100, 70 and 50 nA. Arrows indicate the decreasing stripping current.

time window of the experiment increases at decreasing reduction currents. Then, it is logical that for larger measurement times signals become less irreversible: in one case appears a reduction signal not detected at higher currents and, in the other, the overpotential decreases, shifting the signal to less negative potentials. Finally, the general increase of signals at decreasing currents is an obvious consequence of Eqs. (8) and (9).

After successive additions of Zn^{2+}, when the Zn^{2+}-to-GSH ratio is 4 (Fig. 3b), the chronopotentiograms show also a peak, which increases and shifts with lower stripping currents. At this metal-to-ligand ratio using high negative currents (between −1000 and −100 nA) apart from this peak, a shoulder close to −1.00 V due to the reduction of the free Zn^{2+}, begins to grow. When negative stripping currents lower than −100 nA are applied, which involve longer stripping times, three signals are noticeable. The peaks at ca. −1.04 and −1.17 V and a new peak close to −0.99 V attributed to the (mainly diffusive) reduction of free Zn^{2+}. This fact agrees with the previous considerations that predict a higher proportion of the diffusive signal at smaller stripping currents.

The detailed evolution of the AdSCP measurements during the titration of GSH with Zn^{2+} (stripping current −50 nA) is shown in Fig. 4. At metal-to-ligand ratios lower than 0.5, only the previously described small peak is noticed at quite negative potentials (ca. −1.17 V). This peak is consistent with the formation of the ML_2 complex in Fig. 1 and could be attributed to the reduction of Zn^{2+}-ions bound to two sulfhydryl and two carboxylic groups. At metal-to-ligand ratios higher than 0.5, a second peak appears at less negative potentials which is progressively shifted in the positive direction. This fact is in agreement with the formation of a M_2L_2 complex from ML_2 predicted by the model in Fig. 1: the second signal would correspond to the reduction of Zn^{2+}-ions bound to two sulfhydryl and two amino groups. The progressive shift of the signal could be explained in terms of an increase of the electrochemical reversibility along the titration. Finally, at metal-to-ligand ratios higher than 1, a third signal appears indicating an increasing excess of free Zn^{2+}-ions, also in agreement with Fig. 1.

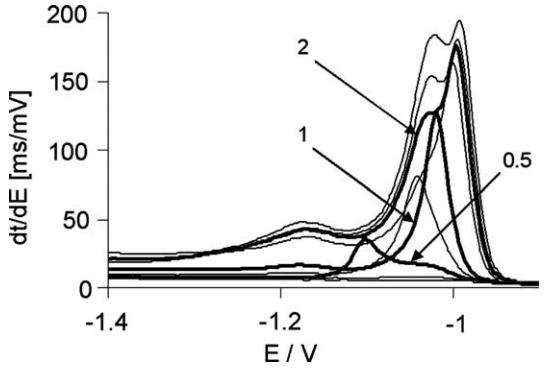

Fig. 4. Chronopotentiometric titration of 1.96×10^{-5} mol l^{-1} GSH with Zn^{2+} solution in borate buffer pH 8.5 on HMDE, using a deposition time of 15 s at −0.7 V and $-i = 50$ nA. Arrows indicate the Zn^{2+}-to-GSH ratio.

In the Zn–GSH system the application of a MCR-ALS analysis is not feasible, due to the progressive shift of the peaks in the course of the titration, which evidences a lack of linearity of the data.

At ratio of Zn^{2+}-to-GSH equal to 2.6, DP voltammetric measurements (Fig. 5a) show only two separate peaks. A high peak at E_p close to −0.94 V and another smaller at ca. −1.11 V are observed due to the two reduction steps in 2:2 complex of Zn with GSH, with the more positive reduction step overlapped by reduction of free Zn^{2+}-ions.

In DC voltammetry (Fig. 5b) the two reductions steps concerning to the 2:2 complex of Zn are observed depending on the scan rate used. With high scan rates the separation of the peaks is not achieved but at scan rate 500–800 mV/s it is possible to observe the two peaks, at ca. −1.07 and −1.17 V, although the resolution is not very good.

This suggests that the two steps involved in the electrode reduction process for the 2:2 GSH:Zn complex are quite irreversible, especially the step attributed to the reduction of the second Zn(II) which could only be seen when long-time measurement methods as chronopotentiometry with small current, DC voltammetry with slow scan rate or differential pulse voltammetry are applied. In the case of the reduction of the first Zn(II) the electrochemical process is

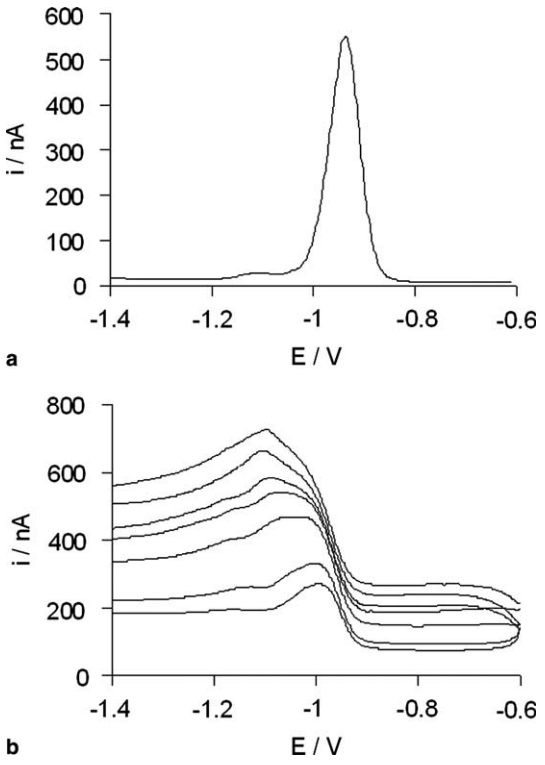

Fig. 5. Voltammetric signals of Zn^{2+}-to-GSH ratio of 2.6 in borate buffer pH 8.5 on HMDE. (a) DPV signal measured from −0.6 V with scan rate 10 mV s^{-1} after rest time of 5 s. (b) DCV signal measured from −0.6 to −1.5 V. Scan rate 100, 200, 500, 700, 800 1000 and 1200 mV s^{-1}.

not so slow to produce no signal but is so close to the irreversible behaviour to exhibit a notorious shift of the signal at increasing scan rates (faster measurements cause more negative peak potentials).

3.3. Study of the Zn(II)–PC_2 system by CCSCP, DCV and DPV

In order to study the behaviour of the Zn(II)–PC_2 system, several DCV, DPV and SCP titrations were carried out in two ways, addition of Zn^{2+} to a peptide solution and addition of the peptide to a Zn^{2+} solution. Fig. 6 shows the signals obtained in some of these experiments.

The evolution of DP voltammograms when the $(\gamma$-Glu-Cys$)_2$Gly peptide is added to a Zn^{2+} solution is shown in Fig. 6a. The initial voltammogram, shows only a peak at ca. −0.96 V attributed to the reduction of the free Zn^{2+}. With the first additions of peptide this peak is increasing and a little shift towards negative potentials is observed, but after successive additions of peptide a progressive decrease of this peak is showed. At −1.25 V a peak is also increasing due to the reduction of a Zn-complex. A peak at potentials between −0.42 and −0.54 V attributed to the reduction of the Hg-peptide complexes formed on the electrode surface is increasing with additions of peptide.

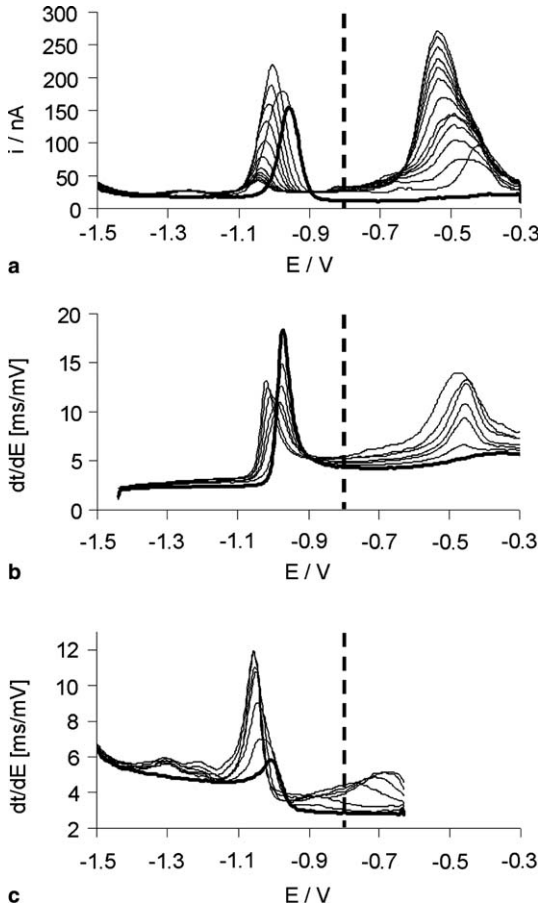

Fig. 6. Signals measured on HMDE at a pH value of 8.5. (a) DPV titration of 1×10^{-5} mol l^{-1} Zn^{2+} with peptide from −0.3 V with scan rate 10 mV s^{-1} and chronopotentiometric titration of 5×10^{-6} mol l^{-1} Zn^{2+} with $(\gamma$-Glu-Cys$)_2$Gly peptide. (b) SCP using a $E_A = -1.4$ V, a deposition time of 15 s and $i = 50$ nA. (c) AdSCP using a deposition time of 15 s at −0.6 V and $-i = 50$ nA. First signals are denoted with a thicker line.

During the reverse titration – additions of Zn^{2+} to peptide solution – two reduction peaks are increasing with the additions of zinc: peak at ca. −1.02 V, shortly overlapped by reduction of Zn^{2+} and peak at about −1.25 V increasing slowly with the additions of zinc (not shown). When $(\gamma$-Glu-Cys$)_2$Gly peptide is added to Zn^{2+} in solution, the initial chronopotentiogram using positive stripping currents after accumulation at −1.4 V shows a peak at ca. −0.97 V corresponding to the reoxidation of free Zn^{2+}. After the progressive addition of peptide, for applied high positive current, the initial peak decreases gradually and a new peak at ca. −0.46 is increasing, which is attributed to the formation of the Hg-peptide complexes. But, if small stripping currents are applied (Fig. 6b) a different behaviour is observed in the Zn-region: the peak at ca. −0.97 V decreases with the addition of peptide at the same time that a shoulder is increasing at E_p close to −1.02 V due to the reoxidation of Zn(II) bound to the peptide. When the concentration of peptide is high, the shoulder at −1.02 is developed into peak and no signal for the reoxidation of free Zn^{2+} is shown.

Applying EVLS measurements when $(\gamma$-Glu-Cys$)_2$Gly peptide is added to an excess of Zn^{2+} or Zn^{2+} is added to an excess of peptide is shown on Fig. 7a and b. In both cases, peak-counterpeak shape is observed for elimination function I_d calculated according to Eqs. (23) or (31) (Section 2.3), which shows that the reduction of Zn(II) in Zn–PC_2 takes place on HMDE in adsorbed state. Therefore, adsorptive accumulation and constant current chronopotentiometry with negative current is again suitable.

On Fig. 6c, chronopotentiogram for additions of $(\gamma$-Glu-Cys$)_2$Gly peptide to Zn^{2+} in solution is presented, after accumulation at −0.6 V and applying negative current. At the beginning, a peak at E_p close to −1.00 V due to the reduction of free Zn^{2+} is observed. With the addition of peptide to the Zn^{2+} solution new peaks are increasing. A peak at −0.69 V and a second peak at potentials between −0.48 and −0.52 V are attributed to the reduction of the Hg-peptide complexes formed on the electrode surface. In the Zn-region using small stripping currents the chronopotentiograms show (Fig. 6c) the developing of new peaks corresponding to the reduction of Zn(II) bound to the peptide in different manners. At ca. −1.05 V a peak is increasing with the addition of peptide, but in the first additions this peak is overlapping with the peak due to the reduction of free Zn^{2+}. After successive additions of peptide the excess of free metal ion is not so large, so that no signal for the free Zn^{2+} is shown. At ca. −1.30 V another peak appears due to the reduction of Zn(II) bound to the peptide, which is in agreement with DPV titrations. The shape and the behaviour of this peak mean that the reduction of the Zn-complex is quite irreversible, in accordance with chronopotentiometric measurements using positive cur-

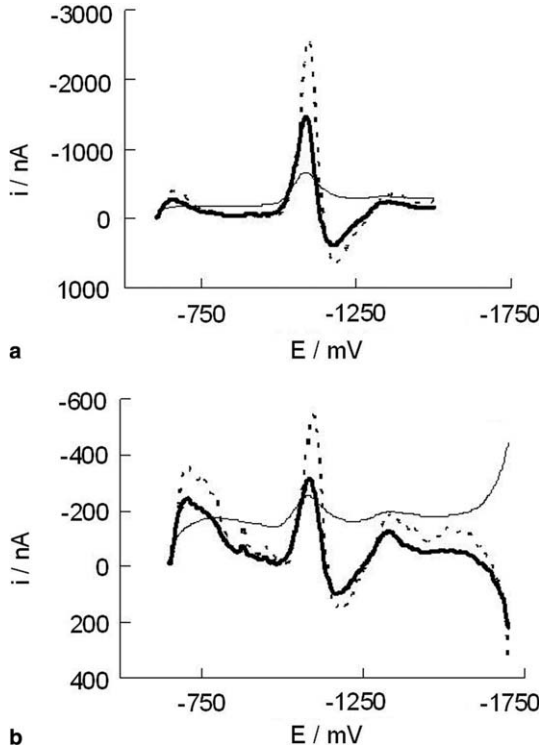

Fig. 7. Elimination voltammetry with linear scan when: (a) (γ-Glu-Cys)$_2$Gly peptide is added to an excess of Zn^{2+} and (b) Zn^{2+} is added to an excess of peptide. — v_{ref} 160 mV s^{-1}, — $f(I_d)$ = Eq. (23) and ---- $f(I_d)$ = Eq. (31).

rents (where no signal for this complex is shown). And it seems that at ca. −1.20 V a small peak is also appearing and it could be attributed to the reduction of another Zn-complex. Different behavior is observed applying a stripping current of −1000 nA: a peak at ca. −1.12 V is increasing (without overlapping with the peak attributed to the reduction of free Zn^{2+}) together with a shoulder at about −1.23 V.

DC voltammograms with slow scan rates, despite of not very good resolution, are in agreement with AdSCP measurements using small negative currents and also show, after a few additions of peptide to a Zn^{2+} solution, the peak at ca. −1.28 V attributed to the reduction of an irreversible Zn-complex and also it seems that at ca. −1.16 V a small peak is appearing. (not shown).

The titration of (γ-Glu-Cys)$_2$Gly peptide with Zn^{2+} in solution could be performed only for few Zn^{2+} additions, due to possibility of peptide oxidation. AdSCP measurements on the Zn–PC$_2$ system when the Zn^{2+}-to-peptide ratio is 0.25, with a wide range of negative stripping currents is shown in Fig. 8. Applying stripping currents between −1000 and −500 nA only a peak at ca. −1.12 V, that increases and shifts to positive potentials with lower currents, is observed. When stripping currents lower than −100 nA are used two new peaks at E_p close to −1.20 and −1.30 V, respectively, appear. Low currents involve longer stripping time; therefore the more electrochemically irreversible complexes could be seen. The presence of these

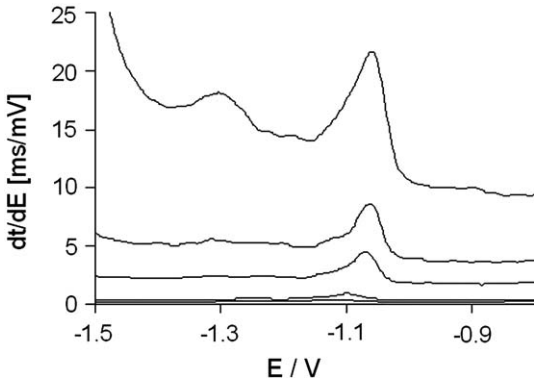

Fig. 8. Chronopotentiograms of Zn^{2+}-to- PC$_2$ ratio of 0.25 in borate buffer pH 8.5 on HMDE, dependence on negative currents at $E_A = -0.3$ V applying a deposition time of 15 s, $-i$ = 1000, 500, 100, 50, 20 nA.

peaks only when small currents are used, suggests that they are connected with strong complexes with a quite irreversible reduction.

The interpretation of chronopotentiometric and voltammetric measurements suggests that using high currents in chronopotentiometry, which involve shorter stripping times, or similarly high scan rates for DC voltammetric measurements, only complexes with quite reversible reduction signals are observed. When long-time measurement is applied (this means chronopotentiometry with small current, DC voltammetry with slow scan-rate or differential pulse voltammetry), there is enough time for the electrochemical reduction of complexes with more irreversible signals, where metal ion is bound.

Multivariate curve resolution method based on an alternating least-square optimization (MCR-ALS) has been proposed as a tool to get as much information as possible from chronopotentiometric and voltammetric data. The appearance of several overlapping signals in the Zn-region suggest the application of MCR-ALS analysis of the matrices in order to establish the assignation of the signals of Zn(II) bound in different ways to the peptide. In Fig. 6 a broken line separates the peaks due to Hg compounds from signals in the Zn-region. The peaks belonging to Hg compounds at the region −0.42 to −0.54 V (which are likely to behave in a non-linear way) are not taken into account in the MCR-ALS analysis. The rest of signals do not change their characteristic potential along the titration in a significant way and this suggests a linear behaviour that allows the application of MCR-ALS to the data matrices obtained in the voltammetric (Fig. 6a) and chronopotentiometric (Figs. 6b and c) titration of Zn^{2+} with (γ-Glu-Cys)$_2$Gly peptide.

The reverse measurements – additions of Zn^{2+} to peptide solution were performed and their results essentially confirm the conclusions from direct titration. However a MCR-ALS analysis has not been applied to them, because oxidation of peptide can easily occur and was detected in many cases, which can seriously affect quantitative conclusions about stoichiometries. These experiments only have

been used to obtain qualitative information about the processes occurred during the titration.

When MCR-ALS analysis is applied on the data matrix obtained in the DPV titration of Zn^{2+} with peptide (Fig. 6a), the best results (lack of fit 6.78%) were achieved using 4 components and the constraints of non-negativity, selectivity and signal shape. Fig. 9 summarises the resulting unitary voltammograms (a) and concentration profiles (b) plotted in front of the peptide-to-metal ratio.

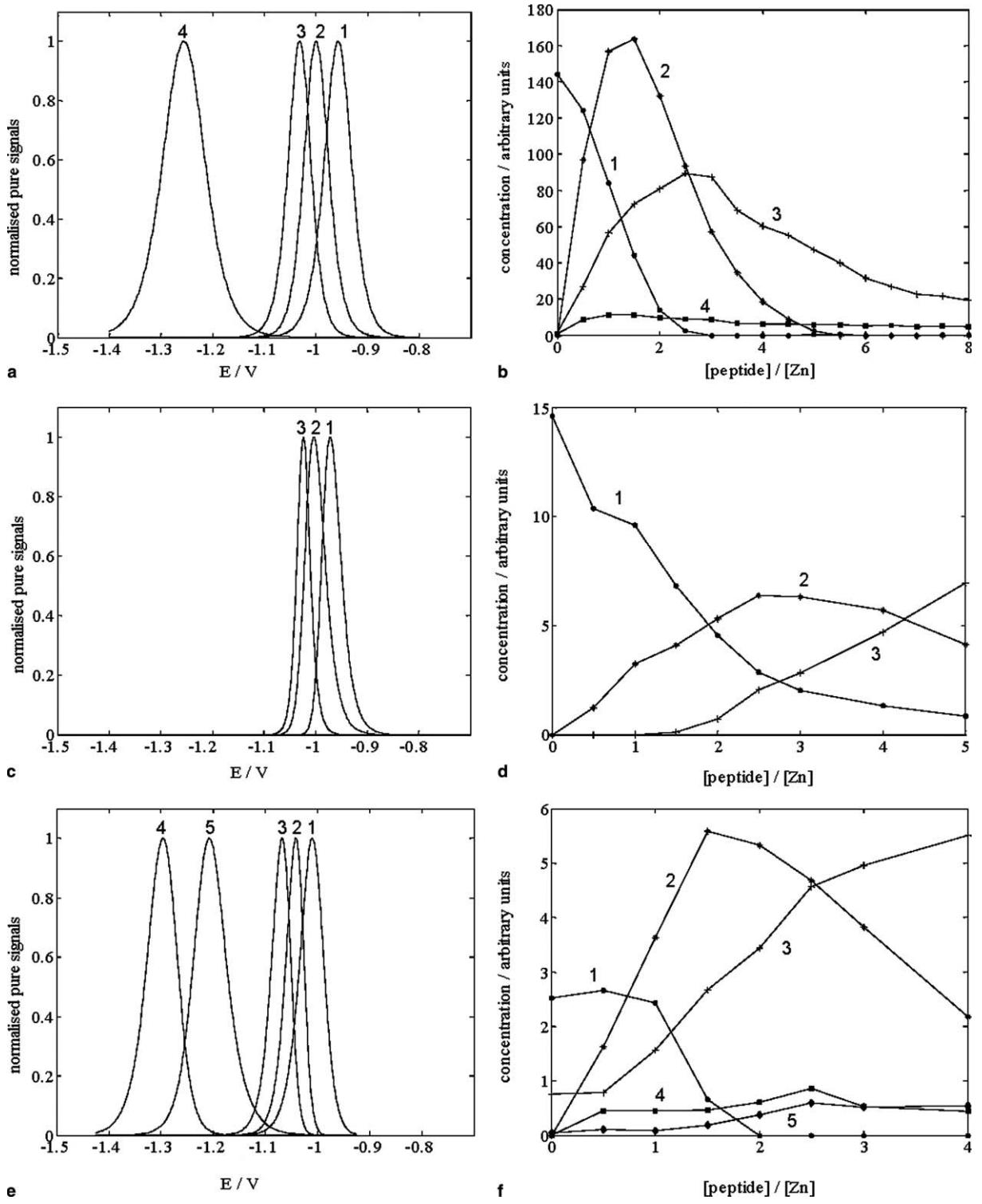

Fig. 9. Normalized unitary signals (a, c, and e) and concentration profiles (b, d, and f) plotted in front of the peptide-to-metal ratio obtained in the MCR-ALS decomposition of DPV data matrix shown in Fig. 6a, lack of fit 6.78% (a and b), of SCP data matrix shown in Fig. 6b, lack of fit 6.86% (c and d) and of AdSCP data matrix shown in Fig. 6c, lack of fit 11.68% (d and f).

The components have been numbered according to the position of their signals. In agreement with previous experiments [15,34], component 1 clearly corresponds to the reduction of free Zn^{2+} and disappears at a peptide-Zn ratio of 2. Components 2–4 are attributed to the reduction of Zn^{2+} bound to the peptide in different manners. Component 2 increases gradually and reaches a maximum at a ligand-to-metal ratio 2 and later progressively decreases. Component 3 is also increasing and for ratios higher than 2 is more predominant than component 2. Finally, component 4 fastly increases until a peptide-to-metal ratio of 1 and from here stabilizes.

Then MCR-ALS analysis is applied on the data matrix obtained in the SCP titration of Zn^{2+} with PC_2 (Fig. 6b), and the best results (lack of fit 6.86%) were achieved using three components and the constraints of non-negativity and signal shape. Fig. 9 summarises the unitary chronopotentiogram (c) and the concentration profile (d) plotted in front of the peptide-to-metal ratio, provided by MCR-ALS. Component 1 is clearly associated with the reduction of free Zn^{2+} which is disappearing during the titration. Components 2 and 3 correspond to the reduction of Zn^{2+} bound to the peptide. Component 2 appears from the start and increases until a peptide-to-metal ratio of 2.5 and later progressively stabilizes while component 3 appears at a peptide-Zn ratio of 2 and progressively increases.

As it was concluded in a recent work [26] the chronopotentiometric methods using small currents are more sensitive and show better signal separation than voltammetric methods. For this reason and due to the little reversibility of these complexes, the application of MCR-ALS analysis on the data matrix obtained in the AdSCP titration (Fig. 6c) shows five components instead of four components needed for voltammetric MCR-ALS analysis. The best results were achieved (lack of fit 11.68%) using 5 components and the constraints of non-negativity, selectivity and signal shape. Fig. 9 summarises the unitary adsorptive chronopotentiogram (e) and the concentration profile (f) plotted in front of the peptide-to-metal ratio, provided by MCR-ALS. The component 1 attributed to the reduction of free Zn^{2+} is stable until a peptide-Zn ratio of 1, later disappears at a ligand-to-metal ratio 2. Components 2–5 corresponding to the reduction of Zn^{2+} bound to the peptide in different manners. Components 2–4 have the same behaviour as in the two previous MCR-ALS analyses. But in AdSCP MCR-ALS analysis another component appears, component 5, which starts to increase at a peptide-Zn ratio close to 2 and later progressively stabilizes.

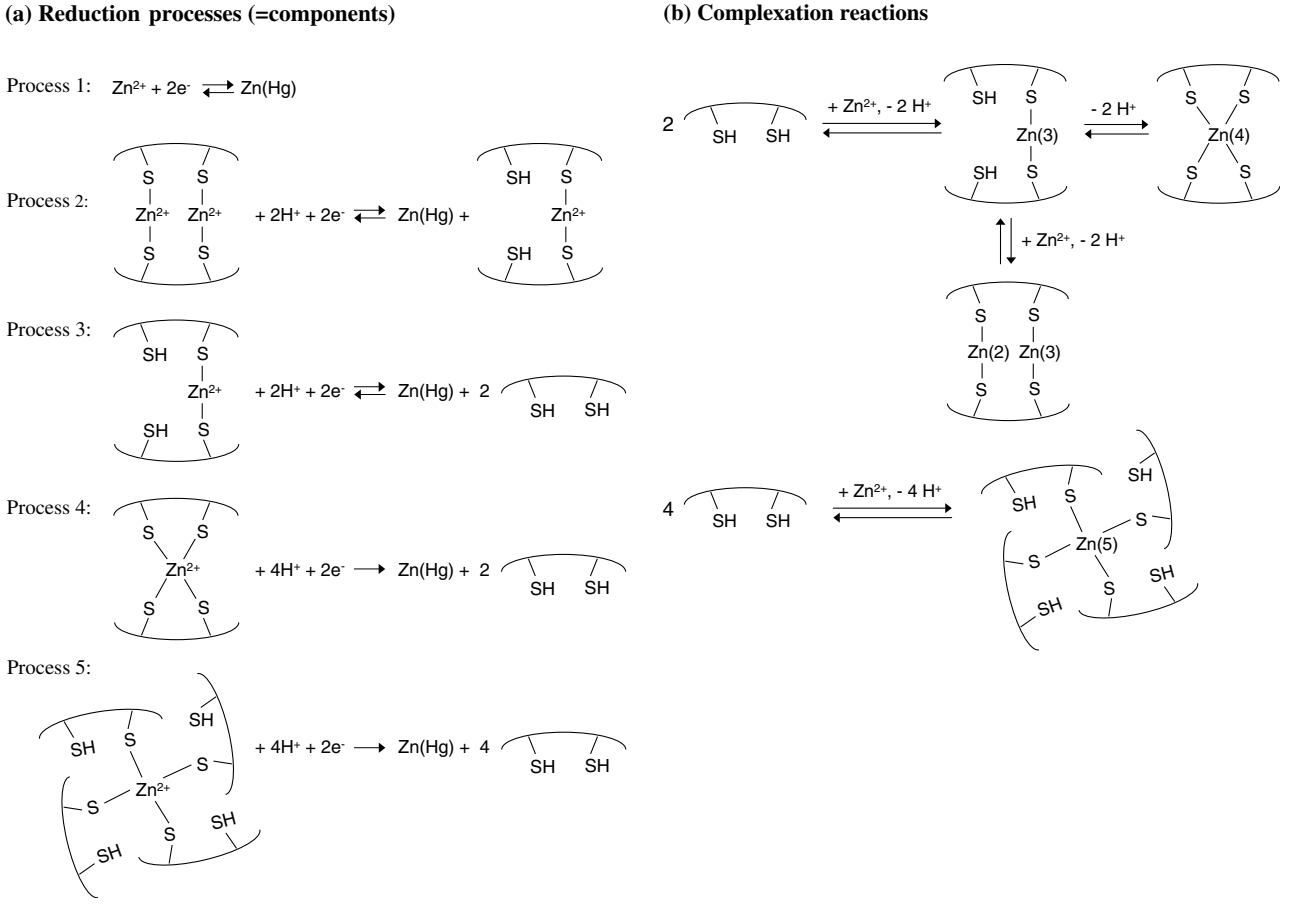

Fig. 10. Proposed electrode reaction for the reduction processes (a) and complexation reactions (b) for the titration of Zn^{2+} with $(\gamma\text{-Glu-Cys})_2$Gly peptide. Numbers in parenthesis state the correspondence between the different zinc atoms and the components 2–5 in Fig. 9.

The evolution of their concentration profiles (Figs. 9b, d, and f) can be explained by assuming that components 2–5 correspond to Zn(II) bound to two or four sulphur atoms of the peptide. Proposed electrode reaction for the reduction processes and complexation reactions are shown in Fig. 10a and b, respectively, where only the sulphur atoms taking part in the complexation of zinc are denoted.

This interpretation suggests that when PC_2 is added to an excess of zinc, complex 2:2 and 1:2 Zn–S are formed. The reduction of these is connected with components 2 and 3, respectively. This suggest that two Zn(II)-ions initially bound to two peptides start to bind the incoming free peptides forming 1:2 Zn–S bonds. At a substantially more negative potentials another zinc-complex would be reduced (component 4), attributed to the reduction of a 1:2 complex, where four sulphur atoms belonging to two peptide molecules are engaged in tetracoordination of one zinc atom. Finally the component 5, which appears only in AdSCP MCR-ALS analysis with a larger excess of peptide, would correspond to the reduction of a quite stable complex, where Zn-(II)-ion bonds four sulphur atoms belonging to four molecules of peptide. It is possible that this complex is formed only in adsorbed phase.

The complexation model here proposed is similar to that deduced for the Cd(II)–PC_2 system [15]. The main differences are the presence of Cd(II)-ions bound to a single S atom (not detected in the case of Zn) and the predominance of the Cd(II)-ions bound to four different peptide molecules at large excess of ligand (Zn(II)-ions prefer the ML_2 stoichiometry).

4. Conclusions

The facts described suggest us the following conclusions:

Adsorptive accumulation constant current stripping chronopotentiometry (AdSCP) is a valuable alternative for the electrochemical study of metal complexation by thiol-containing peptides, as suggested by the study of Zn–GSH and Zn–PC_2 systems.

The behavior of the Zn(II)-complexes, which are reduced with different degrees of electrochemical irreversibility, was studied using voltammetric and chronopotentiometric methods, but only chronopotentiometric methods combine the possibility to study both, long-time and short-time processes with very good sensitivity and signals separation, which is not possible using voltammetric methods (DPV is slow, DC or CV have poor sensitivity using slow scan rates at low concentrations).

AdSCP on HMDE presents experimental simplicity, reproducibility and total depletion regime with a wide range of stripping currents and is also more resistant than SCP to the effects of signal overlapping. In a positive current scan, the evolution of potentials towards more positive values produces an uncontrolled variation in the deposition time of the overlapping more positive signals; in contrast, the evolution to more negative potentials in AdSCP supposes no additional deposition for the signals while the previous ones are registered at more positive potentials, provided that a full coverage of the electrode has been achieved in the deposition step.

The application of MCR-ALS analysis for the resolution of overlapping SCP and AdSCP peaks is only possible under conditions allowing a reasonable linearity of the data. Then, MCR-ALS provides abundant information that permits to propose models of metal–peptide complexation. Moreover, such information is consistent with that obtained by other techniques, thus confirming the applicability of MCR-ALS in these cases.

Acknowledgements

The authors gratefully acknowledge financial support from project COST OC-D21.002 from The Ministry of Education, Youth and Sports of the Czech Republic, Project BQU2003-07587-C02-01 from the Spanish Ministry of Science and Technology and Project 2001SGR-00056 from the Generalitat de Catalunya. Núria Serrano acknowledges the University of Barcelona for a Ph.D. grant and for the financial support for the stay in the J. Heyrovský Institute of Physical Chemistry, Academy of Sciences of the Czech Republic. For the synthesis of PC_2 we thank to Dr. J. Velek from Institute of Organic Chemistry and Biochemistry, AS CR, Prague.

References

[1] D. Dolphin, O. Avramovic, R. Poulson (Eds.), Glutathione. Chemical, Biochemical and Medical Aspects, Part A, Wiley, New York, 1989, pp. 147–186.
[2] W.E. Rauser, Plant. Physiol. 109 (1995) 1141.
[3] E. Grill, E.L. Winnacker, M.H. Zenk, Science 230 (1985) 164.
[4] E. Grill, E.L. Winnacker, M.H. Zenk, Proc. Natl. Acad. Sci. USA 84 (1987) 439.
[5] W.E. Rauser, Annu. Rev. Biochem. 59 (1990) 1141.
[6] B. Ahner, N. Price, F. Morel, Proc. Natl. Acad. Sci. USA 91 (1994) 8433.
[7] M.H. Zenk, Gene 179 (1996) 21.
[8] M.S. Díaz-Cruz, J. Mendieta, R. Tauler, M. Esteban, J. Inorg. Biochem. 66 (1997) 29.
[9] M.S. Díaz-Cruz, J. Mendieta, R. Tauler, M. Esteban, Anal. Chem. 71 (1999) 4629.
[10] M.S. Díaz-Cruz, J. Mendieta, A. Monjonell, R. Tauler, M. Esteban, J. Inorg. Biochem. 70 (1998) 91.
[11] M.S. Díaz-Cruz, J.M. Díaz-Cruz, J. Mendieta, R. Tauler, M. Esteban, Anal. Biochem. 279 (2000) 189.
[12] B.H. Cruz, J.M. Díaz-Cruz, M.S. Díaz-Cruz, C. Ariño, M. Esteban, R. Tauler, J. Electroanal. Chem. 516 (2001) 110.
[13] G. Scarano, E. Morelli, Electroanalysis 10 (1998) 39.
[14] I. Šestáková, H. Vodičková, P. Mader, Electroanalysis 10 (1998) 764.
[15] B.H. Cruz, J.M. Díaz-Cruz, I. Šestáková, J. Velek, C. Ariño, M. Esteban, J. Electroanal. Chem. 520 (2002) 111.
[16] J.M. Estela, C. Tomás, A. Cladera, V. Cerdà, Crit. Rev. Anal. Chem. 25 (1995) 91.
[17] D. Jagner, Analyst 107 (1982) 593.
[18] M.L. Gozzo, L. Colacicco, C. Callà, G. Barbaresi, R. Parroni, B. Giardina, S. Lippa, Clin. Chim. Acta 285 (1999) 53.
[19] R.M. Town, H.P. Van Leeuwen, J. Electroanal. Chem. 523 (2002) 1.
[20] L. Trnková, R. Kizek, O. Dračka, Electroanalysis 12 (2000) 905.
[21] L. Trnková, O. Dračka, J. Electroanal. Chem. 413 (1996) 123.

[22] L. Trnková, Talanta 56 (2002) 887.
[23] L. Trnková, R. Kizek, J. Vacek, Bioelectrochemistry 63 (2004) 31.
[24] L. Trnková, J. Electroanal. Chem. 582 (2005) 258.
[25] I. Šestáková, T. Navrátil, Bioinorg. Chem. Appl. 3 (2005) 43.
[26] I. Šestáková, M. Kopanica, L. Havran, E. Paleček, Electroanalysis 12 (2000) 100.
[27] N. Serrano, I. Šestáková, J.M. Díaz-Cruz, Electroanalysis 18 (2006) 169.
[28] B. Merrifield, Solid phase peptide synthesis, in: B. Gutte (Ed.), Peptides: Synthesis, Structures and Applications, Academic Press, San Diego, 1995, pp. 93–169.
[29] O. Dračka, J. Electroanal. Chem. 402 (1996) 19.
[30] M. Esteban, C. Ariño, J.M. Díaz-Cruz, M.S. Díaz-Cruz, R. Tauler, Trends Anal. Chem. 19 (2000) 49.
[31] R. Tauler, A. Smilde, B.R. Kowalski, J. Chemometr. 9 (1995) 31.
[32] M.S. Díaz-Cruz, M. Esteban, A.R. Rodríguez, Anal. Chim. Acta 428 (2001) 285.
[33] The MATLAB version 5.3 R11, MathWorks Inc., Cochituate Place, MA.
[34] B.H. Cruz, J.M. Díaz-Cruz, C. Ariño, M. Esteban, Environ. Sci. Technol. 39 (3) (2005) 778.
[35] R.M. Town, H.P. van Leeuwen, J. Electroanal. Chem. 509 (2001) 58.
[36] N. Serrano, J.M. Díaz-Cruz, C. Ariño, M. Esteban, J. Electroanal. Chem. 560 (2003) 105.
[37] M. Torres, J.M. Díaz-Cruz, C. Ariño, B.S. Grabaric, R. Tauler, M. Esteban, Anal. Chim. Acta 371 (1998) 23.

DISCUSSIÓ DELS RESULTATS

Estudi dels sistemes Cd-Zn-MT i Zn-MT II

En el treball 10.1 els sistemes Cd-Zn-MT i Zn-MT II s'han estudiat amb un HMDE per cronopotenciometria de redissolució aplicant intensitats constants positives o negatives. L'aplicació d'un ampli interval d'intensitats fa possible l'estudi del comportament elèctroquímicament làbil o inert dels complexos involucrats en funció de l'escala de temps de les mesures electroquímiques. Com ja s'ha dit, un comportament electroquímicament inert és aquell en què el complex pràcticament no es dissocia en l'escala de temps de la mesura, mentre que el comportament làbil apareix quan la dissociació és molt més ràpida que la mesura.

L'estudi cronopotenciomètric amb un HMDE del sistema Cd-Zn-MT mostra inicialment, en un ampli interval d'intensitats, dos pics separats atribuïts al Cd(II) complexat amb la metal·lotioneïna (CdT) i al Zn(II) complexat (ZnT) (figura 3 del treball 10.1). Successives addicions de Cd(II) o Zn(II), mostren un comportament diferent en funció del valor de la intensitat aplicada. Quan s'utilitza una intensitat de reoxidació de -1000 nA, el que implica temps de reoxidació curts, no s'aprecien canvis en la intensitat ni en la posició dels pics CdT i ZnT, mentre que quan els temps de mesura són llargs (intensitats de reoxidació de -100 nA o inferiors) s'evidencien canvis en els pics inicials, ja que el temps de mesura és suficient per a què es pugui produir la dissociació d'alguns ions Cd(II) o Zn(II) enllaçats a la MT.

Les addicions de Cd(II) donen lloc (figura 4b del treball 10.1) a l'aparició d'una espatlla a cadascun dels pics originals (CdT' i ZnT') que tendeix a augmentar amb la concentració de Cd(II), detectant-se, al final, un senyal a E_p=-0.58 V corresponent al Cd(II) lliure.

Successives addicions de Zn(II) a la solució de Cd-Zn-MT mostren (figura 6a del treball 10.1) una disminució del pic CdT a la vegada que creix una espatlla a E_p=-0.65 V (CdT'), mentre que el pic ZnT original creix i es desplaça cap a potencials menys negatius.

Amb l'estudi cronopotenciomètric del sistema Zn-MT II es posa de nou de manifest la dependència amb el valor de la intensitat aplicada (figura 7a del treball 10.1). Per intensitats entre -1000 i -300 nA només s'observa un pic (ZnT), mentre que amb l'aplicació d'intensitats inferiors a -200 nA apareix un segon pic (ZnT').

Quan s'aplica una intensitat de -1000 nA, les addicions successives de Cd(II) a la solució de Zn-MT II produeixen una disminució del pic ZnT a la vegada que creix un pic en la zona del cadmi (CdT) (figura 8a del treball 10.1). Aquest comportament és consistent amb la substitució del Zn(II) pel Cd(II) en la MT. Amb la utilització d'intensitats inferiors es potencia la reorganització, mostrant-se amb les successives addicions de Cd(II) o de Zn(II) a la solució de Zn-MT II un comportament electroquímicament làbil.

L'estudi d'aquests sistemes amb un elèctrode de carboni vitrificat amb pel·lícula de mercuri (MF-GC) no dóna els resultats esperats ja que no s'observa cap tipus de senyal. Aquest comportament fa pensar que la metal·lotioneïna destrueix la superfície de l'elèctrode (possiblement afavorint l'oxidació de la fina pel·lícula de mercuri).

Estudi dels sistemes Zn(II)-GSH i Zn(II)-PC_2

En el treball 10.2 l'aplicació de la cronopotenciometria de redissolució amb acumulació per adsorció als sistemes Zn(II)-GSH i Zn(II)-PC_2 ha permès estudiar, a concentracions d'ordre μM, els processos de reducció irreversibles que no produeixen el corresponent senyal d'oxidació en una redissolució oxidativa.

La presència de senyals solapats, tant en l'estudi voltamperomètric com en el cronopotenciomètric, s'ha solucionat mitjançant l'aplicació d'un tractament quimiomètric de MCR-ALS. L'ús del qual ha permès en cada cas postular models de complexació a partir de l'estabilitat relativa dels enllaços i de les estequiometries.

La complexació del Zn(II) amb el GSH ha estat extensament estudiada per tècniques polarogràfiques i voltamperomètriques. Aquests estudis previs revelen la formació del complex $Zn_2(GSH)_2$ que es correspon amb l'estructura d'un clúster binuclear com a espècie predominant. Mentre que el complex $Zn(GSH)_2$ estaria només present en el moment en què té lloc la reducció del primer Zn del complex $Zn_2(GSH)_2$ (taula 10.1).

El sistema Zn(II)-GSH, on el Zn(II) s'afegeix a una solució de GSH, ha estat estudiat per AdSCP aplicant un ampli interval d'intensitats. Els cronopotenciogrames corresponents a una relació Zn(II)-GSH de 1 (figura 3a del treball 10.2) mostren per intensitats aplicades entre -700 i -100 nA un sol pic (corresponent a la reducció del primer zinc), mentre que amb l'aplicació d'intensitats menors es detecta un segon pic atribuït a la reducció de l'altre Zn(II). Després de successives addicions de Zn(II) els cronopotenciogrames enregistrats a una relació Zn(II)-GSH de 4 (figura 3b del treball 10.2) mostren per intensitats menors de -100 nA els dos pics ja existents i un nou senyal atribuït a la reducció del Zn(II) lliure. Mentre que aplicant intensitats grans només s'aprecia un sol pic.

Aquest comportament observat és consistent amb el fet que intensitats petites incrementen la finestra de temps de la mesura fent que els senyals esdevinguin menys irreversibles i, per tant, revelant senyals no detectats a intensitats més grans.

El comportament del sistema Zn(II)-PC_2 s'ha estudiat voltamperomètricament i cronopotenciomètrica (figura 6 del treball 10.2). Els cronopotenciogrames corresponents a l'addició de pèptid a una solució de Zn(II) aplicant una intensitat positiva, mostren inicialment un pic corresponent a la reoxidació del Zn(II) lliure. Amb les successives addicions de pèptid i aplicant valors d'intensitat petits s'observa la disminució d'aquest senyal a la vegada que es desenvolupa una espatlla a potencials una mica més negatius. Finalment, quan la concentració de pèptid és alta, l'espatlla es converteix en un pic i el senyal corresponent a la reoxidació del Zn(II) desapareix definitivament.

L'estudi per voltamperometria diferencial d'impulsos (DPV) i cronopotenciometria aplicant intensitats negatives petites mostra inicialment un pic atribuït a la reducció del Zn(II) lliure. Però després de les successives addicions de pèptid l'excés de metall lliure ja no és tan gran i s'observa la disminució del senyal corresponent al Zn(II) lliure al mateix temps que apareixen nous senyals, alguns d'ells solapats, a potencials més negatius que es poden atribuir a la reducció dels Zn(II) enllaçat al pèptid de diferents maneres.

La interpretació dels resultats voltamperomètrics i cronopotenciomètrics amb intensitats positives i negatives suggereix que amb l'ús d'intensitats grans en cronopotenciometria,

el que implica temps de redissolució petits, només s'observen els senyals dels complexos amb una reducció totalment reversible. Mentre que, quan s'apliquen temps de mesura llargs (mesures per DPV i cronopotenciomètriques amb intensitats petites), es produeix la reducció electroquímica dels complexos amb senyals més irreversibles.

L'aplicació del mètode de resolució multivariant de corbes per mínims quadrats alternats (MCR-ALS) en aquelles situacions on predominen els complexos inerts, imposant les restriccions de no-negativitat, selectivitat i restricció de forma, als senyals solapats de la zona del zinc permet proposar un model de complexació metall-pèptid (taula 10.1) i assignar els senyals del Zn(II) enllaçat al pèptid de maneres diferents.

Taula 10.1. Resum dels models de complexació proposats pels sistemes Zn(II)-GSH i Zn(II)-PC_2

SISTEMA	MODELS DE COMPLEXACIÓ
Zn(II)-GSH	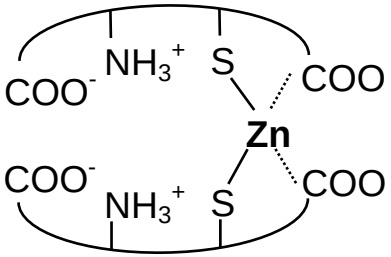 **ML_2** 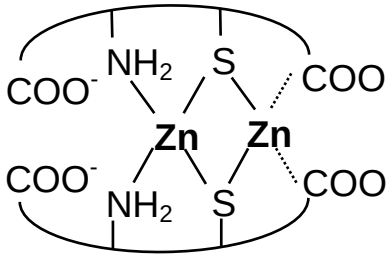 **M_2L_2 PREDOMINANT**
Zn(II)-PC_2	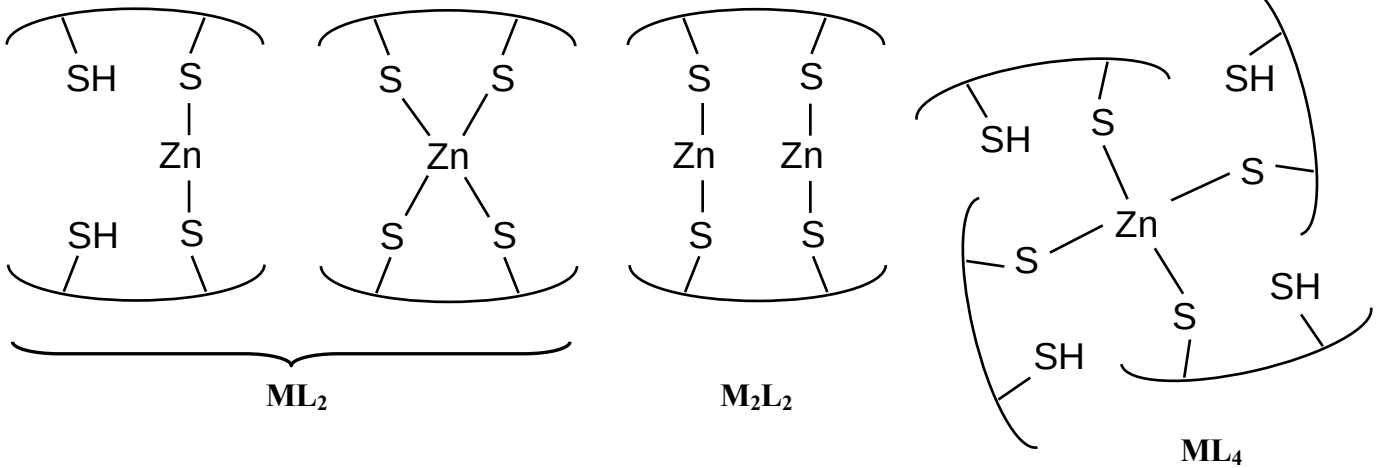 **ML_2** **M_2L_2** **ML_4**